Doctoral Dissertation
Doctoral Program in Energy Engineering (36th Cycle)

Towards sustainable biofuels production for aviation and maritime

By

Lorenzo Testa
* * * * * *

Supervisor
Prof. David Chiaramonti

Doctoral Examination Committee:
Ing. Giacobbe Braccio, Agenzia nazionale per le nuove tecnologie, l'energia e lo sviluppo economico sostenibile (ENEA)
Prof. Jeremiah D.G. Murphy, University College Cork

Politecnico di Torino
June 15, 2024

Declaration

I hereby declare that the contents and organization of this dissertation constitute my own original work and does not compromise in any way the rights of third parties, including those relating to the security of personal data.

……

Lorenzo Testa

Turin, June 15, 2024

* This dissertation is presented in partial fulfilment of the requirements for **Ph.D. degree** in the Graduate School of Politecnico di Torino (ScuDo).

Summary

This doctoral thesis explores the key role of sustainable agro-energy value chains in the advancement of more sustainable and regenerative agricultural practices. With a specific focus on critical factors such as crop rotation, soil carbon sequestration, decentralized production, and the mitigation of indirect land-use change (ILUC) effects, the research project is embedded within the EU Horizon 2020 project *"Biofuels production at low ILUC risk for European sustainable bioeconomy"* (BIKE). This project is aimed to providing evidence, measuring, and widely disseminating the market potential of low ILUC risk value chains for biomass, biofuels, and bioliquids in Europe, aligning with the implementation of RED II. This initiative provides robust evidence and measurements to validate the feasibility of low ILUC risk value chains in the European bioeconomy.

The thesis introduces a comprehensive framework for sustainable biomethane production in Europe, with a specific focus on Italy, and its conversion into sustainable biofuels. Under the light of existing policy targets and regulatory instruments (e.g. Guarantees of Origin for biomethane), the research explores an innovative and sustainable agro-energy chain – biomethane as energy vector for downstream conversion, also characterized by a significant potential to promote more sustainable and regenerative agricultural practices. This biomethane-based value chain under consideration is designed to produce Sustainable Aviation Fuels (SAF) and methanol for maritime, both of which play a key role in the decarbonization of these hard-to-abate sectors.

The work explores the possibility of integrating:

- A decentralized *biogasrefinery* that produces biomethane and Guarantees of Origin;
- Injecting this biomethane into the natural gas (NG) grid;
- Collecting an equivalent amount of natural gas through Guarantees of Origin in a centralized refinery, thus effectively utilizing biomethane for the production of Sustainable Aviation Fuels (SAF) and maritime fuels.

This approach combines the advantages of the decentralized biomass conversion in small farms with the centralized biomethane conversion in large-scale industrial refineries, either through existing or new plants.

The proposed value chain leverages advanced technologies characterized by high Technology Readiness Levels (TRL). These technologies stand as cornerstones of the envisioned production process, promising efficiency and effectiveness. The adoption of the Biogasdoneright (BDR) model, recognized as one of the most sustainable advanced biofuel pathways, further strengthens the sustainable nature of the proposed approach. The proposed value chain also gives the unique opportunity to exploit the EU existing gas infrastructure to rump-up the uptake of the advanced biofuels.

Within this concept, biomethane is utilized in three key Gas-to-Liquid (GTL) technologies: Fischer-Tropsch (FT) synthesis, Methanol (MeOH) synthesis, and Gas Fermentation and Alcohol-to-Jet (ATJ) conversion. These give rise to three distinct routes to be analysed in this thesis, i.e. (i) GTL-FT, (ii) GTL-MeOH route, and (iii) GTL-F_ATJ, respectively.

A computer-aided process simulation model and data collected from a thorough literature review of industrial references have been used to estimate the energy performances. The model provides insights into process yields and energy balances of these biofuel production routes, enabling a data-driven approach to biofuels production modelling. Moreover, preliminary insights into expected investment costs are given.

In the European context, based on the estimated availability of 38 bcm of biomethane at 2030, the GTL-FT route may address 4-9% of kerosene-based jet fuel EU demand, with variable outcomes based on employed technologies; meanwhile, the GTL-F_ATJ route exhibits a 11% potential coverage. For maritime fuels, the GTL-MeOH route could cover from 25 to 56% of the demand, contingent on technology. Alternatively, at 2050, with an estimated biomethane potential of 91 bcm, the GTL-FT route could potentially meet 9-19% of the EU demand for kerosene-based jet fuel: in contrast, the GTL-F_ATJ route shows a potential of 25%. Concerning maritime fuels, the GTL-MeOH potential could range from 48 to 105% coverage.

In Italy, based on the estimated availability of biomethane of 5.6 bcm by 2030, the potential of the GTL-FT route spans 7-14% of jet fuel demand, while GTL-F_ATJ may meet 18%. As for maritime fuels, GTL-MeOH could meet demand ranging from 69% to 152%. On the other hand, at 2050, given an estimated biomethane availability of 8.2 bcm, the GTL-FT route has the potential to meet 8-17% of the demand for kerosene-based jet fuel, while the GTL-F_ATJ route demonstrates a potential coverage of 22%. Regarding maritime fuels, the GTL-MeOH route could span from 91 to an impressive 198% coverage.

However, these processes also yield other very valuable co-products, including naphtha, diesel, waxes, hydrogen, and gasoline: therefore, a fair evaluation should consider these co-products when comparing with the other routes, beyond considering only jet and maritime components, and decide on the different pathways based on sector priorities to meet the set climate targets.

Ultimately, the thesis evaluates the investment costs associated with the implementation of these sustainable agro-energy systems, thereby enhancing our comprehensive understanding of their feasibility and economic viability. It is important to note that these costs are specifically related to the GTL plant (Gas-to-Liquids) part of the refinery. They do not encompass the upstream segment of the value chain, such as the biogas plants, the costs associated with upgrading for grid injection, or the costs of grid connection. While these aspects are certainly interesting and worth studying, our focus is limited to the GTL plant. The investments are estimated, on average, to be 791,970 USD/tonne/day (GTL-FT), 130,275 USD/tonne/day (GTL-MeOH), and 669,740 USD/tonne/day (GTL-F_ATJ), depending on plant scale.

Ringraziamenti

Desidero esprimere la mia profonda gratitudine alle diverse persone che hanno reso possibile il completamento di questo percorso e che hanno contribuito in modo significativo alla mia crescita personale e professionale. Nonostante siano numerose, ho deciso di menzionarle tutte, riconoscendo il valore di ogni singolo contributo.

Innanzitutto, desidero esprimere la mia gratitudine al Professor David Chiaramonti per avermi offerto questa straordinaria occasione di studio e ricerca, aprendomi le porte ad esperienze che altrimenti non avrei potuto vivere. Collaborare con lui mi ha permesso di crescere e affrontare sfide che hanno arricchito il mio percorso formativo in modo significativo.

Un ringraziamento speciale va al gruppo di ricerca del Politecnico di Torino, in particolare a Lorenzo “Pino”, compagno di avventura e grande amico. Un ringraziamento va anche a Gabriele, Michel, Viviana e Giacomo, colleghi e amici fantastici. Grazie anche a Matteo, Marta, Paolo e Daniele per la loro preziosa collaborazione, il loro supporto e la loro simpatia.

Desidero esprimere la mia più sincera gratitudine alla Professoressa Daniela Misul per il suo costante sostegno, la gentilezza e l'affetto sempre dimostrati nei miei confronti.

Un caloroso ringraziamento va agli amici di “Langando”, in particolare ad Arturo, amico “storico”, che è stato un punto di riferimento fondamentale in questi anni a Torino. Grazie a Marco, Vittorio, Eleonora, Silvia, David, Antea, Donato, Alessandra, Cecilia, Daniele e Federica. La vostra accoglienza, il vostro supporto e i momenti meravigliosi condivisi resteranno sempre nel mio cuore.

Un ringraziamento speciale va a tutte le persone che ho incontrato durante il mio periodo come visiting PhD alla FAO, e che ho avuto la fortuna di ritrovare anche adesso in questo nuovo ruolo dopo il dottorato. Innanzitutto grazie alla mia supervisor Michela Morese. Il suo sostegno e la sua guida sono stati fondamentali per il mio sviluppo.

Inoltre, sono grato di aver avuto l'opportunità di lavorare con Marco e Lorenzo, che sono per me più che colleghi, amici.

Grazie a tutto l'Energy team. Mi sono trovato davvero bene con loro e sono felice che il dottorato mi abbia portato a collaborare con persone così eccezionali.

Grazie anche agli amici che ho incontrato in questo contesto, in particolare a Jorge, con cui ho condiviso tanto anche al di là di questa esperienza, a Lapo, Dario, Jacopo, Clara, Marta, Arianna, Isabella, Filippo e gli altri della OG Gang.

Desidero inoltre ringraziare i miei amici, che, sebbene distanti fisicamente durante questo percorso, sono stati un costante sostegno e una fonte di ispirazione. Dario, il cui incoraggiamento e supporto sono sempre fondamentali; Pietro ed Efe, con cui condivido sorrisi, risate ma anche preziosi momenti di confronto; Gabriele, amico importante sin dai tempi della triennale; Andrea, Luca, Elisa, Ivona e gli altri amici della "Linzer Familie". Grazie anche a Rainer, per aver capito le mie scelte ed avermi sempre dimostrato affetto.

Un grazie di cuore alla mia famiglia: mia madre Patrizia, per il suo sostegno costante e amore incondizionato, e mio fratello Francesco, che ha sempre saputo strapparmi una risata anche nei momenti difficili. Grazie per avermi sempre incoraggiato a perseguire i miei sogni e per essere stati al mio fianco in ogni fase di questo percorso. Un ringraziamento speciale anche a tutto il resto della famiglia: i miei innumerevoli cugini, la mia cara nonna, le zie e gli zii.

Infine, desidero ringraziare la mia ragazza Valeria per il suo amore, la sua pazienza e il suo sostegno infiniti. Senza di lei, questo viaggio sarebbe stato molto più difficile. Grazie per essere stata il mio porto sicuro nei momenti di tempesta, e al contempo il sole che illumina le mie giornate serene. La sua presenza nella mia vita è una costante fonte di emozioni e mi sento fortunato ad averla sempre accanto.

Grazie a tutti. Sono profondamente grato di avervi nella mia vita.

Acknowledgements

I wish to express my deep gratitude to the many people who have made the completion of this journey possible and have significantly contributed to my personal and professional growth. Although there are many, I have decided to mention each one, acknowledging the value of every single contribution.

First and foremost, I wish to express my gratitude to Professor David Chiaramonti for offering me this extraordinary opportunity for study and research, opening doors to experiences I otherwise would not have had. Collaborating with him allowed me to grow and face challenges that have significantly enriched my educational journey.

A special thank you goes to my research group at the Polytechnic University of Turin, particularly to Lorenzo “Pino”, a companion in adventure and a great friend. Thanks also to Gabriele, Michel, Viviana, and Giacomo, fantastic colleagues and friends. Thanks also to Matteo, Marta, Paolo, and Daniele for their valuable collaboration, support, and friendliness.

I wish to express my most sincere gratitude to Professor Daniela Misul for her constant support, kindness, and affection always shown towards me.

A warm thank you goes to the friends of the “Langando” group, particularly to Arturo, a longtime friend, who has been a fundamental reference point during these years in Turin. Thanks to Marco, Vittorio, Eleonora, Silvia, David, Antea, Donato, Alessandra, Cecilia, Daniele, and Federica. Their warmth and affection, along with the wonderful moments shared, will always remain in my heart.

A special thank you goes to all the people I had the good fortune to meet during my period as a visiting PhD at FAO, and whom I have been lucky to meet again in this new role after the doctorate. First and foremost, thanks to my supervisor

Michela Morese. Her support and guidance have been fundamental to my development.

Additionally, I am grateful for the opportunity to work with Marco and Lorenzo, who are more than colleagues to me, they are friends. Thanks to the entire Energy team. I truly enjoyed working with them and am happy that the PhD led me to collaborate with such exceptional people.

Thanks also to the friends I met in this context, particularly to Jorge, with whom I shared so much beyond this experience, to Lapo, Dario, Jacopo, Clara, Marta, Arianna, Isabella, Filippo, and the others from the OG Gang.

I also wish to thank my friends, who, although physically distant during this journey, have been a constant support and a source of inspiration. Dario, whose encouragement and support are always essential; Pietro and Efe, with whom I share smiles, laughter, but also valuable moments of reflection; Gabriele, an important friend since undergraduate days; Andrea, Luca, Elisa, Ivona, and the other friends of the "Linzer Familie". Thanks also to Rainer, for understanding my choices and always showing me affection.

A heartfelt thanks to my family: my mother Patrizia, for her constant support and unconditional love, and my brother Francesco, who has always managed to make me laugh even in difficult times. Thank you for always encouraging me to pursue my dreams and for being by my side in every phase of this journey. A special thank you also to the rest of the family: my countless cousins, my dear grandmother, my aunts, and uncles.

Finally, I wish to thank my girlfriend Valeria for her infinite love, patience, and support. Without her, this journey would have been much more difficult. Thank you for being my safe harbor in times of storm, and at the same time the sun that brightens my serene days. Her presence in my life is a constant source of joy and I feel fortunate to have her always by my side.

Thank you all. I am deeply grateful to have you in my life.

Contents

List of Tables

List of Figures

List of Abbreviations

	Definition
AD	Anaerobic Digestion
ADM1	Anaerobic Digestion Model No.1
AMP	Amino-Methyl-Propanol
ASF	Anderson-Schulz-Flory
ASU	Air Separation Unit
ATJ	Alcohol-to-Jet
ATR	Autothermal Reforming
BECCS	Bioenergy with carbon capture and storage
BECCS/U	Bioenergy with carbon capture and utilisation or storage
bpd	barrel per day
BDR	Biogas Done Right
BWR	Boiling Water Reactor
CAPEX	Capital Expenditure
CHP	Cogeneration or combined heat and power
CIB	Consorzio Italiano Biogas

COP21	2015 United Nations Climate Change Conference
CORSIA	Carbon Offsetting and Reduction Scheme for International Aviation
CSTR	Continuous Stirrred Tank Reactor
CTL	Coal To Liquid
DEA	Diethanolamine
DME	Dimethyl Ether
DMR	Dry Methane Reforming
DMTM	Direct Methane to Methanol
ELECNRTL	Electrolyte Non-Random Two Liquid
EOS	Equation of State
EtOH	Ethanol
ETS	Emissions Trading System
EU	European Union / European
FOAK	First Of A Kind level
FT	Fischer Tropsch
GHG	Greenhouse Gases
GO	Guarantees of Origin
GOP	monthly average price of Guarantee of Origin
GTL	Gas To Liquid
GTL_F-ATJ	Gas-to-Liquid with Gas Fermentation and Alcohol-to-Jet conversion
GTL-FT	Gas-to-Liquid with Fischer-Tropsch synthesis

GTL-MeOH	Gas-to-Liquid with methanol synthesis
HPWS	High Pressure Water Scrubbing
HTFT	High Temperature Fischer Tropsch
IGCC	Integrated Gasification Combined Cycle
ILUC	Indirect Land Use Change
IMO	International Maritime Organization
IT	Italy / Italian
LHHW	Langmuir-Hinshelwood-Hougen-Watson
LPG	Liquefied Petroleum Gas
LTFT	Low Temperature Fischer Tropsch
MB	Membrane separation
MDEA	Methyldiethanolamine
MEA	Monoehtanolamine
MeOH	Methanol
MPS	Modular Plant Solutions
MTBE	Methyl Tertiary-Butyl Ether
NGP	Average monthly price of natural gas
NRRP	National Recovery and Resilience Plan
NRTL	Non-Random Two Liquid
NRTL-RK	Non-Random Two Liquid - Redlich-Kwong
PAD	Pressurized Anaerobic Digestion
POX	Partial Oxidation

PR-BM	Peng Robinson with Bostonne-Mathias alpha function
PRF	Plug Flow Reactor
PSA	Pressure Swing Adsorption
PWS	Pressurized Water Scrubbing
RCSTR	Rigorous continuous stirred tank reactor with rate-controlled reactions based on known kinetics
REDII	Renewable Energy Directive II
REDIII	Renewable Energy Directive III
REQUIL	Rigorous equilibrium reactor based on stoichiometric approach
RGIBBS	Rigorous reaction and/or multiphase equilibrium based on Gibbs free energy minimization
RK	Redlich-Kwong
RKSMHV2	Redlich-Kwong-Soave equation of state with Modified-Huron-Vidal mixing rule
RPLUG	Rigorous plug flow reactor with rate-controlled reactions based on known kinetics
RSTOIC	Stoichiometric Reactor based on known fractional conversions or extents of reaction
RWGS	Reverse Water Gas Shift
RYIELD	Nonstoichiometric reactor based on known yield distribution
SAF	Sustainable Aviation Fuels
SCWR	Supercritical Water Reforming
SMR	Steam Methane Reforming
SRK-ML	Soave Redlich Kwong equation of state with T dependent

TP	Feed-in premium
TR	Reference fare
TRL	Technology Readiness Level
UASB	Upflow Anaerobic Sludge Blanked
VFA	Volatile Fatty Acids
WGS	Water Gas Shift

Chapter 1 Introduction

1.1 Framework

Nowadays fossil resources still represent the main global energy source, covering about 80% of the world's energy consumption [1]. However, their production and use cause severe impacts on the environment, as they release carbon dioxide and other greenhouse gases (GHG), responsible for global warming and climate change: according to J. G. J. Olivier and J. A. H. W. Peters [2], fossil fuel combustion accounts for 89% of all CO_2 emissions and 68% of all GHG emissions.

Climate change is today a well-recognized global concern, and the urgent need to develop and implement alternative processes for sustainable energy generation is promoting research and development worldwide.

At International level, a major commitment to GHG emission reduction came with the adoption of the COP21 Paris Agreement in 2015, signed by 196 Parties. This binding international treaty marked the beginning of a new global effort in contrast to climate change, setting the aim of limiting global warming to well below 2°C (possibly 1.5 °C) compared to pre-industrial levels (intended as 1850-1900) [3]. In this context, an unprecedent boost to market deployment of renewable energies is an unavoidable component of a wider climate change fighting strategy.

Along with wind and solar energy, another crucial solution involves utilizing biomass to produce biofuels, thus replacing conventional fossil fuels, as they provide a renewable carbon-based source, being CO_2 utilized by crops and forests during the natural photosynthesis process [4]. However, biofuel production itself could induce other land-related emissions, either directly and/or indirectly [5]. In fact, when biofuels are produced on existing agricultural land and conventional agronomic practices, the demand for food and feed crops might lead to the extension of agriculture land into areas with high carbon stock such as forests, wetlands and peatlands, to provide the same amount of feed/food replaced by biofuel production. If and when this happens, it may originate greenhouse gas emissions that will negatively impact on biofuels GHG balance [6] [7], and thus on climate. This effect is known as Indirect Land-Use Change (ILUC). ILUC is a very complex

phenomenon, which accounting requires the understanding of large number of different factors. It can be anyway contrasted by adopting sustainable agricultural rotations, photosynthetic intensification in agriculture, soil carbon accumulation, improved Nitrogen and Carbon use Efficiency, etc.

The urgent need to fight climate change has driven the European Union (EU) to set ambitious decarbonization goals to accelerate the transition to a low-carbon economy, advancing the adoption of renewable energy sources and promoting sustainable energy practices.

The European Renewable Energy Directive II (RED II) [8] set the overall EU target for Renewable Energy sources consumption by 2030 to 32%. As biofuels are crucial in helping the EU meet its greenhouse gas reduction targets, the RED II outlined a goal for 2030, aiming to increase the share of renewable energy used in transport to 14%, with a minimum share of 3.5% designated for advanced biofuels. RED II also established the minimum threshold for reducing greenhouse gas emissions for biofuels, including biomethane for transport, by means of sustainability criteria.

In 2021, the European Commission adopted the "Fit for 55" [9] climate package, aimed at achieving the Green Deal objectives set by 2030: more specifically, the reduction of greenhouse gas emissions by 55% compared to 1990 levels, towards achieving carbon neutrality by 2050. One of the pillars of the package is the review and strengthening of the EU system for trading GHG emission allowances, which comprises a further reduction of emissions obtained through the EU Emissions Trading System (ETS) sectors by 61% at 2030 compared to 2005. Beyond a significant reduction of the amount of free allowances, the strengthening of the EU ETS system also passes through its extension to new sectors. It is expected the gradual extension, from 2023, of the ETS system [10] to the emissions produced from maritime transport, and in particular from ships exceeding 5,000 tonnes, and the creation from 2025 of a separate quota trading system for buildings and transport on the road. In the aviation sector, the compensation and reduction scheme will be implemented carbon emissions from international aviation (CORSIA).

Also due to the geopolitical events occurred in 2022, and the related evolution of the energy market in the same year, the REPowerEU [11] plan set a series of measures to rapidly reduce dependence on fossil fuels and accelerate the green transition, while increasing the resilience of the EU energy system and reducing dependency. Besides, on March 2023, the EU Institutions provisionally agreed on stronger legislation to accelerate the deployment of renewable energy, raising the EU's binding renewable energy target for 2030 to 42.5%, increasing from the prior

32% target, with an ambition to reach 45% [6]. The so-called RED III [12] was then published on the 31st of October 2023.

In the context of aviation, Sustainable Aviation Fuels (SAF) are gaining prominence as a necessary and immediate solution to reduce the carbon footprint of air travel. Indeed, the European Union (EU) has emphasized the adoption of SAF as a pivotal decarbonization strategy for the sector, suggesting a gradual increment in the amount of SAF at EU airports [13]. The ReFuelEU aviation initiative thus introduced a mandate for SAF [14] for all flights departing from the EU territory. The recent agreement between the EU Parliament and the EU Council on April 26, 2023, surpassed the initial Commission's proposal [15], outlining a progressive and accelerated SAF adoption: 2% by 2025, 6% by 2030, rising to 20% by 2035, with a potential peak of 70% by 2050 at EU airports. This equates to a substantial demand for SAF, as the global aviation industry seeks to align with emission reduction targets and regulations.

Similarly, in the maritime sector, the demand for sustainable fuels is expected to significantly grow. As regulations progressively tighten on both GHG and non-GHG maritime emissions, and shipping come under greater scrutiny, maritime transport faces mounting pressure to transition toward cleaner energy sources. The International Maritime Organization (IMO) has set targets to reduce greenhouse gas emissions from international shipping by at least 50% by 2050 compared to 2008 levels [16]. This shift implies a substantial increase in the demand for sustainable maritime fuels, in particular deploying advanced biofuels. At EU level, the FuelEU Maritime regulation introduce progressive targets for carbon intensity reduction compared to average in 2020 for vessels larger than 5000 gross tonne: 2% by 2025, 6% by 2030, 14.5% by 2035, 31% by 2040, 62% by 2045, to 80% by 2050. These vessels represent 55% of all ships, and 90% of emissions from the maritime sector.

1.2 Scope of the work

Given this scenario, an imperative emerges to quickly ramp-up the production of these sustainable alternatives to conventional fossil fuels, while actively exploring innovative pathways for their development.

However, designing, authorising, building, commissioning, and starting to commercially operate new industrial biofuel facilities based on innovative sustainable technologies is complex, needs very large investments and requires significant time to complete. Moreover, in order to provide a quantitatively relevant contribution to the current and short-/medium-term volumes of EU liquid fuel demand, only process at or close to the FOAK (First Of A Kind) level, i.e. TRL 9, should be considered. In addition, building sustainable supply chains for these

sectors is a significant challenge, given the constraints set by the EU legislation in terms of eligible feedstocks, particularly in the lipid-based biofuel route.

The combination of all these factors represents a major limitation to achieve the planned targets.

Biomethane, produced from organic waste and agricultural residues, is a very mature bio-based process that holds significant potential, not only as final product but also as intermediate energy carrier for further processing.

In fact, while the direct uses of biomethane already gathered attention over the past decades, there is a need to explore additional valorisation strategies to maximize its potential in achieving decarbonization objectives in the liquid fuel sector. The production of biomethane, often called as *biogasrefinery* given the multiple products and benefits that this value chain delivers, is a well proven but innovative solution deployable at full commercial scale (TRL 9), thus delivering immediate contributions to achieving EU climate targets.

The production of biomethane is particularly attractive in those EU Countries where a significant gas infrastructure already exists, as Germany or Italy. The map of the EU natural gas grid is shown in **Figure 1**.

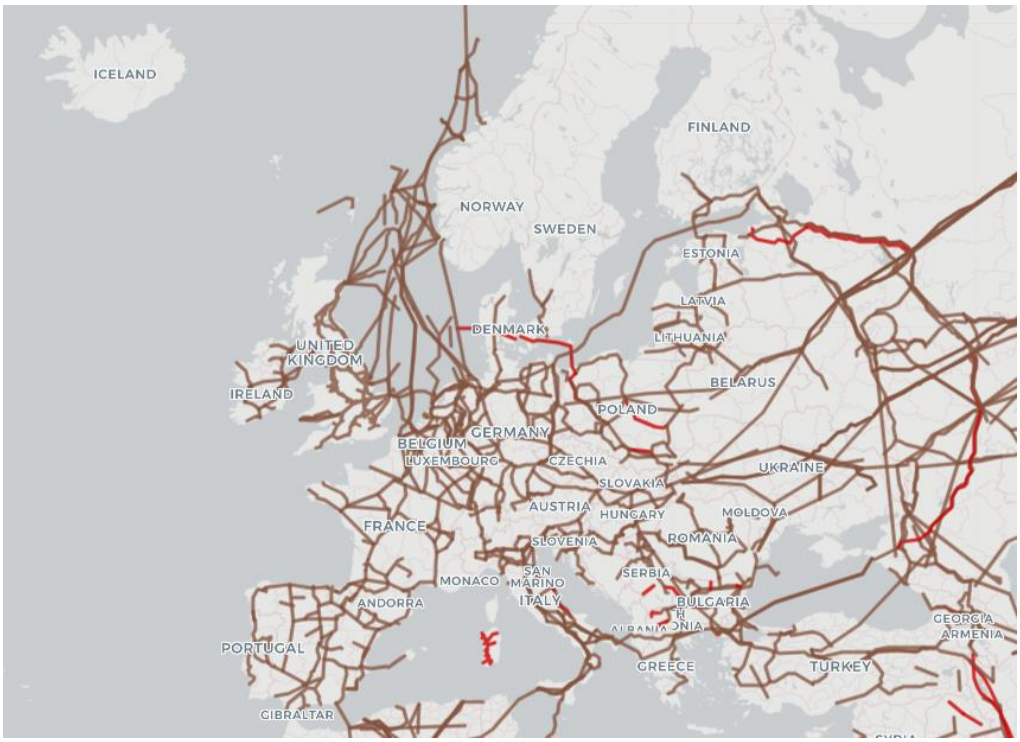

Figure 1. 2023 EU natural gas grid in operation (brown) and under construction (red) [17]

Italy has supported the use of biogas for energy generation in the last decades, through a series of economic incentives for electricity generation plants. As a result,

there are currently more than 2,000 biogas power plants in Italy, with a total nominal power of 1.34 GW (as of April 2023 [18]).

A limited number of biogas plants have already been upgraded to biomethane production, mostly thanks to a previous incentive scheme (Ministerial Decree of 2 March 2018 [19]). Based on the most recent data [20], there are currently 27 biomethane plants in operation in Italy.

In Germany there are approximately 9,600 biogas facilities. Among them, approximately 200 plants are equipped with an upgrading system to convert biogas into biomethane, which is subsequently integrated into the natural gas distribution grid [21].

Moreover, in some these Countries – as Italy – a regulatory system already exists to implement a Guarantee of Origin system (primarily governed by Ministerial Decree of July 6, 2012, no. 120 [22], which implements European Directive 2009/28/EC [23]). This allows the injection of biomethane in the National Grid by a multitude of biomethane plants, and the collection of the same amount of biomethane in a centralized collection point, where the conversion to other products can be carried out at the appropriate scale in existing refineries.

Thus, the possibility of combining:

- Decentralised *biogasrefinery*, delivering biomethane and Guarantees of Origin (GO)
- The injection of this biomethane in the national natural gas grid (or transport to refineries via other means)
- Conversion of the corresponding amount of this bio-based natural gas (via the related GO) in a centralised refinery, thus virtually using Biomethane

appears as a very attracting option.

The concept of the proposed approach is illustrated in **Figure 2**.

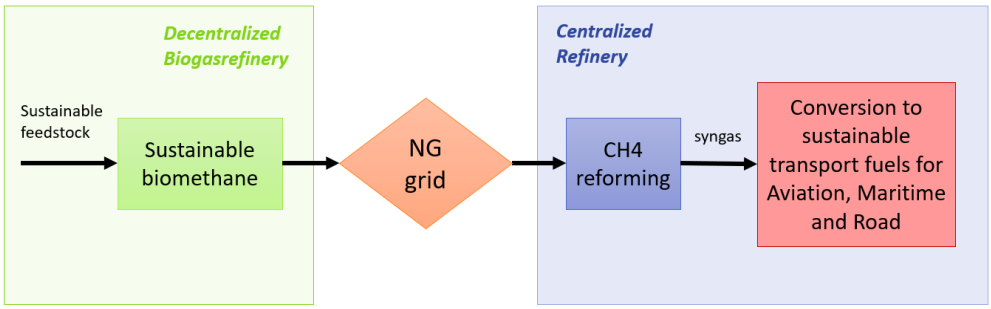

Figure 2. Centralized/Decentralized scheme for liquid biofuels production (NG = natural gas)

In fact:

- The scheme offers the advantages of connecting decentralised biomass conversion (AD plants are relatively small scale in nature, reducing the needs for transporting large volumes of solid biomasses - associated to environmental impacts, as well as higher costs), with the centralised conversion in existing large-scale industrial refineries to sustainable liquid transport fuel products;
- The whole system is based on high-TRL fully commercial solutions. Biomethane is a technologically very mature bioprocess (even if open to further innovation), as well as the conversion of Natural Gas into fuels through technologies such as Fischer-Tropsch, Partial Oxidation, Steam Reforming, and Gas Fermentation.

This work aims to address these novel routes, that in fact combines sustainable advanced biomethane technology with some Gas-to-Liquid (GTL) technologies and provide a preliminary insight into the investment costs. In a subsequent article, a technical and economic feasibility analysis will be developed.

The goal is thus to demonstrate the technical possibility to generate substantial volumes of Sustainable Aviation Fuel (SAF) and Maritime Fuels, employing an integrated approach that encompasses various dimensions.

Moreover, our study considers one of the most innovative and sustainable approaches to biomethane production, which is the Biogasdoneright model [24], which is already able to deliver high GHG performances and environmental benefits, in addition to the biomethane production itself.

As said, the proposed value chains leverage advanced technologies and processes characterized by high Technology Readiness Levels (TRL), such as Biomethane and GTL technologies as Fischer-Tropsch (FT) synthesis, methanol (MeOH) synthesis, Gas Fermentation and Alcohol-to-Jet (ATJ). These technologies serve as the pillars of the proposed production process, ensuring efficiency and effectiveness.

However, our study will assume biomethane is produced through one of the most innovative and sustainable models, the Biogasdoneright [24], that is already delivering today high GHG performances and environmental benefits to the farming system and GHG savings/removals. This further strengthens and remark the sustainable character of the proposed approach.

Beyond deploying the latest technological innovation, the proposed value chain also offers the unique opportunity to exploit the existing EU gas infrastructure to rump-up the uptake of the advanced biofuels.

Furthermore, the conversion of existing fossil-based technologies and refineries by integrating renewable feedstock, such as biomethane, represents the key element

of the strategy. This reconfiguration not only maximizes the utilization of existing resources but also aligns with the broader sustainability goals.

Under the socio-economic point of view, these pathways would also allow to convert existing fossil refinery sites, with clear benefit to the local communities, with creation of permanent jobs, both direct and indirect, as well as investment in the entire chains.

The work also considered the regulatory mechanisms already in place in some EU Member States, which allows to speed up the achievement of EU targets and implementation of EU Policies.

1.3 Manuscript contents

The remainder of this manuscript is structured as follows.

Chapter 2 delves into the sustainable value chain under consideration and its integration within the regulatory framework and investment landscape in Italy. Furthermore, it provides detailed explanations of the three different routes that will be the focus of this study, offering insights into the technologies involved and industrial references, including existing facilities with their associated investment costs related to the GTL part of the value chain.

Chapter 3, on the other hand, will focus on modelling the three pathways. It will begin with an in-depth and critical literature review of the technology models that can be utilized along the value chains outlined in existing literature. The second part of the chapter will describe the model developed based on the references gathered from the literature.

Chapter 4 will showcase the results of the developed model and will feature a discussion section where considerations on energy aspects, such as efficiencies, etc., will be made, contextualizing these results within the Italian and European contexts, while also addressing the demands for aviation and maritime fuels.

Finally, there will be a concluding chapter dedicated to summarizing the findings.

Chapter 2 Exploring biomethane-to-liquid routes for aviation and biofuels

2.1 Value chain and routes description

As introduced, the proposed advanced liquid biofuels production scheme consists in: (i) biogas production in decentralized plants and upgrading to biomethane; (ii) biomethane injection into the natural gas grid and emission of Guarantees of Origin for the biomethane; and (iii) equivalent volume of biomethane processing in a centralized refinery, where methane is first reformed to syngas and then synthetized to liquids (kerosene, diesel, methanol, ethanol, etc.).

The decentralized biogas production we considered in this work is based on the adoption of the Biogasdoneright (BDR) model at farm scale, encompassing the production low indirect land use change (ILUC) feedstock. The primary goal of this model is to contrast the adverse effects on land from bioenergy demand, with a focus on improving soil efficiency and promoting sustainable farming. This objective is supported by the following principles: (i) reducing the reliance on primary crops as digester feed; (ii) mitigating greenhouse gas emissions in agriculture by utilizing digestate as a renewable fertilizer that sequesters CO_2 in the soil, implementing sustainable agricultural practices and recovering nutrients; (iii) integrating agricultural production with these appropriately sized bioenergy units to enhance competitiveness in the food, feed, and energy sectors. Thus, according to the BDR scheme, the feedstock to be provided to the digester should be based on double cropping, with a primary crop for food and a secondary crop for energy [24].

As for the centralized conversion of biomethane into advanced sustainable liquid biofuels, the proposed value chain involves the Gas-To-Liquid (GTL) technology. GTL traditionally allows for the conversion of natural gas into liquid hydrocarbons and oxygenates through chemical reactions. These hydrocarbons are fully equivalent to fuels and chemicals produced in a conventional oil refinery in the range of gasoline and middle distillate range. These therefore include naphtha, diesel, kerosene, lubricants, and waxes. GTL products may include other chemicals such as ammonia, methanol, or methyl tert-butyl ether (MTBE), a major motor gasoline additive. The chemical conversion of methane to liquids allows for an alternative source of liquids to the traditional refinery products deriving from crude

oil. In addition, GTL facilitates the transportation of methane from remote production sources to consumption destinations [25].

The GTL technology is based on three main steps: (i) reforming of methane to synthesis gas (syngas), primarily constituting a mixture of carbon monoxide and hydrogen; (ii) catalytic conversion of syngas to liquid hydrocarbons; (iii) products separation and upgrading [25].

Specifically, this study explores three different routes, notably:

1) GTL-FT: syngas is converted to Fischer-Tropsch (FT) liquids. The GTL plant capacity being considered in this case is 10,000 barrels per day (bpd) of FT products (syncrude);
2) GTL-MeOH: syngas is converted to methanol (MeOH). The capacity of the GTL plant under consideration in this case is 2,000 tonne/d of MeOH;
3) GTL-F_ATJ: syngas undergoes a fermentation process to be converted to ethanol (EtOH) and then further processed to jet fuel through the alcohol-to-jet (ATJ) technology. In this case, the capacity being considered for the GTL plant is 1,000 tonne/d of products.

These sizes have been selected based on the typical dimensions of industrial plants typically available on the market or, alternatively, on possible minimum industrial sizes (details in [26] [27]).

Figure 3 shows the conceptual scheme of the proposed value chain, encompassing both the sequence of steps and the diverse routes that may be undertaken.

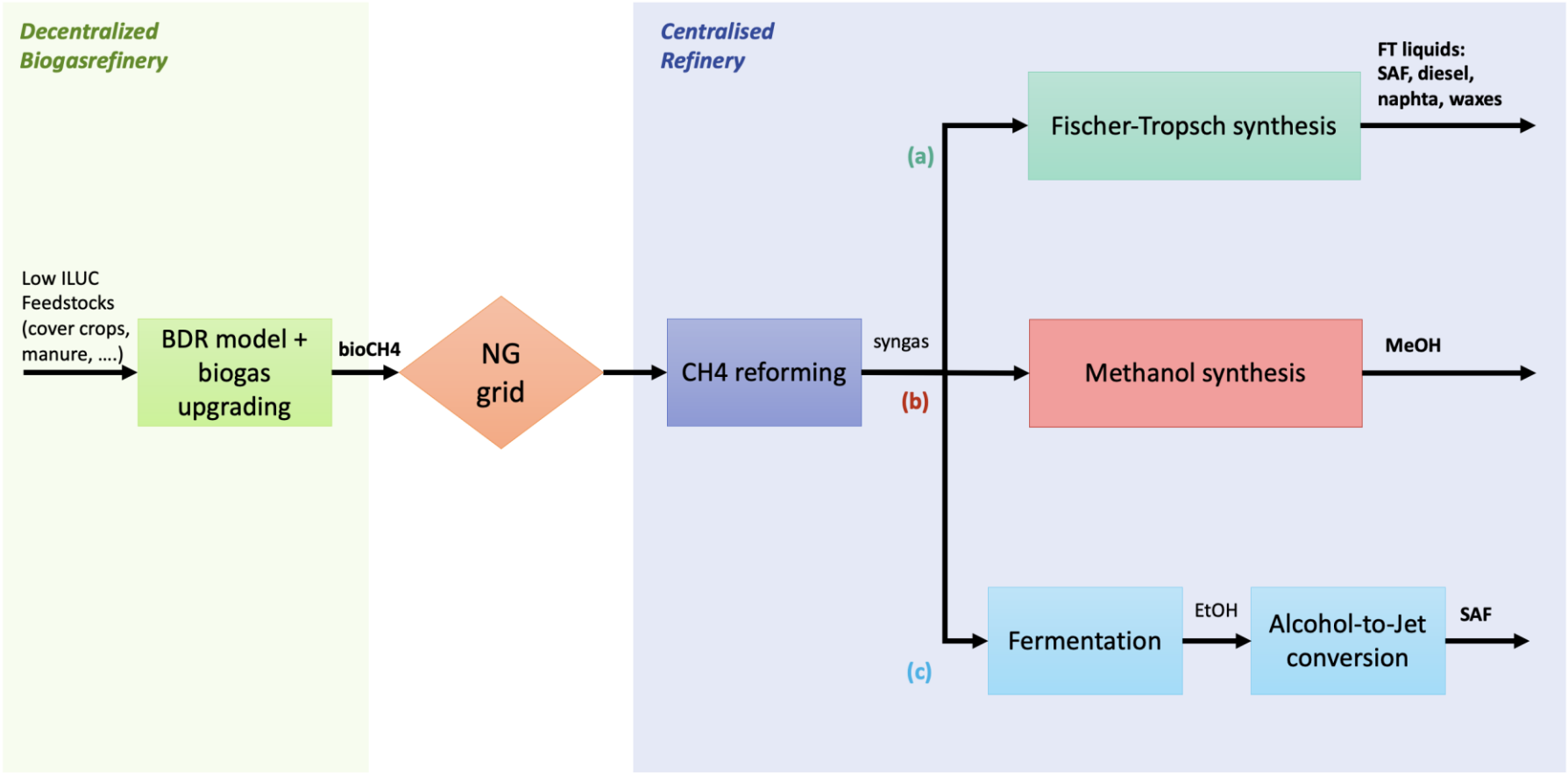

Figure 3. Liquid biofuels production chain scheme (BDR = Biogasdoneright model; NG = natural gas; FT = Fischer–Tropsch; MeOH = methanol; EtOH = ethanol; SAF = Sustainable Aviation Fuels)

2.1.1 The value chain within the IT regulatory system

To gain a comprehensive insight into the value chain, it is vital to integrate it within the Italian regulatory framework. Notably, these value chains align well with the Italian incentive scheme specified in the National Recovery and Resilience Plan (NRRP) "*Development of biomethane, according to criteria for the promotion of the circular economy*". This measure was approved by the Italian Minister for Ecological Transition (MiTE) on the 15th September 2022 [28]. It is aimed to support investments to increase the efficiency of existing agricultural biogas plants and to convert them into sustainable biomethane production plants. In addition, this Ministerial Decree (DM) has the scope to encourage the construction of new biomethane plants.

The measure, composed of 15 Articles and presented as a means of implementation of the circular economy, regulates the modalities of allocation of 1,7 billion €, and is fundamental to reduce Italy's dependence on foreign gas.

The Decree provides for:

a) A CAPEX incentive up to a maximum of 40% of the eligible investment costs;
b) An incentive tariff applied to net production of biomethane and injected into the natural gas grid, for a period of 15 years.

The base amount of the incentives is based on the size of the plant, the feedstock type, the kind of investment (new plant or converted), and the year. The incentives are issued through a series of public competitive auctions.

As concerns the CAPEX incentive, the investment costs considered as eligible are:

- Costs of realization and efficiency improving of the biomethane production plant;
- Equipment costs for biomethane monitoring and oxidation, exhaust gases and fugitive emission monitoring;
- Costs of connection to the natural gas network;
- Costs for the purchase or acquisition of operating software for plant management;
- Costs of design, construction management, testing, consultancy, feasibility studies, purchase of patents and licenses related to the implementation of the above investments, a maximum total of 12% of the total eligible expenditure; and
- Costs for the digestate composting phase.

Further details concerning the CAPEX incentive are reported in **Table 1**.

Type of biomethane production plant	Biomethane production capacity (Cp)	Specific maximum investment cost [€/Smc/h]		Percentage of capital contribution [%]
		New plants	Conversions	
Agricultural plants	Cp≤ 100 Smc/h	33.000	12.600	40%
	100 Smc/h <Cp≤ 500 Smc/h	29.000	12.600	40%
	Cp>500 Smc/h	13.000	11.600	40%
Plants fed by organic waste	Any	50.000	-	40%

Table 1. CAPEX incentive: Maximum specific values of the CAPEX to be covered with incentives (40% of expense incurred), with Cp= plant production capacity

The Decree refers to the Guarantee of Origin (GO), a certificate that allows biomethane producers to demonstrate the renewable origin of their product. In this case, the GO is released to the biomethane producer, who can sell it to users/refineries.

Concerning the incentive tariff applied to net production of biomethane, the biomethane producer can choose between an *all-inclusive tariff* (TO) and a *premium tariff* (TP). Being the incentive tariff paid on the basis of net production and fed into the natural gas grid, the fossil energy consumption attributable to auxiliary plant services must be subtracted from the amount, which is anyway increased by any auto consumption of biomethane.

The *all-inclusive tariff* (TO) is equal to a reference tariff (TR), reduced of the percentage of discount offered and accepted during the competitive auctions, including the economic value of the sale of natural gas and the value of the guarantees of origin (PGO).

On the other hand, *premium tariff* (TP) is equal to a reference tariff (TR), to which the sum of the average monthly price of natural gas (NGP) and the monthly average price of guarantees of origin (GOP) must be subtracted. In this case, the guarantees of origin (GO) remain available to the producer.

The TR, which set as a basis for auctions, is differentiated between plants fed by from agricultural or waste matrices. The NGP is under continuous negotiation and managed by the GME, Gestore dei Mercati Energetici - the Energy Market Authority. The GOP is registered on the market platform for the exchange of guarantees of origin (M-GO) in relation to GOs of biomethane used in transport or other uses, and is managed by the GME.

The scheme for the incentive tariff is summarized in **Table 2**, while **Table 3** reports details regarding the reference tariff (TR).

INCENTIVE TARIFF: applied to net production of biomethane and injected into the natural gas grid		
	PREMIUM TARIFF (TP)	*ALL-INCLUSIVE TARIFF (TO)*
Calculation method	TP = TR — NGP — GOP	TO = TR
Natural gas sales	Sale in the availability of the biomethane producer	Withdrawal by the GSE
GO handling	Issued to the biomethane producer and in his availability	Issued to the biomethane produce and transferred free of charge to the GSE

Table 2. Incentive scheme (TP= premium tariff, TR= reference tariff, NGP= average monthly price of natural gas, GOP= monthly average price of guarantees of origin, GO= guarantees of origin, GSE= Gestore dei Servizi Energetici)

Type of biomethane production plant	**Biomethane production capacity (Cp)**	**Reference tariff [€/MWh]**
		New agricultural and bio-waste plants and reconversion only for agricultural plants
Small Agricultural plants	Cp≤ 100 Smc/h	115
Other agricultural plants	Cp>100 Smc/h	110
Plants fed by organic waste	Any	62

Table 3. Reference tariffs set as a basis for auctions [€/MWh]

The main requirements to access to the incentives of the DM are:

- Possession of the qualification for the construction and operation of the relevant plant for biomethane production;
- Compliance with the sustainability requirements with regard to the reduction of greenhouse gas emissions to be guaranteed depending on destination of biomethane;
- In the case of conversion, assistance shall be granted on existing agricultural plants;
- Projects must include the digestate storage tanks of the facilities, of a volume equal to the production of at least 30 days, which must be gas tight and equipped with gas collection and recovery systems to be reused for the production of electricity, thermal or biomethane;
- Quote of the of connection to the gas grid, if provided in the project.

In our case, within the proposed value chain scheme, biomethane producers would receive a premium tariff (PT) on their production and obtain a guarantee of origin (GO). They would inject the biomethane into the grid, and downstream, a refinery would extract the biomethane, purchasing both the biomethane and the guarantee of origin. Consequently, the refinery purchasing the biomethane also gains ownership of the GO, enabling them to demonstrate the renewable origin of

their products to final customers, even if not physically connected to the anaerobic digestion unit. The conceptual scheme of the overall process is shown in **Figure 4**.

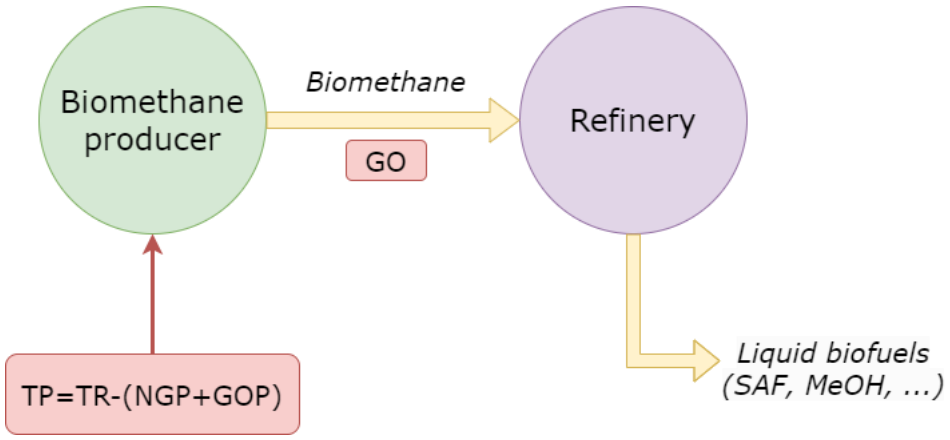

Figure 4. Conceptual scheme of the value chain proposed (TP= feed-in premium, TR= reference fare, NGP= average monthly price of natural gas, GOP= monthly average price of guarantees of origin, GO= guarantees of origin, SAF=Sustainable Aviation Fuels, MeOH=methanol)

2.2 Identification of bio/thermo-chemical conversion technologies

This section extensively explores and analyses a diverse range of industrial and innovative technologies for converting biomass to liquid fuels, providing valuable insights into key process parameters.

2.2.1 Anaerobic digestion

Biogas can be produced through the biological process known as Anaerobic Digestion (AD), which involves a complex microbiological pathway. Various groups of bacteria and archaea collaborate to break down organic matter into a gas mixture comprising CH_4 (53-70% vol), CO_2 (30-50% vol), N_2 (2-6% vol), O_2 (0-5% vol), and smaller proportions of H_2, H_2S, NH_3 [29]. The specific composition depends on the type of biomass being digested and the prevailing process conditions. Possible substrates encompass dedicated crops, agricultural residues, household and food wastes, animal manure, and industrial byproducts.

The AD process is composed of four key phases: hydrolysis, acidogenesis, acetogenesis, and methanogenesis. In the hydrolysis stage, intricate substrates rich in carbohydrates, fats, and proteins undergo breakdown into their respective monomers—glucose, fatty acids, and amino acids. Subsequently, these monomers transform into volatile fatty acids (VFA), such as valeric, butyric, caproic, iso-valeric, iso-butyric, propionic, and acetic acids during acidogenesis. The next

phase, acetogenesis, sees the conversion of VFAs into acetic acid, hydrogen, and carbon dioxide. Finally, methanogenesis completes the process by converting these products into methane and carbon dioxide. The end-products of AD include a slurry or solid fraction referred to as digestate, comprising the remnants of the treated substrate and being rich in organic carbon and nutrients.

The trophic chain's dynamics hinge on various operational factors such as temperature, redox potential, pH, feeding procedure, mixing, retention time, type of substrates, reactor configuration, organic loading rate, and the presence of inhibitors.

2.2.2 Biogas cleaning and upgrading

As mentioned, biogas primarily comprises CH_4, water vapor, and CO_2, along with contaminants like H_2S, NH_3, N_2, and siloxanes. The concentration of these impurities depends on the composition of the digested substrate. It is crucial to reduce these impurities due to potential issues such as corrosion, toxicity, catalyst deactivation, and a decrease in gas heating value. Meeting gas specifications and standards is also essential. Biomethane, derived from biogas, can be injected into natural gas grids, prompting many countries to establish standards for gas quality before injection [30]. In Italy, for instance, biomethane quality for injection is regulated by specific decrees and technical reports.

The process of purifying biogas from contaminants is commonly known as "biogas cleaning", while the removal of CO_2 and steam is termed "upgrading" [31]. Although some upgrading technologies address both impurities and CO_2, there is an advantage in cleaning the gas before upgrading. The technology used for cleaning biogas is influenced by the intended final use of the gas. For instance, the purification process for biogas intended for heat and power generation differs significantly from that required for producing biomethane. This is because volatile organic compounds (VOCs), which are typically present in biogas streams, need to be managed differently depending on the final application.

Various technologies for biogas upgrading are available, continually improving, with new techniques in development [32]. Widely adopted technologies include:

a) Physical absorption, utilizing water or organic solvents.
b) Chemical absorption, employing amine or saline solutions.
c) Pressure swing adsorption (PSA).
d) Membrane separation (MB).
e) Cryogenic upgrading [33].

Physical absorption (a) exploits the different solubility of CH_4 and CO_2 in the absorbent liquid. Chemical absorption (b) involves the chemical reaction of CO_2

with solutions like amine or saline. PSA (c) uses porous materials at high pressures to adsorb CO_2 and other trace components. Membrane separation (d) uses permeable layers to separate CH_4 from other impurities. Cryogenic upgrading (e) relies on the principle that gases liquefy at different temperatures at a fixed pressure.

In Europe, PWS is used in 35.5% of plants, followed by 20% for MEA, 20% for MB, 17% for PSA, and 8% for emerging technologies [30]. After cleaning and upgrading, the resulting gas stream is termed biomethane, a renewable source of methane (CH_4 >95%, CO_2 from 1 to 5%), suitable for direct use as automotive fuel or injection into the natural gas grid [34].

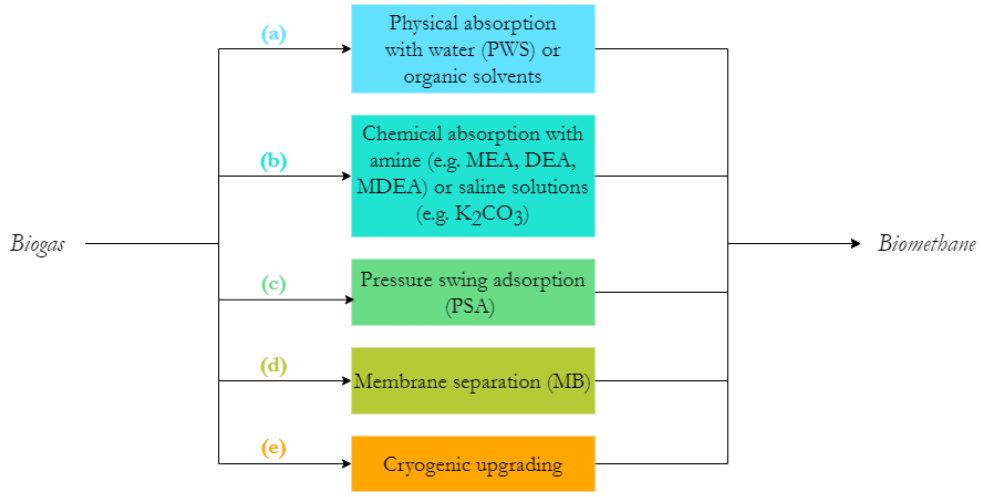

Figure 5. Biogas cleaning and upgrading main conversion technologies

2.2.3 Biomethane reforming to syngas

Both the production routes here considered to generate Fischer-Tropsch fuels and methanol are fed with syngas: therefore, in our scheme reforming of biomethane to syngas is necessary, representing a critical step of the process.

Synthetic gas, or syngas, is a gaseous mixture of H_2 and CO, at different ratios, that can be used as a chemical building block for the synthesis of a variety of chemical products and carbon-based fuels. The selectivity of the final products depends upon the H_2/CO ratio [35]. Both Fischer-Tropsch and methanol synthesis require H_2/CO ratio equal to 2 [36] [37]. Syngas is traditionally obtained from coal, natural gas, residual oils, and petroleum, but it is possible to generate syngas also from biomass, a sustainable and renewable substitute to the fossil-based syngas [38].

The industrial process for converting natural gas, methane, or biomethane into syngas varies depending on the desired downstream products. These processes break down the hydrocarbons into hydrogen and carbon monoxide, which can then be used to produce a range of valuable chemicals and fuels like ammonia, pure

hydrogen, methanol, and more. The choice of conversion method and downstream processes depends on factors like cost, efficiency, and the specific applications of the end products.

In the scheme encompassed in this study, the syngas is obtained from the biomethane, the upgraded product of Anaerobic Digestion of organic materials [39]. Also, it can be generated from methane extracted from the gas grid, if an equivalent amount of biomethane is injected in the gas pipeline elsewhere from the AD-biomethane production site (in a certified accounting mode, ensuring renewable carbon is not double counted using guarantees of origin).

The main processes used to convert methane to syngas can be summarised ([40],[36], [41]) as follows:

(i) Steam methane reforming (SMR);
(ii) Partial oxidation (POX);
(iii) Autothermal reforming (ATR); and
(iv) Dry methane reforming (DMR).

SMR (i) is a well-established and large-scale technology, mostly used for hydrogen production from methane. In this route, CH_4 and steam react in a reformer over a nickel-alumina catalyst [42], at a temperature of 1073.15 to 1173.15K and a pressure of 15 to 30 bar. The primary reaction is:

$$CH_4 + H_2O \rightarrow CO + 3H_2 \quad (1)$$

The process is strongly endothermic [43], and the resulting H_2/CO ratio is ~3, well above FT- and MeOH- synthesis requirements (H_2/CO ~2).

However, it also generates carbon dioxide (CO_2) emissions as a by-product through the water gas shift (WGS) reaction. In this case CO and water react, producing hydrogen and carbon dioxide, as in reaction (2):

$$CO + H_2O \rightarrow CO_2 + H_2 \quad (2)$$

Toward Net Zero, Carbon Capture and Sequestration (CCS) should be used in combination with SMR and fossil feeds. Indeed, the CO_2 emissions generated during SMR could also be further valorised through Carbon Capture and Utilization (CCU), which however necessitates the availability of supplementary hydrogen.

POX (ii) instead uses oxygen to convert methane. The methane partial oxidation reaction is the following:

$$CH_4 + \frac{1}{2}O_2 \rightarrow CO + 2H_2 \quad (3)$$

The process is exothermic and generates a H_2-lean syngas (H_2/CO=1 to 1.6) and the reaction occurs at high temperature (>1473 K) if no catalyst is used [36]. The employment of catalyst can lower the reaction temperature to ~1000 K. The catalysts employed could be divided into three groups: Ni, Co and Fe, noble metal and early transition metal carbide [44].

Combining POX with SMR reforming allows for achieving H_2/CO ratio in the range 1.6 to 2.6 [36], a process is called autothermal reforming (iii). In ATR, the heat produced by the POX is used to provide the endothermic heat of SMR reaction.

These three technologies are well employed in the industry. For instance, Shell and Sasol utilize POX [45], [46], [47], Rentech uses SMR [48], and Exxon Mobil utilizes ATR [49].

In DMR (iv), CO_2 is used as an oxidant to convert CH_4 to syngas. The technology is thus very attractive from a sustainability perspective, as it uses two types of greenhouse gases, i.e. CO_2 and CH_4, to form a valuable product. The process is described by equation (4).

$$CH_4 + CO_2 \rightarrow 2CO + 2H_2 \quad (4)$$

The syngas produced is normally characterized by a H_2/CO ratio close to 1 [36]. This could also be further adjusted for methanol and Fischer-Tropsch synthesis by reacting CO with H_2O to produce CO_2 and H_2 in water gas shift (WGS) and partial oxidation reactions [29], [40].

Catalysts for DMR can be noble metal-based (Rh, Ru), which have a good activity and stability but high cost, or Ni-based ones (Ni/Al_2O_3), commonly used for their low cost, high H_2 yield and fast turnover rates.

This approach is particularly interesting as it can tolerate the varying concentration of CO_2 associated with biomethane. Nevertheless, the commercialization of this technology is still in its preliminary stage [42], [50]. However, there are some drawbacks linked to these reforming routes, such as catalyst deactivation (mainly due to carbon deposition), and high energy demand, as the reforming reaction is endothermic and requires to be operated at high temperatures (1123.15 to 1273.15K) to obtain higher conversion rates and minimize carbon deposition.

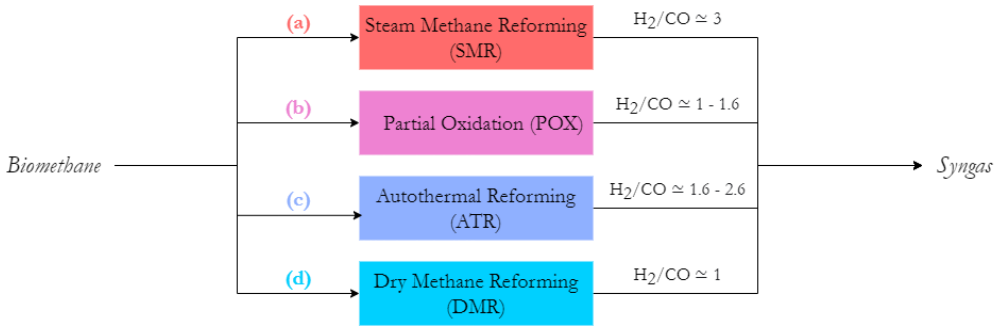

Figure 6. Methane reforming to syngas conversion technologies

2.2.4 Fischer-Tropsch synthesis

Once syngas has been produced and purified, it can be used in the Fischer-Tropsch process to produce a mixture of hydrocarbons at different chain lengths, used as synthetic fuels. These products may be used directly in a gas turbine or distilled into kerosene (C-10 to C-16), diesel- (C-14 to C-20), light naphtha (C-5 to C-6), heavy naphtha (C-6 to C-12) and waxes (C-20+).

The Fischer-Tropsch synthesis is a polymerization reaction, in which CO is hydrogenated with H_2 to the C-1 intermediate, which then grows to form different hydrocarbon chains of variable lengths. Syngas is thus converted into a variety of products, such as alcohols, aldehydes, olefins, paraffins, and especially liquid transportation fuels [51]. After the FT synthesis, the last stage is upgrading and separation of the FT syncrude in order to obtain high-quality products.

Fischer-Tropsch synthesis was developed in the early XX century by Franz Fischer and Hans Tropsch at Kaiser Wilhelm Institute [55], with the aim of producing synthetic fuels from coal reserves in Germany during World War II [52]. The process found only limited commercial application [53] [57]. This relatively well-known technology has recently drawn a renewed interest for its application to cellulosic biomass and agricultural waste [56], to convert them to linear-and branched-chain synthetic hydrocarbon [54], representing thus a very promising and sustainable solution for the production of clean fuels at competitive costs ([58], [59], [60]).

The polymerization reaction requires syngas at a H_2/CO ratio of about 2 [61], which is processed over a metal catalyst (Fe or Co), at pressure range of 20 to 60 bar. Temperatures can be in the range of 473.15 to 523.15 K (low temperature FT synthesis or LTFT), or 573.15 to 623.15 K (high temperature FT synthesis or HTFT). In both cases, the process is highly exothermic, and therefore a heat exchange system is necessary to cool the reactor and maintain under control the process temperature: it is also an energy-recovery opportunity for waste heat [62].

At first, reagents, hydrogen and carbon monoxide, form monomer units, which are then polymerized to yield a wide spectrum of products (mainly paraffin), ranging from C-1 to C-40 hydrocarbons.

The FT synthesis consists in four main reactions, shown in equations (5) to (8), i.e.

- Paraffins formation:

$$nCO + (2n + 1)H_2 \rightarrow C_nH_{2n+2} + nH_2O \quad (5)$$

- Olefins formation:

$$nCO + 2nH_2 \rightarrow C_nH_{2n} + nH_2O \quad (6)$$

- Alcohols formation:

$$nCO + 2nH_2 \rightarrow C_nH_{2n+1}OH + (n-1)H_2O \quad (7)$$

- Carbonyls formation:

$$nCO + (2n-1)H_2 \rightarrow (CH_2)_nO + (n-1)H_2O \quad (8)$$

Catalysts play a crucial role in FT synthesis, as they must guarantee a good conversion yield of reactants, as well as selectivity towards products. Catalysts in FT are often supported on metal oxides, typically alumina or silica [53]. Suitable catalysts for FT synthesis are Group VIII elements, in particular Cobalt (Co), Iron (Fe), Nickel (Ni), and Ruthenium (Ru), able to chemisorb CO dissociatively (into C and O) and H_2, and have a noticeable activity. However, other elements, such as Rhodium (Rh), Iridium (Ir), Palladium (Pd), and Platinum (Pt), are also used in FT synthesis. Though the selectivity of these elements is even higher compared to Ru, Ni, Co, and Fe, they are not considered in industrial applications because of their costs [52], and only Co and Fe are used in commercial processes. Co-based catalysts are mainly used in LTFT: these are characterized by high activity, significantly stability and tendency to produce relatively higher molar-weight hydrocarbons. On the other hand, Iron-based catalysts are cheaper than Co-based ones, can be used in both HTFT and LTFT configurations, and promote relatively higher fraction olefins. Additionally, Iron catalysts also promote the WGS secondary reaction.

There are four main different types of Fischer-Tropsch reactors: (a) fixed-bed multi-tubular reactor, (b) fluidized-bed reactor, (c) slurry-bed reactor, and (d) microchannel reactor. The type of reactor influences the operational parameters of the synthesis process, the product selectivity, the product distribution with chain growth probability, the catalyst activity, and the conversion of carbon monoxide [53]. Details about FT reactors design can be found in [63].

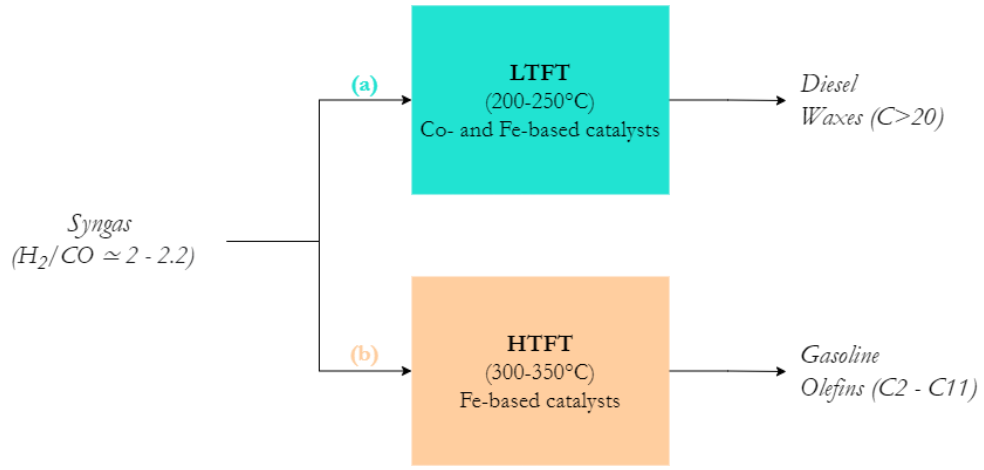

Figure 7. Fischer-Tropsch synthesis – configurations and products

2.2.5 Methanol synthesis

Methanol (CH_3OH) is a valuable chemical product with a variety of uses, either as a clean fuel, mixed with other conventional fuels, or as a bulk chemical building block for the synthesis of other chemicals such as acetic acid, formaldehyde, methyl methacrylate and methyl tertiary-butyl ether (MTBE) and many others [64]. CH_3OH is extremely stable and liquid at the room temperature, and this minimizes problems with storage and transportation, even if accidental release in soil and dwells can be a serious health risk ([65], [66], [67], [68]).

Currently, the most used industrial route for methanol production is based on using syngas produced via reforming of natural gas, even if also biomethane can obviously be used. Nevertheless, there are also attractive routes that involve a single step, such as oxidative coupling of methane, e.g. methane partial oxidation to methanol (i.e., DMTM) [69], which will be discussed in a separated section of this work.

Methanol is obtained through the hydrogenation of carbon oxides over a suitable (copper oxide, zinc oxide, or chromium oxide based) catalyst [70][71]. The conversion is exothermic and very selective, and the synthesis is followed by a distillation column to separate methanol from water, which is the by-product of the conversion [72].

The main reactions of methanol synthesis are [73]:

$$CO + 2H_2 \rightarrow CH_3OH \quad (9)$$

$$CO_2 + 3H_2 \rightarrow CH_3OH + H_2O \quad (10)$$

$$CO_2 + H_2 \leftrightarrow CO + H_2O \quad (11)$$

Equation (9) represents the CO hydrogenation, (10) the CO_2 hydrogenation, and (11) the reverse water gas shift (RWGS) reaction. It is noted that the required H_2/CO ratio of the syngas at the inlet is equal to 2.

The typical operating conditions are in the ranges of 50 to 100 bar and 493.15 to 553.15 K, depending on catalyst supplier.

There are several commercial types of methanol synthesis reactors, i.e. quench reactor, adiabatic rectors in series, or boiling water reactors (BWR) [74]. A detailed description of reactor types is available in [75].

DMTM route

As an alternative to methanol synthesis from syngas, the straight conversion of methane into methanol is also a possible and interesting route. This method allows to by-pass the very energy intensive step required to reform CH_4 into CO and H_2, and thus represents an economical-advantageous and environment-friendly option [76].

The technologies for the direct conversion of methane to methanol might be catalytic oxidation processes, photo-catalysis technologies, plasma technologies, supercritical water oxidation technologies, membrane technologies and other methods.

Da Silva et al. [69] and Zakaria et al. [77] performed a review of the different DMTM routes.

However, to date, this method is not yet applied at full industrial and commercial scale. The process is particularly difficult, since the target product CH_3OH is more prone to oxidation than CH_4, and thus the process needs to activate the C-H bonds on one hand, and avoid over-oxidation of CH_3OH on the other [78]. Moreover, the current technologies do not provide a relevant methanol yield [79].

2.2.6 Syngas fermentation

Syngas fermentation is an advancing technology that has undergone extensive research and industrial scaling in the past decade. This innovative process enables microbial production of essential chemicals and fuels from mixtures of H_2, CO, and/or CO_2. Acetogenic bacteria play a key role in converting syngas into valuable compounds such as acetic acid and ethanol. Unlike traditional chemical synthesis, syngas fermentation operates at ambient temperatures and pressures, thereby reducing operational costs. Additionally, the flexibility of biocatalysts allows for greater tolerance to impurities in the gas mixture, eliminating the need for complex gas conditioning. The microbial conversion pathway, primarily via the reductive acetyl-CoA or Wood-Ljungdahl pathway, facilitates the transformation of CO, H_2, and CO_2 into acids and alcohols. Several globally recognized companies, including LanzaTech, INEOS Bio, and Coskata Inc., have already demonstrated the

feasibility of syngas fermentation through various projects. Notably, LanzaTech's innovative approach involves fermenting waste gases from industrial processes, such as steel mill flue gas, into ethanol, offering a sustainable and cost-effective solution for chemical production while mitigating carbon emissions [80]. Further details can be found in [81]

2.2.7 Alcohol-to-Jet (ATJ) conversion

Alcohol-to-Jet (ATJ) conversion is a cutting-edge process that transforms various alcohols like ethanol or butanol into aviation fuel, presenting a promising alternative to conventional fossil fuels. This innovative technology aims to reduce greenhouse gas emissions and lessen dependence on petroleum-based products in the aviation sector. Typically, ATJ involves catalytic reactions converting alcohols into hydrocarbons suitable for jet engines. By utilizing renewable feedstocks such as biomass or agricultural residues, ATJ holds significant potential for sustainable aviation, aligning with efforts to combat climate change and bolster energy security.

In most instances, ATJ conversion routes leverage established technologies in novel configurations, typically involving dehydration, oligomerization, and hydrogenation steps. The route is shown in **Figure 8**.

Dehydration chemically removes oxygen, converting C-1 to C-4 alcohols into C-2 to C-5 alkenes through catalytic processes like zeolite and metal oxides.

Oligomerization combines short-chain molecules into long-chain ones, converting C-2 to C-4 alkenes into alkenes with carbon numbers between 8 and 16. The oligomerization of alkenes and short chain olefins to form higher is a well-established reaction in the petrochemical industry with a variety of forms dating back to the 1930s and using a variety of homogeneous or heterogeneous catalysts in single or multiple reactor configurations.

Hydrogenation, using metal catalysts like nickel, platinum, or palladium dispersed on activated carbon, converts alkenes into alkanes by adding hydrogen, eliminating instability in the jet fuel [80]. For this step, a supply of hydrogen is required.

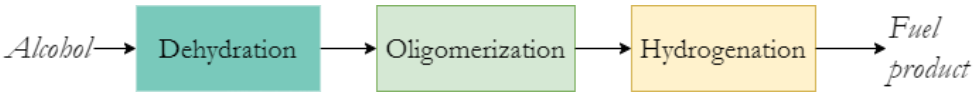

Figure 8. ATJ conversion route

2.3 Reference plants and investment costs

In this section, a brief overview of reference industrial GTL plants and their associated investment costs is presented, as an outcome of the literature review conducted within this research. The focus here is specifically on the GTL plant segment of the value chain. The upstream aspects, including biogas plants, costs related to upgrading for grid injection, and grid connection costs, are not included in this evaluation. Although these areas are indeed significant and merit further study, the scope is confined to the GTL plant.

2.3.1 GTL-FT route: CAPEX

The leading technology in the market is the FT technology by Shell and Sasol [82], with large-scale GTL plants. Traditional GTL facilities normally utilize coal or natural gas to attain economies of scale, producing over 10,000 bpd of liquid products [26]. The Oryx GTL plant and the Pearl GTL plant in Qatar and Bintulu, Malaysia are two examples.

Table 4**Table 4** reports the main commercial-scale GTL-FT plants in operation around the world.

Plant	Company	Capacity [bpd]	CAPEX [USD Billion]	Location	Year
Mossel Bay GTL	PetroSA	22,500	4	South Africa	1992
Bintulu GTL	Shell	12,000	0.85	Malaysia	1993
Oryx GTL	Qatar Petroleum and Sasol	34,000	6	Qatar	2007
Pearl GTL	Shell and Qatar Petroleum	140,000	19	Qatar	2011
Escravos GTL	Chevron, Sasol and Nigerian National Petroleum Corp	33,000	10	Nigeria	2014
Turkmenistan	Turkmenistan's state-owned	15,500	2.5	Turkmenistan	2018
Uzbekistan	Sasol, Petronas, and Uzbekneftegaz	38,000	3.7	Uzbekistan	2020

Table 4. Main GTL FT-based plants worldwide [26]

As regards investment costs, information derived from **Table 4** Table 4to show the capacity in barrels per day (bpd) and the pertaining Capital Expenditures (CAPEX).

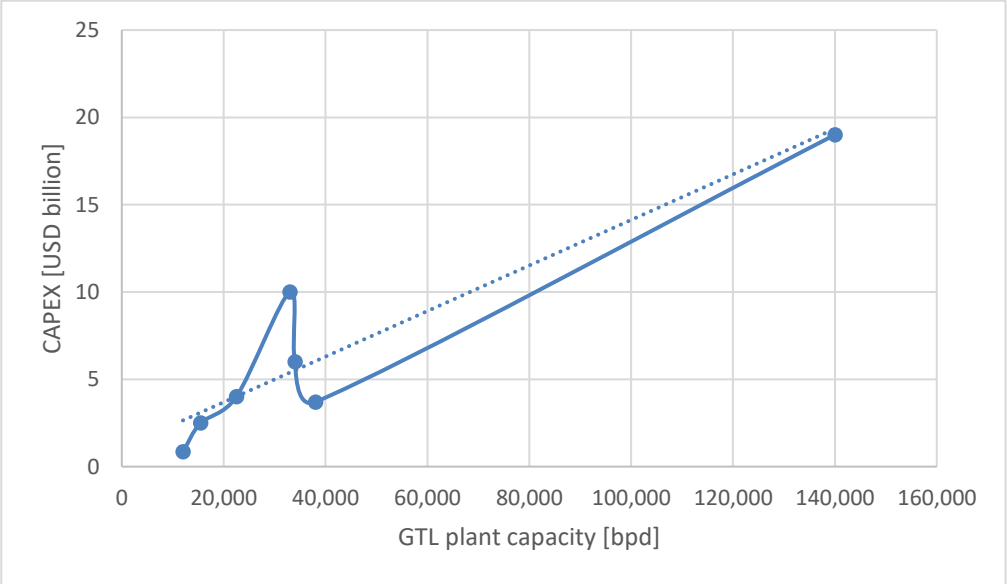

Figure 9. Existing GTL FT-based plants capacity and related CAPEX

As **Figure 9** suggests, the trendline is about 94,800 USD/bpd. Nevertheless, the figure also shows how the capacity GTL FT-based plants and related CAPEX do not have a linear relationship.

Moreover, other data available in literature show some volatility as concerns the Capital Expenditure of GTL plants. For instance, Wang and Economides [25] stated that the capital expenditure for a GTL plant in the 1950s was about 120,000 USD/bpd and decreased in the first decade of the 2,000s to less than 50,000 USD/bpd, with a target to reach below 20,000 USD/bpd. Arno De Klerk [83] indicates a CAPEX of 62,000 UDS/bpd (price in 2010), with a cost breakdown shown in **Figure 10**.

Also, in the presented case study, it was assumed the existence of an operational refinery. In this scenario, certain costs would be inherently absorbed by the presence of pre-existing infrastructure.

Considering the high volatility of the data, we can assume CAPEX at 80,000 USD/bpd of products, which corresponds to about 791,970 USD per metric tonne per day of product.

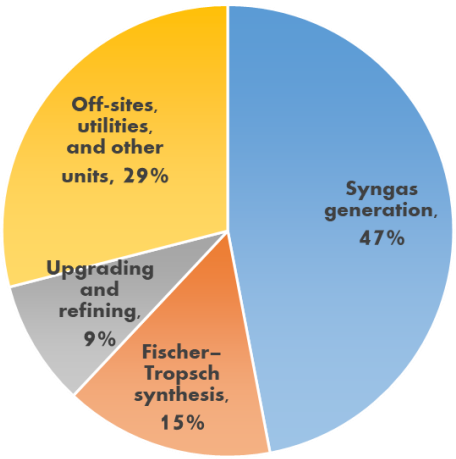

Figure 10. Breakdown of CAPEX for a GTL plant [83]

2.3.2 GTL-MeOH route: CAPEX

As for the GTL-MeOH plant, similarly to the GTL route from natural gas, methanol production from syngas is a commercially demonstrated technology, and the average size of the current top-tier methanol facilities worldwide is in the range of 2,000 to 2,500 tonne/d. Larger-scale applications (5000 tonne/d) are also possible [84]. Nowadays, the largest producer and supplier of methanol is Methanex Corporation. As examples of MeOH plants, we can report the Titan plant (850,000 tonnes per year) and the Atlas plant (1.7 million tonnes per year, world's largest methanol plant), both in Trinidad.

Among the most recent news, the construction of Methanex Geismar 3 is approaching completion, with a budget of 1.23-1.3 billion USD, aimed at an annual methanol production capacity of 1.8 million tonnes [85]. Geismar 3 leverages a significant portion of the existing infrastructure originally developed for Geismar 1 & 2.

In addition, in the United States, the Koch Methanol St. James [86] plant was previously commissioned, initially estimated at USD 1.85 billion for constructing a greenfield plant with a capacity of 1.7 million metric tonnes.

Table 5 presents the primary operational commercial-scale GTL-MeOH plants in the United States [27].

Company	Location	Year	Capacity [tonnes/day]	CAPEX [USD]
Methanex	Alberta, Canada	2011	1,392	60,000,000
OCI	Texas, US	2012	2,227	60,000,000
LyondellBasell	Texas, US	2013	2,172	150,000,000
Celanese/Mitsui	Texas, US	2015	3,619	900,000,000
Geismar #3	Louisiana, US	2023	4,932	1,300,000,000

Table 5. Recent US MeOH plants (2011-2015) [27]

Concerning investment costs, data in **Table 5** are graphically represented in **Figure 11**, showing the capacity in tonnes per day (tonne/day) alongside the corresponding CAPEX. As highlighted in the figure, the capacity of the reviewed GTL-MeOH plants and their associated CAPEX do not have a linear relationship. However, referencing the information in **Table 5**, we can derive an average figure and estimate a specific CAPEX cost of 130,276 USD/(tonne/day).

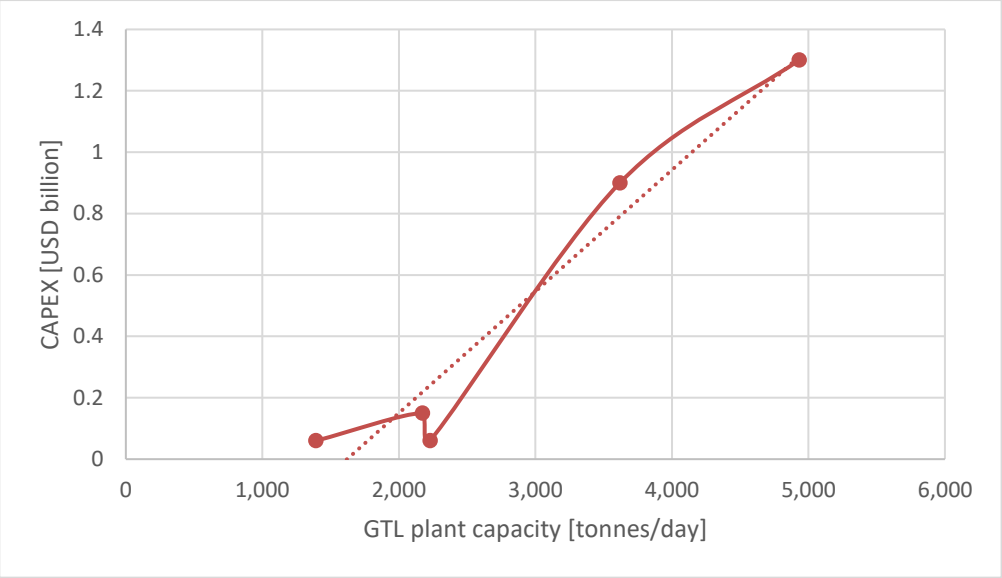

Figure 11. Existing GTL MeOH-based plants capacity and related CAPEX

Methanol, in addition to its role as a biofuel, is a bulk chemical, serving as key building block to various chemicals and materials. It finds demand across diverse sectors, including formaldehyde, acetic acid, olefins, polymers, fuel blending, and solvents. Examples of methanol projects for chemical applications are provided in **Table 6**.

Table 6. MeOH projects around the world, 2022 (Chemical Market Analytics by OPIS, a Dow Jones Company)

Methanol Projects [ktonne]							
COMPANY	**LOCATION**	**2021**	**2022**	**2023**	**2024**	**2025**	**2026**
Methanex	Geismar, LA	-	-	-	1,800	1,800	1,800
Big Lake Fuels	Lake Charles, LA	-	-	-	-	-	1,400
US Methanol	Institute, WV	-	17	200	200	200	200
Koch Methanol St. James, LLC	St James Parish, LA	144	1,700	1,700	1,700	1,700	1,700
Celanese Mitsui JV	Clear Lake, TX	1,300	1,500	1,530	1,620	1,620	1,620
Caribbean Gas Chemical	La Brea, Trinidad	1,000	1,000	1,000	1,000	1,000	1,000
Alpont LLC	Ohio, US	-	-	91	91	91	91
JSC Shchekinoazot	Shchekino, Russia	-	500	500	500	500	500
Dena Petrochemical	Iran	-	-	-	-	1,650	1,650
Sabalan	Iran	140	1,650	1,650	1,650	1,650	1,650
Assam PC	Namrup, India	-	14	165	165	165	165
Jiutai Energy	Inner Mongolia, China	-	-	1,000	1,000	1,000	1,000
Guangxi Huayi Energy Chemical	Guangxi, China	1,008	2,000	2,000	2,000	2,000	2,000
Guoneng Yulin Chemical	Shaanxi, China	1,504	1,800	1,800	1,800	1,800	1,800
Zhongmei Mengda	Inner Mongolia, China	500	1,000	1,000	1,000	1,000	1,000
Sarawak Petchem	Sarawak, Malaysia	-	-	-	568	1,700	1,700
Others		561	1,750	2,768	2,858	2,858	2,858
Closures	Various	-	1,000	2,000	2,400	2,400	2,400
	NET TOTAL INCREASE	**-**	**5,774**	**1,450**	**2,171**	**2,782**	**1,400**

Currently, the global supply of renewable methanol is estimated at approximately 300,000 tonnes, while global demand stands at around 86 million tonnes. Most of this renewable methanol supply is derived from bio-methanol. In the United States, companies like OCI, Methanex, Proman, Mitsui/Celanese have obtained ISCC certification to manufacture bio-methanol using the mass balance method. Within existing natural gas-based methanol production facilities, these companies can procure biogas or biomethane injected into the pipeline system. Maersk is fuelling its inaugural voyage of the first carbon-neutral container ship with bio-methanol supplied by OCI Fuels [87] [88]. Methanex has, as well, embarked on its inaugural carbon-neutral ocean voyage, utilizing a mixture of bio-methanol and traditional fossil natural gas-derived methanol [89].

2.3.3 GTL-F_ATJ route: CAPEX

A number of companies have been developing and started to commercialize the Alcohol-To-Jet (ATJ) process. Leading these efforts are LanzaTech and Gevo, specialized in ethanol and isobutanol, respectively. LanzaTech demonstrated successful production of sustainable aviation jet fuel (SAF) from gas fermented ethanol in partnership with Virgin Atlantic and Pacific Northwest National Laboratory [90]. In 2016, Gevo's ATJ pathway received approval for a 30% blend mix with jet fuel, whereas Lanzatech's ATJ pathway obtained approval for a 50% blend mix with jet fuel in 2018 [91].

As for the CAPEX of this specific route, according to the reviewed literature, the syngas fermentation section would cost about 235,881 USD/(tonne/day EtOH) [92], while the ATJ section would be around 229,906 USD/(tonne/day) [90]. Therefore, considering all the products generated along the route, the capital cost per unit of product is estimated at 669,740 USD per tonne per day.

2.3.4 GTL plant operational costs (OPEX)

Operational Expenditure (OPEX) is an important parameter in assessing the economic viability of a Gas-to-Liquids (GTL) project. Among its components, catalysts and chemicals primarily utilized for syngas generation typically represent approximately one-third of the OPEX. Additionally, expenses associated with personnel, general administration, and mechanical maintenance of the plant constitute the remaining portions of the OPEX (as outlined by Peter M. Maitlis and Arno de Klerk [83]).

However, estimating the precise annual cost of OPEX can be challenging. Following the rule of thumb within the oil and gas industry, OPEX typically ranges from 10 to 15 percent of Capital Expenditure (CAPEX) [82]. However, given the

complexity of GTL plants, accurately predicting OPEX becomes even more challenging. Some studies[1] have suggested that OPEX for GTL facilities may deviate from this norm, potentially amounting to as low as 5% of CAPEX.

Nevertheless, this thesis has primarily focused, albeit to a limited extent, on CAPEX. The examination of OPEX nonetheless warrants a more in-depth study, which could be the subject of future research endeavours to ensure a comprehensive evaluation of the project's economic feasibility and long-term sustainability.

[1] For example, Al-Saadoon, Faleh. (2007). Economics of GTL Plants. SPE Projects Facilities & Construction. 2. 1-5. 10.2118/94380-PA.

Chapter 3 Value chain process modelling

3.1 Literature review

As introduced in Chapter 1, the core of this thesis revolves around constructing a model to simulate a sustainable supply chain for the production of liquid biofuels for aviation and maritime purposes. The aim is to extract information on mass balances, energy consumption, and draw conclusions, which will be discussed in Chapter 4. As mentioned, three alternative pathways have been identified (i.e. GTL-FT, GTL-MeOH, and GTL-F_ATJ), involving decentralized biogas production using the BiogasDoneRight model, upgrading to biomethane, injection into the natural gas grid, methane extraction from the grid, and conversion in gas-to-liquid plants into liquid biofuels for aviation and maritime use.

This chapter provides a critical review of available literature to gather insights into the modelling of various steps within the selected conversion processes. Thus, it scrutinizes and provides commentary on the modelling approaches found in papers, covering aspects such as assumptions, schematization, and process conditions.

For the modelling, a commercial simulation software, i.e. Aspen Plus, has been chosen. Consequently, the modelling studies under consideration are those employing this software. This applies to the GTL-FT and GTL-MeOH routes, for which the level of analysis is notably comprehensive. However, for the GTL-F_ATJ pathway, the analysis is not as extensive as the others, as it has recently attained full industrial scale compared to the more established pathways.

Many of the contents of this chapter have been previously published in [1].

3.1.1 Materials and methods

A methodical examination of peer-reviewed journal articles, book chapters, theses, and conference papers was conducted to compile a comprehensive literature review. Databases, including Springer and Elsevier, along with various journals such as Energies and Chemical Engineering Transactions, were explored. The search spanned the last two decades and was limited to publications in English, Italian, and German.

Concerning modelling papers, the initial step involved selecting simulation software capable of representing technologies within the identified value chain. Several process modelling software packages were considered, with Aspen Plus ultimately chosen for its extensive use in both industrial and research applications.

The focus on modelling studies was narrowed down to those specifically utilizing Aspen Plus.

The screening process involved examining titles, abstracts, and reference lists, applying inclusion criteria that emphasized similarity to the study's technologies, clear modelling descriptions, and the ability to extract pertinent information from complex processes. Preference was given to papers featuring model validation with experimental data.

The collected modelling studies underwent a thorough analysis, exploring aspects such as process configuration, modelling assumptions, process yield, and energy consumption. To ensure effective comparisons, data were harmonized, ensuring uniform units across the gathered information.

3.1.2 Results of the review

This section provides a detailed overview of the selected modelling studies, focusing on key components of the modelling process, exploring plant configurations and their associated resource consumption.

Modelling anaerobic digestion

The process of anaerobic digestion is highly intricate, encompassing various intermediate reaction mechanisms, including bacterial metabolic reactions, parameters, interactions with inhibitors, and more.

In the literature, several models have been proposed to describe anaerobic digestion [93]. These models can be single-step models [94], involving a single bacterial population with a limited description of inhibition effects, or models of intermediate complexity [95], considering a higher number strains of bacteria with a more accurate description of inhibition factors, or, finally, complex models [96] [97] [98] [99], entailing a high number of processes, inhibition effects, and specific bacterial populations.

Among the complex AD models, Anaerobic Digestion Model No. 1 (ADM1) [96] is considered as the most comprehensive one and is widely applied for AD description [100]. ADM1, developed by the International Water Association (IWA) task group, assumes that the reaction system consists of biochemical reactions (involving enzymes) and physico-chemical reactions (involving acid-base reactions and the gas-liquid transfer). The substrate fed to the digestor is assumed to be composed of carbohydrates, proteins, and fats [101]. Another important and complete complex model is the one developed by Angelidaki et al. [99], in which the substrate is assumed to be composed of basic organic components (i.e. carbohydrates, lipids, and proteins), intermediates (i.e. volatile fatty acids and long-chain fatty acids), and inorganic components (i.e., ammonia, phosphate, cations, and anions). The model includes 2 enzymatic hydrolytic steps, 8 bacterial steps and involves 19 chemical compounds [99].

Implementing modelling schemes of AD in Aspen Plus is quite challenging, as it involves microorganisms, whose microbial activity is difficult to describe in software language. In literature, several studies simulating the anaerobic digestion in Aspen Plus have however been found and are analysed below.

Al-Rubaye et al. [100] developed a two-stages simulation model: one first step for the hydrolysis phase, and a second one for the other three phases, i.e. acidogenesis, acetogenesis and methanogenesis. The *Property Method* (a collection of methods and models that the software uses to compute thermodynamic and transport properties [102]) chosen for the simulation is the Non-Random Two-Liquid (NRTL). In line with ADM1, the substrate feed rate is assumed to be made of carbohydrates, proteins, and fats, and therefore the introduction of material components is treated accordingly. The feed stream is mixed with H_2 and H_2O through a mixer and a heat exchanger is employed to model heating of this stream, necessary to maintain the required temperature in the ranges favourable for AD. The hydrolysis step is simulated using a stoichiometric reactor (RSTOIC), a type of reactor block in Aspen Plus in which the reaction kinetics are not considered, but stoichiometry and conversion of a reactant must be specified. 13 chemical reactions are considered for this step, and the reaction rates have been calculated by Aspen Plus calculator blocks, using a FORTRAN code. The subsequent AD steps have been simulated in a continuous stirred tank reactor (in Aspen Plus named as "RCSTR"), which requires the reaction kinetics to be known; thus, specifications from ADM1 and comprehensive models have been used, involving more than 33 kinetic reactions. The reaction rates have been calculated through calculator blocks, using a FORTRAN code. The RCSTR reactor releases two streams at outlet: one is the gas stream, which is the biogas and small traces of other gases, and the liquid stream. The gas stream goes through a splitter and then a flash separator, which separates the water from the biogas. Subsequently, the biogas stream passes through a gas filter, which separates the hydrogen component from the produced biogas. On the other hand, the liquid stream goes through a splitter to separate a part of it as recycle and is connected to the feed stream. The model was validated against experimental data in terms of % CH_4 in the produced biogas. Three different feed cases have been tested, i.e. (i) cattle manure, (ii) cow manure, and (iii) wastewater generated from industrial and agricultural activities. Results match the literature data; in detail, the deviation from simulation results and experimental data are: 5.4% for the case of cattle manure, 8.54% for the case of cow manure, and 15.83% for the case of wastewater generated from industrial and agricultural activities. In the study, a sensitivity analysis has also been carried out to study the effect on CH_4 yield in case of introduction of hydrogen in the process. The investigation revealed that, for H_2 feeding rates below a maximum value, there is increase of methane gas composition in the produced biogas.

The model developed by Rajendran et al. [103] shows similarities with Al-Rubaye's one. Here as well hydrolysis is separated from the other AD phases, and has a separate reaction set (made of 13 reactions) including carbohydrates, proteins,

and fats. Carbohydrates were modelled as cellulose, starch, and hemicelluloses, proteins as soluble proteins and insoluble proteins, while fats as tripalmate, triolein, palmito-olein, and palmitolinolein. Acidogenesis, acetogenesis, and methanogenesis are modelled using a different reaction set (made of 33 reactions) to calculate the kinetics of the reactions, whose constants were obtained following models such as ADM1 and comprehensive models. A FORTRAN code has been used to compute the reaction rates. Also in this case, the simulation model uses NRTL as *Property Method*, and the reactors chosen for the hydrolysis and the other three phases are respectively a stoichiometric reactor (RSTOIC), with specified reaction extents, and a continuously stirred tank reactor (RCSTR), with specified kinetic constants. The model was validated against experimental and industrial data, using the biogas production rate as validation parameter, for different substrates at different process conditions (7 case studies). The deviations from simulation results and experimental data span from 0.3 to 12.4% (absolute values).

Nguyen et al. [104] developed a simple one-step AD model to estimate the energy potential from the anaerobic digestion of food waste in municipal solid waste stream of urban areas in Vietnam. A stoichiometric reactor (RSTOIC) has been chosen to simulate the digester, in which the calculations are based on the Buswell equation, describing the overall process of anaerobic degradation. The global *Property Method* selected for the simulation is NRTL. The resulting biogas stream is separated in a flash separator, which separates the gas components and the digestate. The gaseous phase (raw biogas) is then treated to reduce the presence of H_2S and then introduced into a CHP unit, or into a boiler unit, or to an upgrading unit for biofuel production, depending on the model scenario chosen.

Scamardella et al. [105] simulated a pressurized anaerobic digestion process (PAD) using a RCSTR reactor operating at a pressure range of 1.5 to 5 bar. Reaction kinetics were taken from the ADM1 and comprehensive models. ELECNRTL (Electrolyte Non-Random Two Liquid) *Property Method* is chosen here, as it allows to simulate dissociation equilibria that affect the CO_2 solubility in the liquid phase.

Peris Serrano [101] implemented the Angelidaki and the ADM1 models. The hydrolytic step is not considered in this simulation, and thus only three phases are modelled. The process consists of two-stages, i.e. two digesters, in which all the AD reactions occur. The reactor type selected is the RCSTR, for which total mixed flow and constant volumes are assumed, with residence time chosen as user-defined parameter. The kinetic reactions in the model follow the power law and kinetic constants are computed in calculation blocks written in FORTRAN. The *Property Method* chosen for the simulation is NRTL.

Llanes et al. [106] developed an Aspen Plus model for the AD of vinasses, which integrates ADM1, Flow pattern and Biofilms characteristics with the inclusion of sulphate reduction reactions. Vinasse is usually treated in UASB (Upflow Anaerobic Sludge Blanket) reactor types instead of completely mixed flow pattern reactors, so the authors employed two stoichiometric reactors (one for the

hydrolysis stage and one for the methanogenic step) and two RCSTR reactors for the other phases. Kinetics are calculated in FORTRAN programmed blocks. Here as well, cellulose, hemicellulose and dextrose were added as carbohydrates, proteins as soluble and insoluble, while lipids comprised of tripalmate, triolein, and palmito-olein. The *Property Method* adopted is the NRTL. The model has been validated against experimental data for three different case studies. A mean relative error lower than ±15% has been observed, with no significant differences between simulation results and experimental data in terms of biogas composition and methane yield.

Table 7 summarizes the main Aspen Plus models for AD reviewed in this work. The analysis has shown that the AD, though very complex to be fully described, can be simulated in Aspen Plus. Overall, the number of studies addressing AD modelling is not very large: only six Aspen Plus simulation models have been found.

Table 7. Reviewed Aspen Plus models for AD

Authors	Publication year	Property method	Reactor configuration in Aspen Plus	Reference model	Remarks
Al-Rubaye et al. [100]	2017	NRTL	RSTOIC (13 reactions) + RCSTR (33 reactions). Calculation blocks programmed in FORTRAN for kinetics computations	ADM1 and comprehensive models	Two-stages model (hydrolysis in RSTOIC and the other phases in RCSTR)
Llanes et al. [106]	2019	NRTL	two RSTOIC, two RCSTR, with calculation blocks programmed in FORTRAN for kinetics computations	The model integrates ADM1 – Flow pattern – Biofilms characteristics with the inclusion of sulphate reduction reactions	Two-stages model (hydrolysis in RSTOIC and the other phases in RCSTR)
Nguyen et al. [104]	2014	NRTL	RSTOIC	Buswell equation	One-stage model
Rajendran et al. [103]	2014	NRTL	RSTOIC (13 reactions) + RCSTR (33 reactions), with calculation blocks programmed in FORTRAN for kinetics computations	ADM1 and comprehensive models	two-stages model (hydrolysis in RSTOIC and the other phases in RCSTR)
Scamardella et al. [105]	2019	ELECNRTL	RCSTR	ADM1 and comprehensive models	PAD model (pressurized anaerobic digestion)
Serrano Peris [101]	2011	NRTL	two RCSTR in series with calculation blocks programmed in FORTRAN for kinetics computations	Angelidaki + ADM1	The hydrolytic step is not taken in account

Modelling biogas upgrading

Several studies simulating biogas upgrading in Aspen Plus have been retrieved in literature.

Ashraf et al. [29] developed a model for the PWS process: absorption and stripping columns are modelled as two RADFRAC distillation blocks, which is a column type designed for general vapour-liquid multistage separation. The thermodynamic method used is electrolyte non-random two-liquid (ELECNRTL): absorption of biogas components in water is accounted by Henry coefficients, while dissolution of H_2S and based on a first stage in which biogas is compressed to 12 bar, cooled to 313.15 K and then sent at the bottom of the absorption column, which is also fed from the top with water. The column is operated at 12 bar. Upgraded biogas leaves the column from the top of the column, and impurity-rich sour water leaves from column bottom. Sour water is then sent to a flash separator (operated at 3 bar) to remove residual CH_4, and then fed to the stripping column for regeneration at 1 bar, which uses air as stripping medium. In the reported case study, biogas is fed at 2000 ppm of H_2S. For a better removal of H_2S, activated carbon impregnated with ZnO is considered, and the resulting cleaned biogas has a composition characterized by less than 10 ppb of H_2S and NH_3, 99%, and 79% recovery of CH_4 and CO_2.

Cozma et al. used an Aspen Plus model to simulate a high-pressure water scrubbing (HPWS) system applied to biogas upgrading in [107] and [108] studies. The simulation model is characterized by operational conditions based on data taken from literature (in particular, the work by Götz et al. [109]). The model is equilibrium-stage, and the thermodynamic method chosen for the analysis is a non-random-two-liquid model with ideal gas and Henry's Law (NRTL); the method has been chosen based on a preliminary study in which the authors compared the performance of different thermodynamic models available in the software to calculate the solubility of the main biogas components (CO_2, CH_4, H_2S, N_2, and O_2) in pure water. The simulation model assumes pressurization at 10 bar and cooling to 293.15 K of the biogas stream (60% vol CH_4, 38.9% vol CO_2, 300 ppm vol H_2S, 0.5% vol N_2, and 0.5% vol O_2), which is then sent to the bottom of the absorber, which is also fed with water from the top. The scrubber is a RADFRAC column, working at T=293.15 K, p=10 bar. The number of stages and the absorbent flow rate required to achieve equilibrium have been determined through a preliminary study. The bottom stream (CO_2-enriched water) is transferred to a flash column, where the pressure is reduced from 10 to 3 bar to minimize methane loss. The gas containing CO_2, CH_4, H_2S, N_2, O_2, and water, released from the flash column is mixed with the raw biogas and re-circulated to the inlet of the compressor. After leaving the flash column, the rich solution is sent to the stripper, also modelled as a RADFRAC column, where it meets a counter flow of air. Here CO_2 and H_2S are released from the water at atmospheric pressure and at a temperature of 293.15 K.

Subsequently, the water is recirculated back to the top of the scrubber. Based on these conditions, it was calculated that the gas leaving the absorber contains: 96.72% vol CH_4, 0.937% vol CO_2, 0.006 ppm vol H_2S, 1.1% vol N_2, and 0.976% vol O_2. The calculated energy demand for producing 309.36 Nm^3/h of upgraded biogas is 171.5 kWh.

The work done by Götz et al. [110], which also described and modelled in Aspen Plus the HPWS technology for biogas upgrading, represented a reference also for the studies by Cozma et al. [107] [108]. Thus, the process conditions and scheme are nearly the same for both simulation models. The model is based on equilibrium and uses ELECNRTL thermodynamic model. The calculations take into account the gas quality requirements for biogas injection according to the German law. Biogas feed has a composition of 53.7% vol CH_4, 45.2% vol CO_2, 101.8 ppmv H_2S, 0.93% vol N_2, and 0.19% vol O_2. The gas exiting the simulated process is composed by 96.8% vol CH_4, 0.47% vol CO_2, <<1 ppm vol H_2S, 2.1% vol N_2, 0.56% vol O_2, and 0.32% vol H_2O.

The PWS technology to convert biogas into biomethane has also been modelled in the thesis work by Menegon [111]. Similarly to Cozma et al. [107], the author carried out a preliminary study to select the most suitable *Property Method*, finally choosing the NRTL-RK model. The process conditions and scheme are very similar to those used by Cozma et al. [107]: biogas (45% vol CO_2, 55% vol CH_4) is compressed and cooled to 10 bar and 293.15 K and fed to an absorption column. The bottom stream is sent to a flash separator operating at 3 bar, from which gas is recirculated to the second compression stage, while liquid is sent to a stripper using air as stripping medium. Regenerated water is sent back to the absorber. The simulation is rate-based, and the absorption and the stripping column reach a CH_4 purity of 98.7% vol. The CH_4 recovery is 99.08%.

The biogas water scrubbing technology has been also simulated in Aspen Plus by Bortoluzzi et al. [112]. The simulation scheme is similar to those cited above. The *Property Method* chosen is the Predictive Soave Redlich Kwong equation of state (SRK). In the simulated process, biogas is compressed to the absorption pressure of 10 bar through a two-stages intercooled compression, and water is removed via condensation. Then, biogas enters a packed column, which also receives a stream of liquid water; here, biogas upgrading occurs, thus a stream containing biomethane and a stream containing water, CO_2, H_2S and small amounts of CH_4. This latter stream is flashed to 3 bar to recover methane; two streams exit the flash: one, containing vapour CO_2 and CH_4, is recycled to the second compression stage, while the second one, liquid, is sent to a stripper. An air stream entering the stripper desorbs CO_2 (and H_2S) from the feed, and the solvent is then re-generated and recirculated to the absorber. The biomethane stream produced in the absorber is then dried: the CH_4 recovery of the process is 99.6%. For the base case, the molar percentage of CH_4 in the product stream is 98.7% mol.

The same modelling approach has been adopted also Seman et al. [113]. Authors used the NRTL *Property Method*, adopting the same process conditions

used in the study by Cozma et al. [108], as well as the simulation flowsheet. The specifications related to the absorption column are slightly different between the two studies, as the number of stages and the pressure is slightly higher in the work of Seman et al. [113]. This leads to a percentage of CO_2 removal and biomethane purity a little higher (97.6% mol CH_4 in the absorber product gas stream) in this latter case.

Ashraf et al. [29] also simulated the chemical absorption with MEA as absorption solvent for syngas upgrading (CO_2 removal after desulphurization). The processing scheme is similar to water scrubbing, i.e. an absorption and a stripping column, to remove CO_2 and to regenerate the solvent respectively, modelled as RADFRAC distillation columns.

Chemical absorption for biogas upgrading was simulated also by Lingelem [114], who used AMP solvent (2-amino-2-methyl-1-propanol), more specifically 30% wt AMP in aqueous solution. For the base case process, the author used the ELECNRTL thermodynamic model and RADFRAC columns (rate-based absorption, equilibrium-based desorption). The purified biogas stream is characterized by a CH_4 molar concentration of 97% mol. Six modifications of the base case have been also simulated.

Gamba et al. [115] simulated both water scrubbing and chemical absorption processes for biogas upgrading by means of a rate-based approach, according to modelling details from the by Pellegrini et al. [116]. The thermodynamic model used is Electrolyte-NRTL. In the PWS simulation, biogas is treated in a one packed column at 20 bar with pure water at 298.15 K. There is no water regeneration step in the process. The inlet gas composition is 60% vol CH_4 and 40% vol CO_2. Other components have been neglected. Concerning the chemical absorption simulation, a 30% vol and 15% vol MEA aqueous solutions have been considered. The distillation column has the same characteristics as in the case of PWS, with the only differences in the packing material (metal instead of plastic) and the absorption pressure (atmospheric pressure). Both PWS and chemical absorption have been simulated find the absorbent flowrate needed for obtaining a 98% vol biomethane concentration on a dry basis.

Gamba et al. [117] simulated water scrubbing, MEA (monoethanolamine) scrubbing, and MDEA scrubbing when applied to obtain biomethane from municipal sewage sludge AD. Also in this case, the modelling approach is rate-based, and biogas components considered are only CH_4, CO_2 and water. For what concerns PWS, there is no water regeneration step, and the biogas is first sent to a three-stage intercooled compression, then to the absorption column. Regarding the MEA chemical scrubbing, the model accounts for an absorption and a regeneration step in backed columns, operating at atmospheric pressure with a solution composed of 15% wt MEA. The MDEA chemical scrubbing case has the same process scheme of the MEA case. Here, absorption is carried out at 2.7 bar, using a 50% wt MDEA solution in water, and the regeneration at atmospheric pressure. All three simulated upgrading processes reach a biomethane purity higher than is 98%

vol on a dry basis. For what matters the PWS case, the upgraded biogas has a molar percentage of CH_4 of 98.86% mol on a dry basis, with a methane recovery to fed biogas of 95.8%. Regarding the MEA case, the upgraded biogas has a molar percentage of CH_4 of 98.71% mol on a dry basis, with a methane recovery to biogas of 99.9%. About the MDEA case, the upgraded biogas has a molar percentage of CH_4 of 98.73% mol on a dry basis, with a methane recovery to fed biogas of 99.98%.

The biogas upgrading technologies of PWS and chemical absorption with alkanolamine solutions have also been simulated in Aspen Plus by Pellegrini et al. [118]. In this study, three different biogas compositions have been tested, representing landfill gas, biogas from wastewater treatments and gas from co-fermentation. The gases considered in these feed streams are CH_4, CO_2, N_2 and O_2. The layout of the water scrubbing process takes as a reference the one developed by Bortoluzzi et al. [119]. The biogas inlet stream is first compressed to 8 bar and cooled, then purified in a packed absorption column also fed with water. The bottom stream is then sent to a flash chamber and afterwards to a stripping column using air. Compression is here carried out in more steps. In each step separation of water from methane takes place too, using flash separators. The chemical scrubbing has been simulated referring to the process scheme of the study carried out by Gamba et al. [117]. The raw biogas is fed to the absorption column (2.7 bar), after being subjected to a single-stage compression and cooling down to 308.15 K. Both the absorption and stripping columns are packed columns (packing: metal Pall rings). The column specifications have been adjusted from the ones used in a previous work [115]. In all the case studies, the total flow rate of feed biogas is such that the volumetric flow rate of biomethane leaving the plant is 500 Sm^3/h, to have a common basis for an economic feasibility comparison.

Similarly, Worawimut et al. [120] used Aspen Plus to simulate and compare the processes of water scrubbing and chemical scrubbing with diethanolamine (DEA) solution with regeneration and recirculation. The studies by Cozma et al. [108] (PWS) and Niu et al. [121] (chemical absorption) have been taken as references to set process conditions and for results validation. The NRTL property method has been selected and RADFRAC distillation columns without condenser and reboiler have been used to model the absorber and the desorber, both set as equilibrium based. Biogas from swine farm wastes was used in this work, with a composition of 68% vol CH_4, 24% vol CO_2, 3000 ppm vol H_2S, 2% vol N_2, 0.1% vol O_2 and 5.6% H_2O. The biogas flow rate of the plant is 1000 kmol/hr. Both water scrubbing and chemical scrubbing were simulated to find the absorbent flow rate needed to obtain at least 96% v/v biomethane purity. Total water flow rate of the plant is 16,000 kmol/hr, which is the same amount of the total DEA solution flow rate of the plant. The product gas of the PWS process is characterized by a composition of 96.005% vol CH_4, 0.32% vol CO_2, <<0.001% vol H_2S, 3.098% vol N_2, 0.154% vol O_2, 0.424% vol H_2O. The methane recovery is 89.96%, while the energy consumption of the process is 11309 kW. The product stream of the

chemical absorption with DEA has a composition of: 96.026% vol CH_4, 0.310% vol CO_2, <<0.001% vol H_2S, 3.114% vol N_2, 0.155% vol O_2, 0.395% vol H_2O. The process has a methane recovery equal to 89.47%, with an energy consumption of 11331 kW.

Gangadharan et al. [42] also simulated the technology of chemical scrubbing with DEA in Aspen Plus for acid gas removal from natural gas. The simulation is rate-based, the thermodynamic property method is ELECNTRL, and also here the main blocks of the flowsheet are the absorber and stripper (RADFRAC distillation columns), but no solvent recirculation is included. The cleaned gas then enters 20-stages distillation column, operating at 44.6 bar, where methane gets separated from C-2 and C-3 components. A 99.5% mole recovery of methane is obtained from the process.

Membrane separation technique has been simulated by Scamardella et al. [105]. The authors adopted a user-defined model (user 2 block), interfacing the block with an Excel file. The *Property Method* selected is ELECNRTL. The model refers to Fick's law with diffusive model assumptions. In the model, the output of the membrane are two streams, i.e. a CH_4-rich gaseous stream, a CO_2-rich gaseous stream and the off-gas of the process. The resulting biomethane can reach high purity percentages (>95% vol) for operating pressures higher than 3 bar.

As Aspen Plus is a steady state calculator, no dynamic options are available in the software. Therefore, since PSA is a dynamic process, examples of PSA process simulations have been found mainly on Aspen Adsorption, e.g. Menegon et al. [111], Abdeljaoued et al. [122]. Anyway, some studies simulating the PSA process in Aspen Plus have been found and are reported below.

Gamero et al. [65] simulated the PSA process to clean the outlet gas of gasification to obtain high quality syngas and simultaneously capture the greenhouse gases. The system consists of four units, composed by ideal column separators operating at pressure and temperature conditions (30.6 bar and 308.15 K), to separate H_2 (first PSA unit), CO (second PSA unit), CO_2 (third PSA unit), and CH_4 (fourth PSA unit). The components obtained are then mixed, to obtain the H_2/CO ratio required for the downstream utilization. Multistage compressors and valves are also used in the process. The Peng-Robinson with Boston Mathias function method was selected for the simulation. As a result, about 80% of the CO_2 and 95% of CH_4 fed in the PSA system were sequestrated.

Similarly, Ortiz et al. [123] simulated the PSA process to clean syngas obtained by supercritical water reforming of glycerol. The PSA system is composed by three units: in the first unit, highly pure H_2 is separated as a non-adsorbed stream; in the second one, CO is separated as the adsorbed component; in the third one, separation of CO_2 and CH_4 occurs. The obtained gas streams are then mixed to obtain the H_2/CO ratio required for downstream utilization. Distillation columns for purification and valves for depressurization are involved in the process. NRTL property method has been selected. The system reaches 95% H_2 recovery, 98% CO recovery, 90% CO_2 as well as CH_4 recovery.

Table 8 summarizes the Aspen Plus simulation models reviewed in this work for biogas upgrading. The analysis revealed that upgrading processes have been largely simulated in literature: more than 15 studies have been found, most of which addressing the processes of physical and chemical absorption.

Table 8. Reviewed Aspen Plus models for upgrading processes

Authors	Publication year	Technology	Property method	Main simulation blocks	Process Yield	Remarks
Ashraf et al. [29]	2015	PWS	ELECNRTL	RADFRAC distillation columns for absorption and stripping	CH_4 recovery of about 99%	biogas upgrading
		Chemical absorption with MEA	ELECNRTL	RADFRAC distillation columns for absorption and stripping	not specified	syngas upgrading
Bortoluzzi et al. [112]	2014	PWS	SRK	Distillation columns for absorption and stripping	98.97% mol, with a CH_4 recovery of 99.6%	natural gas cleaning
Cozma et al. [107] [108]	2013, 2015	PWS	NRTL	RADFRAC distillation columns for absorption and stripping (equilibrium-based)	about 96.72% vol CH_4 in the product stream	biogas upgrading
Gamba et al. [115] [117]	2013, 2015	PWS	ELECNRTL	RADFRAC distillation columns for absorption and stripping (both rate-based)	about 98.86% mol CH_4 on a dry basis in the product stream, CH_4 recovery of about 95.8%	biogas upgrading
		Chemical absorption with MEA			about 98.71% mol CH_4 on a dry basis in the product stream, CH_4 recovery of about 99.9%	
		Chemical absorption with MDEA			about 98.73% mol CH_4 on a dry basis in the product stream, CH_4 recovery of about 99.98%	
Gamero et al. [65]	2018	PSA	PR-BM	Ideal column separators, multi-stage compressors and valves	about 80% CO_2 and 95% CH_4 from the feed stream captured	cleaning the outlet gas of gasification to obtain syngas
Gangadharan et al. [42]	2012	Chemical absorption with DEA	ELECNRTL + RK for vapour	2 RADFRAC distillation columns for absorption and stripping	CH_4 mole recovery of about 99.5%	natural gas cleaning
Götz et al. [110]	2011	PWS	ELECNRTL	Distillation columns for absorption and stripping	about 96.8% vol CH_4 in the product stream	biogas upgrading

Lingelem [114]	2016	Chemical absorption with AMP	ELECNRTL	RADFRAC distillation columns for absorption and stripping (rate-based absorption, equilibrium-based desorption)	97% mol on the base case	biogas upgrading
Menegon [111]	2017	PWS	NRTL-RK	Distillation columns for absorption and stripping (equilibrium-based first, then rate-based)	98.7% vol, with a CH_4 recovery of 99.81%	biogas upgrading
Ortiz et al. [123]	2012	PSA	NRTL	Ideal column separators, multi-stage compressors and valves	95% H_2 recovery, 98% CO recovery, 90% CO_2 recovery, 90% CH_4 recovery	cleaning syngas obtained by supercritical water reforming of glycerol
Pellegrini et al. [118]	2015	PWS	No information	Distillation columns for absorption and stripping	not specified	biogas upgrading
		Chemical absorption with MEA	No information		not specified	
Scamardella et al. [105]	2019	Membrane separation	ELECNRTL	User-defined model	>95% vol	biogas upgrading
Seman et al. [113]	2019	PWS	NRTL	Distillation columns for absorption and stripping	97.6% mol	biogas upgrading
Worawimut et al. [120]	2018	PWS	NRTL	RADFRAC distillation columns for absorption and stripping (equilibrium-based)	96.005% vol, with a CH_4 recovery of 89.96%	biogas upgrading
		Chemical absorption with DEA			96.026% vol, with a CH_4 recovery of 89.47%	

Modelling methane reforming

Gangadharan et al. [42] simulated dry reforming and steam reforming for syngas production from natural gas. The simulation scheme consists of a first step dedicated to acid gas removal (H_2S and CO_2) from natural gas through chemical absorption with DEA, followed by methane separation from higher hydrocarbons in a distillation column, steam production in heat exchanger and finally SMR. Methane exiting the acid gas removal step is mixed with steam in a mixer, which uses heat from the SMR reactor output stream. The mixture is then sent to another heater and then to the plug flow reactor (RPLUG), where the SMR and WGS reactions take place over a Ni/Al_2O_3 catalyst at a constant temperature of 890 K. The output stream is then sent to a heat exchanger, used to generate steam, and then to a flash separator, where syngas and water are obtained. The thermodynamic property method selected is Peng-Robinson, and the convergence criteria have been relaxed due to issues in the PFR convergence with the default criteria. The rate expression for the catalytic reactions occurring in the PFR reactor have been modelled using the Langmuir-Hinshelwood-Hougen-Watson kinetics formulation (LHHW), obtained from the work of Xu and Froment [124]. The produced syngas is characterized by a composition of: 72.22% mol H_2, 21.71% mol CO, 3.56% mol H_2O, 1.77% mol CO_2, 0.48% mol CH_4, 0.26% mol N_2. Authors also simulated a combination of SMR and DMR. In this process, the syngas generated by SMR is sent to a heat exchanger. Here the syngas is cooled and passed through a CO_2 membrane separator, separating CO_2 from the syngas mixture, which contains CO, H_2, CO_2, H_2O and unreacted CH_4. Then, the stream is sent to a flash separator, where separation of syngas and water takes place. The CO_2 separated by membrane filtering is sent to the dry reformer, where the methane reacts with CO_2 for increased production of syngas. As for the SMR process, LHHW kinetic expressions are used to determine the rate of reaction of the DMR process. The resulting syngas has a composition of 73.61% mol H_2, 23.85% mol CO, 1.20% mol H_2O, 0.51% mol CO_2, 0.55% mol CH_4, 0.27% mol N_2.

Giwa et al. [125] simulated the SMR for hydrogen production. The authors modelled two different versions of the process, i.e. with and without feed (CH_4 and H_2O) mixer. For reforming, an equilibrium reactor was chosen, in which the stoichiometry of the reaction was specified, i.e. the reforming reaction (1) and the water-gas-shift reaction (2). Several case studies have been simulated. In case of reactor operating at 1173.15 K temperature and 1 bar pressure of, the syngas compositions obtained in both versions of the model were characterized by the same molar composition, i.e. 62.56% mol H_2, 16.06% mol CO, 17.77% mol H_2O, 3.59% mol CO_2, 0.02% mol CH_4.

The SMR process of natural gas has been also modelled by Amran et al. [126], using a kinetic-based approach with Redlich-Kwong-Soave equation of state with

modified Huron-Vidal mixing rules (RKSMHV2) thermodynamic model. Natural gas and steam are first mixed, fed to a heat exchanger and then to a RPLUG reactor to model the methane reforming reaction, and finally to another RPLUG reactor for WGS reaction. Both reactors follow a rearranged LHHW kinetic model. It is assumed that natural gas does not contain H_2S and CO_2. The modelling approach was validated against data from other published studies, showing a good agreement with literature. A sensitivity analysis of the reaction performance has also been performed.

Gopaul et al. [127] simulated the syngas production from biogas through dry reforming. In particular, three different cases have been simulated, i.e. (i) DMR alone, (ii) DMR and POX, (iii) DMR and hydrogen oxidation (HOX). The target H_2/CO ratio is 1.6-1.7, for downstream Fischer-Tropsch synthesis. The study also compares different types of biogas in terms of H_2 and CO yield: landfill, corn cob, whole stillage, and combined cob and stillage. The compositions of the analysed biogas types do not include H_2S or NH_3. Biogas is not upgraded to biomethane prior to reforming; thus the reforming reactor is directly fed by the biogas stream. About the thermodynamic model, the *Property Method* chosen here is IDEAL, which uses both Raoult's law and Henry's law. The DMR alone case was simulated using a RGIBBS reactor, i.e. an equilibrium reactor whose output is computed following the method of Gibbs free energy minimization at specified operating conditions (pressure, temperature, flowrates). Biogas is fed into the reforming reactor at 1123.15 K and 1.01325 bar. The reactor operates at 1223.15 K and 1.01325 bar. The DMR+POX case is similar to the previous one in terms of reactor configuration and operating conditions. However, in this case, a second feed stream containing oxygen at 1.01325 bar and 473.15 K is used, and therefore the exothermic partial oxidation reaction satisfies the energy demand of the endothermic DMR process. The amount of oxygen required was determined using the Design Specification function available in Aspen Plus, taking also into account the desired syngas H_2/CO ratio of 1.6-1.7. The case of DMR+HOX modelling comprises two RGIBBS reactors, one for DMR and one for H_2 combustion to provide energy to the DMR process. Biogas feed and DMR reactor have the same conditions of the other two cases. The HOX reactor is fed under stoichiometric excess conditions of O_2 at 473.15 K and 1.01325 bar, H_2 at 1123.15 K and 1.01325 bar, and combustion occurs at 1273.15 K and 1.01325 bar. Also in this case, the required H_2 and O_2 feed rates were determined through the Design Specification function in Aspen Plus. The optimal process conditions to maximize syngas yield and quality were determined through a sensitivity analysis on the DMR case with landfill biogas type, which turned out to be similar also for the other biogas types. The analysis showed that, however, the desired 1.6-1.7 H_2/CO ratio is found at temperatures and pressure ranges for which syngas quality is low. Therefore, other values of H_2/CO ratio, slightly outside the desired range have been accepted in favour of a better CH_4 conversion (from 96% to 100%) and syngas quality (meaning, for high quality syngas, a syngas composed mainly of H_2 and CO, with a minimal amount of by-

products). Authors also performed an energy analysis of the processes, which are both exothermic and endothermic. DMR reactor heat duty ranges from +14.88 to +28.74 kW_{th}/kmol, while the DMR+HOX process values of -23.93 and -4.58 kW_{th}/kmol depending on biogas type (resulting in exothermicity); the combined DMR+POX process was able to counterbalance the high energy demand of DMR, achieving thermal-energy neutrality.

The DMR process has been modelled in Aspen Plus also by Ashraf et al. [29]. In this case the RGIBBS reactor block was used, fed by cleaned biogas, steam, and air (to lower coke formation and external energy demand). A sensitivity study to find the optimum process conditions has also been carried out. As a result, a syngas stream characterized by a H_2/CO ratio of about 1.58 was obtained, with a methane conversion of about 99%.

Er-rbib et al. [128] simulated a combination of DMR and SMR processes to produce syngas from natural gas. The reforming unit is composed by two parts: a pre-reformer and a reformer. In the pre-reformer, a complete conversion of the higher hydrocarbons of natural gas into methane occurs over a nickel catalyst at 823 K and 5 bar. Then, in the reformer, the primary SMR reaction (1), the primary DMR reaction (4) and the RWGS reaction (11) take place. The chosen reactors are equilibrium reactors, and thus no kinetic models are considered, whereas the thermodynamic model used is the Peng Robinson with Bostonne-Mathias alpha function (PR-BM).

Table 9**Table 9** summarizes the main Aspen Plus models on upgrading processes reviewed in this work. A large number of studies was identified, most of them dealing with SMR. The analysis however revealed that there is also a good number of papers addressing the DMR, also in combination with SMR, as well as POX, while a smaller number of articles addressing ATR was found.

Table 9. Reviewed Aspen Plus simulation models for reforming

Authors	Publication year	Technology	Thermodynamic model	Main simulation blocks	Methane conversion	Resulting syngas H_2/CO	Study objectives
Amran et al. [126]	2017	SMR	RKSMHV2	RPLUG reactor with LHHW kinetics	can reach 30% for reactor length of about 10 m	not reported for specific conditions	hydrogen production from natural gas
Ashraf et al. [29]	2015	DMR	not specified for this part of the process	RGIBBS reactor	about 99%	1.58	syngas production from biogas
Er-rbib et al. [128]	2012	DMR + SMR	PR-BM	two REQUIL reactors	not specified	not specified	syngas production from natural gas
Gangadharan et al. [42]	2012	SMR (Ni/Al_2O_3 catalyst)	PENG-ROB	RPLUG reactor with LHHW kinetics	not specified	3.33	syngas production from natural gas
		combined SMR and DMR process	PENG-ROB	RPLUG reactor with LHHW kinetics	not specified	3.09	
Giwa et al. [125]	2013	SMR	not specified	REQUIL reactor	not specified	3.90	hydrogen production from methane
Gopaul et al. [127]	2015	DMR	IDEAL	RGIBBS reactor	96%÷100% depending on the feed type	0.96÷2.80 depending on the feed type	syngas production from biogas
		DMR + POX		RGIBBS reactor	96%÷100% depending on the feed type	0.96÷2.80 depending on the feed type	
		DMR + HOX		two RGIBBS reactors	96%÷100% depending on the feed type	0.96÷2.80 depending on the feed type	
Hao et al. [129]	2008	ATR	IDEAL	RGIBBS reactor	not specified	not specified	syngas production from natural gas

Modelling Fischer-Tropsch synthesis

Modelling the Fischer-Tropsch process is particularly challenging due to the high number of species existing in equilibrium, the variety of reaction products, the complexity of the CO catalyst chemistry, and the large amount of process parameters relevant for the process [38]. Indeed, the identification of a plausible mechanism, as well as the formulation of a representative expression addressing the consumption rate of the primary component CO and an accurate description of the product distribution are crucial and complicated steps in modelling the Fischer-Tropsch synthesis [130] [131]. A comprehensive review of the FT kinetics has been carried out by Van Der Laan and Beenackers [132]. The Anderson-Schulz–Flory (ASF) model is normally used to represent the FT product distribution, based on one parameter, namely the chain probability factor α, which describes the addition of carbon atoms into the molecule chain [133]. However, in most cases the real Fischer-Tropsch product selectivity does not obey the ideal ASF distribution [134], and deviations (essentially higher selectivity to CH_4, and lower to C_2H_4 than expected in the model) are well documented in the literature [130]. Dependence of the chain probability factor α on process conditions (pressure, temperature, composition, catalyst type, etc.) has been largely studied and correlations have been formulated, e.g. [135], [136], [137].

In this section, different models found in literature simulating the Fischer-Tropsch synthesis in Aspen Plus are analysed.

Ashraf et al. [29] simulated the FT synthesis in a slurry reactor from bio-syngas. A RYIELD reactor block with CO conversion of 80% has been selected. This block does not require exact information about the stoichiometry or kinetics, but models a reactor by specifying the reaction yields of each component [102]. The product distribution follows the ASF distribution, with α values computed according to Kruit et al. [137] parameters. After the synthesis, the FT syncrude is then sent to a distillation column (RADFRAC) to separate products according to the following classification: C-1 to C-4 lights, C-5 to C-9 naphtha, C-10 to C-16 kerosene, C-17 to C-22 diesel, and C-22+ waxes. As the selectivity of FT-crude products depends on reaction temperature and feed syngas (H_2/CO ratio), a sensitivity study has been carried out, and these parameters optimized to maximize kerosene and diesel fraction using solver function in MS Excel. In order to achieve 80% CO conversion and maximise kerosene and diesel yield fractions, the optimal values have been estimated between 1.6 and 2 for the H_2/CO ratio, and between 473.15 and 573.15 K as regards the reaction temperature. Considering the whole process (biogas to liquid fuel conversion process using pressurized water scrubbing, dry methane reforming, and FT-synthesis), the overall carbon conversion efficiency reaches 45%, while the energy efficiency is 30%.

Adelung et al. [61] simulated the production of synthetic hydrocarbons (in particular kerosene and diesel) from syngas derived from captured CO_2 and H_2 obtained though water electrolysis. In the proposed approach, syngas is generated

through reverse water-gas-shift (RWGS) reaction, and then converted through the FT reaction into a broad range of hydrocarbons. A product separation is performed downstream hydrocarbon production: long chain hydrocarbons are sent to a hydrocracker to increase the yield at the desired chain length for transport fuel production (<C-22). Gas products and unreacted species are recycled to increase the carbon efficiency of the process. Operational parameters are optimized to maximize the energy efficiency. In Aspen Plus, the thermodynamic method here selected is the Peng-Robinson with Boston-Mathias modifications (PR-BM), H_2, CO, CO_2, H_2O, N_2, O_2 and alkanes are the chemical species considered in this model. It is assumed that Carbon is not a possible product. The FT reactor is a tubular fixed bed: it has been simulated as a stoichiometric reactor (RSTOIC) with Co catalyst, without considering reaction kinetics. The reactor operates at 493.15 K and 25 bar, while the H_2/CO ratio is set at 2. CO conversion is assumed equal to 40%, and inert gas share is fixed at 50%. Under these conditions, the chain growth probability factor α is equal to 0.839, calculated using the expression proposed by Vervloet et al. [136]. The stream from the reactor is first sent to a flash separator, where heavy hydrocarbons are separated, and then to a hydrocracker. The product from the hydrocracker is then subject to further separation through 8 different flashes into hydrocarbons, water and recycling gases. The carbon efficiency of the overall process is 88%, thanks to the recycles, while the Power-to-Liquid efficiency for the base case is 38.7%.

Campanario et al. [123] simulated the production of low-temperature Fischer-Tropsch products from syngas obtained by supercritical water reforming of bio-oil aqueous phase. The overall process is composed of four different sections, i.e. (i) supercritical water reforming (SCWR) of the bio-oil aqueous fraction, (ii) upgrading of the syngas to increase H_2 and CO molar flow rate and to achieve the desired H_2/CO ratio through water-gas-shift and dry reforming reactors and PSA systems, (iii) Fischer-Tropsch synthesis loop, and (iv) refining and upgrading of FT products by means of distillation columns and hydrocracking. Focusing on the FT synthesis section, the selected reactor is a stoichiometric one (RSTOIC) operating in a temperature range of 493.15 to 513.15 K and 20 to 40 bar, fed by syngas at 2 H_2/CO ratio. FT products were assumed to be composed only of olefins and paraffins, and the probability parameter of chain growth propagation, α, has been computed using the expression obtained by Song et al. [135]. The stream leaving the FT reactor is then cooled to condense heavier hydrocarbons and separate them from the gas. The gas stream is recycled back to the FT reactor to maximize the overall CO conversion and to increase the production of liquid fuel, while the liquid phase is sent to a decanter for separating H_2O from heavier hydrocarbons, which are first expanded through a valve and finally sent to the distillation section. The thermodynamic methods used are UNIQUAC for the distillation train and Peng-Robinson EOS for the FT section. The effect of the main operating parameters on the process performance, such as feed composition and operating conditions of the Fischer-Tropsch reactor, was studied by a sensitivity analysis. Optimal conditions

were identified, thus for a mass flow of aqueous phase of 60 t/h with a total organic concentration of 35% wt, biofuels production was estimated equal to 4596 kg/h (2804 kg/h FT-diesel, 1491 kg/h FT-jet fuel and 301 kg/h FT-gasoline), the carbon efficiency with refining to 38.53% (without refining, it was estimated at 43.50%), while net electrical power was 5297 kWe.

Niassar et al. [138] simulated the FT synthesis in the context of development and optimization of an Integrated Process Configuration for IGCC Power Generation Technology, with a Fischer-Tropsch fuels from coal and biomass. Basically, the process consists in a first part related to syngas generation from gasification, which is then split and sent into the FT unit, where it is converted to fuel, and the combined power cycle generates electricity and power. Focusing on the Aspen Plus model section related to the Fischer-Tropsch unit, the reactor chosen by the authors is a stoichiometric reactor (RSTOIC) in which 31 reactions have been considered. The property method selected is Peng-Robinson. The feed syngas is characterized by H_2/CO ratio of about 2, and the process is carried out at about 513.15 K and 20 bar. The syngas is thus mainly converted to C-1 to C-30 hydrocarbons and water. Chemical reactions have been defined up to C-30 as the database of software does not contain hydrocarbons that are heavier than the C-30. The products of the Fischer-Tropsch reactor undergo downstream separation under gradual cooling in the three separators. Lightweight and heavyweight hydrocarbons liquids are the main products of the process, while gases are sent to the power plant for power generation. A sensitivity analysis has been carried out, and the simulation results compared with an experimental work [139], [140], indicating that the difference in results is about 4%.

In the context of assessing Biogas-to-Liquid processes for bagasse utilization, Michailos et al. [141] developed an Aspen Plus model to simulate the Fischer-Tropsch synthesis of bio-syngas. The studied production route included a gasifier unit, syngas quenching and cleaning, a FT synthesis reactor, product recovery and separation, and finally a heat and power generation system. The biomass, i.e. sugar cane bagasse, undergoes a pre-treatment constituted by bagasse crushing to small particles and drying before entering the system. With regards to Fischer-Tropsch modelling, authors used a product distribution reactor (RYIELD), following the Anderson-Schultz-Flory distribution model (α=0.9), through which the mass yield of the products of the synthesis were determined. The reactor module interfaces with an Excel Spreadsheet where these calculations are carried out. The feed syngas is characterized by H_2/CO ratio of 2.05. The product stream exiting the FT unit is then sent to a flash to separate the hydrocarbons from the unconverted syngas, which is recycled back. The hydrocarbons stream is then sent to a purification zone, consisting of four distillation columns and a hydrocracking unit for waxes, with a conversion efficiency of 88%. The *Property Method* chosen for conventional components is the Redlich–Kwong–Soavecubic equation of state with Boston–Mathias alpha function (RKS–BM). For a feed consisting of 100 tonne/h of sugar cane bagasse (before being subjected to the pre-treatment process), the product flow

rates of the system are: 9,100 kg/h diesel, 6,050 kg/h gasoline, 1,175 kg/h LPG. The energy efficiency of the process is about 68%.

Hao et al. [129] used Aspen Plus to simulate a Gas-to-Liquid (GTL) process involving syngas generation through ATR and Fischer-Tropsh synthesis. The FTS has been simulated based on detailed kinetic models considering two kinds of industrial catalyst, i.e. iron and cobalt. Authors tested two different Aspen Plus reactor blocks, i.e. PRF (plug flow reactor) and CSTR (continuous stirred tank reactor). The detailed kinetic models for the two different catalyst types have been programmed in FORTRAN and compiled as user-defined functions for the simulation software. Authors performed a sensitivity analysis for both the catalysts to understand the performances of the two models (PFR and CSTR), by varying operating conditions and H_2/CO ratio of the syngas. Different recycling options for the FT tail to the ATR have been simulated to find the optimal flowsheet structure, which was selected according to the overall thermal efficiency to crude products, the overall carbon efficiency to crude products and the energy value of the purge gas. The study concluded that the thermal efficiency to crude products for cobalt-based catalyst is about 60%, while for the iron-based catalyst it is in the range of 49–55%. Additionally, FT synthesis with Fe-based catalyst generates CO_2, its carbon efficiency (61–68%) turns out to be lower with regards to the cobalt-based catalyst (73–75%).

Er-rbib et al. [142] developed an Aspen Plus model to describe the production of synthetic gasoline and diesel fuels. The process consists of four different stages: (i) production of syngas from the combination of dry reforming and steam reforming of natural gas, (ii) Fischer-Tropsch synthesis to produce long chains of hydrocarbons, (iii) separation of fuel and wax hydrocracking, and (iv) recovery of hydrogen. The FT synthesis was modelled using a stoichiometric reactor (RSTOIC), specifying 42 reactions for which information about selectivity and efficiency has been found in the literature. The operating conditions are 513 K and 20 bar. At these conditions, the conversion of synthesis gas was estimated at 87%. The reactor products are cooled and separated from water and oxygen compounds, and then sent to a distillation column for the separation of heavy and light components. Waxes are finally converted into high quality diesel through a hydrocracking unit, which has been simulated as a RYIELD reactor. The *Property Method* used for the reactors and the distillation columns is Peng Robinson with Boston-Mathias alpha function (PR-BM). The results show that the overall process can produce synthetic fuels composed by 72% of diesel, 26% of gasoline and 2% of LPG.

Sudiro et al. [143] used Aspen Plus to simulate synthetic fuels production through LTFT synthesis of syngas obtained from coal and natural gas. Three processes have been simulated, i.e. (i) gas to liquid (GTL), (ii) coal to liquid (CTL) and (iii) a hybrid process coupling features of both CTL and GTL. Focusing on the Fischer-Tropsch section of the model, a RYIELD reactor block has been chosen, with syngas conversion assumed equal to 87% at 513.15 K and 15 bar operating

conditions. Selectivity values (ratio between moles produced and moles of syngas converted) have been specified, taken data from literature. 44 reactions of type (6) and (7), respectively olefins formation and alcohols formation, have been used for all components from CH_4 to $C_{60}H_{122}$ and ethanol. Product distribution on a weight basis is: gasoline (C-5 to C-11) 25.6%; diesel (C-12 to C-18) 40.3%; waxes (C-19 to C-60) 31.6%; light gases 1.6%; oxygenated compounds 1%. The products are then subject to hydrocracking, separation, water treatment and recycling. The *Property Method* used for the process parts involving reactors, distillation columns and two-phase separators is The Peng-Robinson equation of state with Boston-Mathias alpha function, while for separations involving three phases the NRTL equation was applied. Simulated product yields for three cases are 66.7% for GTL, 32.5% for CTL, and 44.4% for the hybrid process., on a weight basis. The estimated thermal efficiency, i.e. ratio between the energy contents in the products and in the feedstock, is 54.2%.

Bao et al. [144] simulated the FT synthesis in the context of process design optimization of a GTL plant. In the study, authors assumed a feed H_2/CO ratio of ~2 and that the process follows the ASF product distribution, with a fixed chain growth probability factor α equal to 0.95. The syncrude is fed into a distillation column to separate LPG, naphtha and wax. NRTL-RK is the property method used, while the reactor configuration is not specified. The simulated plant converts 900,000 kg/h of natural gas into 118,000 BDP of products.

Cinti et al. [145] used Aspen Plus to model the FT synthesis as a part of a study addressing the production of synthetic green fuels through a system integrating a Solid Oxide Electrolyser and the Fischer Tropsch process. The plant is divided in two main sections, i.e. (i) the electrolyser unit and (ii) the liquid fuel synthesis unit. In (i) H_2O and CO_2 are converted into H_2 and CO (syngas) via co-electrolysis, whereas in (ii) syngas conversion into hydrocarbons occurs. In the process modelled, the FT synthesis occurs at 20 bar and 503.15 K, and only a first FT crude separation is considered, which divides purge water from hydrocarbons and light refinery gases. The main Aspen Plus simulation blocks considered for the FT modelling part are: a splitter, a stoichiometric reactor, a mixer and a flash separator. The splitter divides the feed syngas (H_2/CO = 2.1) into two streams: one enters the RSTOIC block, while the other bypasses the reactor and is mixed with the FT products. The FT reactor (Co-based) accomplishes several reactors, and the product distribution is assumed to follow the ASF products distribution model with a chain growth probability factor α equal to 0.94. The synthesis of alcohols, aromatics and other oxygenated compounds is neglected; only alkanes and alkenes are considered as products. The syncrude is then sent to a flash separator preforming the separation of light gases, liquid phase, and water. For a given syngas feed characterized by a molar composition equal to 51.2% mol H_2, 24.4% mol CO, 24.3% mol CO_2, 0.1% mol CH_4, the products at FT reactor outlet (without any separation) is composed by 8.16% mol H_2, 40.78% mol H_2O, 3.58% mol CO, 43.94% mol CO_2, 0.4% mol CH_4, 0.24 mol C_3H_6, 0.38% mol C_3H_8, 0.06% mol C_6H_{12}, 0.32% mol C_6H_{14}, 0.06% mol

C_8H_{16}, 0.57% mol C_8H_{18}, 0.01% mol $C_{16}H_{32}$, 0.94% mol $C_{16}H_{34}$, 0.53% mol C_{30+}. The total energy efficiency of the FT system is 52.57%, while considering just the crude fraction of FT products as a valuable product, the energy efficiency is 40.95%.

Also, Pondini et al. [146] developed an Aspen Plus model considering low temperature Fischer-Tropsch to simulate synthetic fuels production from biomass-derived syngas. The FT reactor (Co-based catalyst) has been modelled using a RSTOIC reactor, for which the fractional conversion of each reaction is imposed as calculated in an integrated Excel file according to an estimated chain-length distribution. Hydrocarbons (olefins and paraffins) with carbon number up to 30 are considered, and the Song et al. [135] correlation for the chain growth probability factor α is considered. The mole fraction calculations for products with carbon number C-1 to C-4 have been adjusted to take into account the ASF deviation (i.e., higher methane selectivity) with reference to Rane et al. [147]. Different operating conditions (H_2/CO ratio, reactor pressure, temperature, CO conversion) have been tested.

Marchese et al. [148] modelled the Fischer-Tropsch synthesis in the context of analysing different power-to-liquid options, in which the FT section is integrated into a complete carbon capture and utilization from a biogas upgrading unit producing about 1 tonne/h of CO_2. The recovered CO_2 is turned into syngas through either a reverse water gas shift reactor or to a solid oxide electrolysis unit operating in co-electrolysis mode; the produced syngas is fed to a Fischer-Tropsch reactor operating at 25 bar and 501 K, whose products are then separated into light gas, naphtha, middle distillates, light waxes and heavy waxes. The process model implements a detailed kinetic model developed in the author's previous study [149] based on real experimental data, which accounts for deviations from the Anderson-Schulz-Flory (ASF) distribution (i.e., higher methane and lower ethylene formation). For the implementation in Aspen Plus, a plug flow reactor (RPLUG) was selected, integrated with an external kinetic subroutine for rates definition up to C-80 for paraffins and C-40 for olefins. The *Property Method* chosen for the FT unit was the RKS-BM. The simulation results show that, for the case of solid oxide electrolyser to produce syngas, the best model configurations can reach a plant efficiency of 81.1%, while for the reverse water gas shift option, the plant efficiency reaches 71.8%.

The same modelling approach was used also in another study [150] addressing the energy and economic analysis of plant configuration integrating the direct air capture technology for CO_2 recovery and the Fischer-Tropsch synthesis. In this case, the carbon number of alkanes and alkenes considered spans from C-1 to C-70.

In another study [151], aimed at analysing the techno-economic feasibility of a biomass-to-X plant, Marchese et al. modelled the FT synthesis using a different approach. The synthesis of paraffin was described up to C-40 and for olefins up to C-19, using the ASF distribution with α dependent over the temperature and syngas

composition according to Song et al. [135] correlation. CH_4 yield was assumed equal to 20%-mol, to account the ASF deviation for this compound. Moreover, a 90% internal recirculation for unconverted syngas was considered. The reactor configuration in Aspen Plus is not specified in the paper, while the thermodynamic method used for the FT section of the overall process is Redlich-Kwong-Soave with Boston-Mathias modification (RKS-BM) EoS.

Gabriel et al. [152] modelled the FT synthesis in the context of a GTL process composed of three sections, i.e. synthesis gas production from natural gas and conditioning, FT reaction, and FT product upgrading and separation. Different plant configurations have been evaluated; changes are limited to the syngas production technologies and conditioning sections. Focusing on the part of the process model in Aspen Plus assessing the Fischer-Tropsch synthesis, the authors used a RSTOIC reactor with a per pass conversion of 70%. The products follow the ASF distribution, with a constant α=0.92, used along to reverse calculate the stoichiometric coefficients of the produced hydrocarbons from C-1 to C-100. Only paraffins are considered, and the stoichiometric coefficients are adjusted for the C-30+ lumping assumption. The syncrude is then sent to a refining section.

Hamad [153] developed an Aspen Plus model for the FT synthesis as part of an analysis of the solvent selection for supercritical Fischer-Tropsch Synthesis reactors, in order to provide a basis for future supercritical phase simulations. The method used for this research is derived from the ASF distribution and the calculations of the stoichiometric coefficients are done in an Excel spreadsheet. For the calculation of α as temperature dependent, the Levenberg–Marquardt algorithm was used. Products are assumed to be composed only by paraffins. The Aspen Plus reactor type chosen is not specified, as well as the *Property Method* used.

Dahl [154] modelled the FT process in the framework of a study evaluating a Power & Biomass to Liquid (PBtL) process concept, which consists of a biomass gasification to produce syngas, hydrogen addition to the syngas to increase its H_2/CO ratio, FT synthesis to produce hydrocarbons, which are then separated, and the longer hydrocarbons cracked. The author developed two Aspen Plus models for the Fischer-Tropsch reactor: a conversion-based model, whose operating conditions were varied, and a kinetic-based model, using plug-flow reactor (RPLUG) in which the conversion of CO is studied. The *Property Method* used is Peng Robinson - Boston Mathias (PR-BM). The conversion-based involves two stoichiometric reactors (RSTOIC). In the first reactor the three main FT reactions occur (paraffins, olefins and alcohols formation), modelled according to the ASF distribution with a method of lumping high-weight hydrocarbons described in Hillestad et al. [155]. The products are assumed to be composed by paraffins (up to C-20 with a C-21+ lump), olefins (up to C-10 with a C-11+ lump) and alcohols (up to C-5 with a C-6+ lump). Each FT product is characterized by its specific probability function α: in case of paraffins and olefins, α is assumed to be temperature and pressure dependent and formulated through Todic et al. correlation [156], while for the oxygenates, α is assumed to be constant (i.e. equal to 0.5). To figure out the ASF underestimation

of methane in the products, a stand-alone reaction describing the CH_4 formation from CO and H_2 is added in the reactor, as well as an additional reaction for CH_4 among the olefins' formation. A total CO fractional conversion has been set to 60%, which is split between the four reactions involved in the first RSTOIC reactor; its values were adjusted for each reaction to yield approximately the same carbon selectivities found in the experimental study carried out by Shafer et al. [157]. The second RSTOIC reactor considers the ethylene deviation, referring to Pandey et al. [130]. Computations have been performed in Aspen Plus calculation blocks. The kinetic-based model uses Langmuir-Hinshelwood (LHHW) adsorption kinetics and the consorted vinylene mechanism, a modified ASF distribution model. The model considers also ASF deviation and the effect of water over the reaction rate. The oxygenates are not included in this model. The products separation flowsheet is the same for both the reactor configurations. After the Fischer-Tropsch synthesis, the liquid and gaseous FT products are separated in a FLASH at the temperature of the FT reactor outlet; in facts, at this temperature (more than 450 K) the hydrocarbons of 17 carbons or higher are liquid and unreacted syngas and hydrocarbon of 16 or lower are gaseous. The gaseous stream is then cooled in a counter current heat exchanger, which recovers the heat to warm the syngas feed, and then further cooled to 283.15 K. The cooled gaseous stream enters a three-outlet FLASH separator, which gives: (i) a C1-C5 hydrocarbons gaseous stream, (ii) a C6-C16 hydrocarbons stream, and (iii) a water stream. The C6-C16 hydrocarbons stream undergoes a further separation, involving a pressure decrease to 5 bar through a VALVE, a temperature increase to 483.15 K, in order to evaporate the C6-C7 hydrocarbons, and then a separation of the C6-C7 hydrocarbons from C8-C16 hydrocarbons in a second FLASH. Different operating conditions have been tested (i.e. 493.15 K, 27.6 bar, $H_2/CO = 2$; 483.15 K, 25 bar, $H_2/CO = 1.95$; 483.15 K, 25 bar, $H_2/CO = 1.60$; 483.15 K, 20 bar, $H_2/CO = 1.95$; 493.15 K, 25 bar, $H_2/CO = 1.95$) for both reactor configurations, and the simulations results showed that, at the same operating conditions, the conversion-based reactor results in higher selectivity towards lower-weight hydrocarbons. For both models, carbon selectivity increases with carbon number and has a peak around C-13.

Table 10 summarizes the selected research works modelling Fischer-Tropsch synthesis in Aspen Plus. Seventeen different studies have been identified.

Table 10. Aspen Plus simulation models reviewed for FT synthesis

Authors	Publication year	Thermodynamic method	Main simulation blocks	Reference model(s)	Remarks
Adelung et al. [61]	2020	PR-BM	RSTOIC reactor with CO conversion of 40%, flash separator, hydrocracker unit	Vervloet et al. expression for the calculation of α	synthetic kerosene and diesel from syngas derived from captured CO_2 and H_2 obtained though water electrolysis
Ashraf et al. [29]	2015	not specified for this part of the process	RYIELD reactor with CO conversion of 80%, RADFRAC distillation column for product separation	ASF distribution model with α parameters from Kruit et al.	FT liquids from biogas
Bao et al. [144]	2010	NRTL-RK	Reactor block type not specified	ASF distribution model with constant α	optimal process design of a GTL plant
Campanario et al. [123]	2017	PENG-ROB for FT, UNIQUAC for distillation train	RSTOIC reactor, cooler, decanter, distillation section	ASF distribution model, Song et al. correlation for α calculation	low-temperature Fischer-Tropsch products from syngas obtained by supercritical water reforming of bio-oil aqueous phase
Cinti et al. [145]	2015	not specified	RSTOIC reactor, splitter and mixer blocks, flash separator	ASF distribution model with constant α	synthetic green fuels produced by a system integrating a Solid Oxide Electrolyser and the Fischer Tropsch process
Dahl [154]	2020	PR-BM	RSTOIC	ASF distribution, and deviations Hillestad et al. [155], Shafer et al. [157], Pandey et al. [130], Todic et al. correlation [156]	evaluate a Power & Biomass to Liquid (PBtL) process concept
			RPLUG with LHHW kinetics		
Gabriel et al. [152]	2014	not specified	RSTOIC reactor	ASF distribution model with constant α	Gas-to-Liquid (GTL) process involving syngas generation from natural gas and Fischer-Tropsch synthesis
Hao et al. [129]	2008	not specified	RPLUG reactor with detailed kinetic models programmed in FORTRAN	User-defined detailed kinetic models	Gas-to-Liquid (GTL) process involving syngas generation through ATR and Fischer-Tropsch synthesis

		not specified	RCSTR reactor with detailed kinetic models programmed in FORTRAN	User-defined detailed kinetic models	
Hamad [153]	2011	Not specified	Not specified	ASF distribution model with Levenberg-Marquardt correlation for α calculation	Analysis of Solvent Selection for Supercritical Fischer-Tropsch Synthesis Reactors
Er-rbib et al. [142]	2012	PR-BM	RSTOIC reactor with 42 reactions for FT, distillation columns, RYIELD reactor for hydrocracking	Specified equations	Synthetic gasoline and diesel fuels from syngas
Marchese et al. [148]	2020	RKS-BM	RPLUG with LHHW formulation	ASF distribution model and ASF deviations	Power to Liquid routes analysis (carbon capture and utilisation from biogas upgrading)
Marchese et al. [151]	2021	RKS-BM	Not specified	ASF distribution model, Song et al. correlation for α calculation	Biomass-to-X-plant: FT synthesis from digestate gasification
Marchese et al. [150]	2021	RKS-BM	RPLUG with LHHW formulation	ASF distribution model	CO_2 from direct air capture as feedstock for FT synthesis
Michailos et al. [141]	2017	RKS–BM	RYIELD reactor interfacing an Excel Spreadsheet, flash separator, hydrocracking unit	ASF distribution model	FT fuels from bio-syngas
Niassar et al. [138]	2018	PENG-ROB	RSTOIC reactor with 31 reactions, coolers, separators	Specified equations	development and optimization of an Integrated Process Configuration for IGCC Power Generation Technology with a Fischer-Tropsch Fuels from Coal and Biomass
Pondini et al. [146]	2013	not specified	RSTOIC reactor	ASF distribution model, Song et al. correlation for α calculation, Rane et al. [147]	FT crudes from biomass-derived syngas (gasification)
Sudiro et al. [143]	2009	PR-BM, NTRL	RYIELD reactor, distillation columns, RYIELD reactor for hydrocracking	Selectivity values from Mulder H.	synthetic fuels production through LTFT synthesis of syngas obtained from coal and natural gas

Methanol synthesis modelling

In the literature, several studies for simulating methanol production in Aspen Plus can be found; these describe the conversion of syngas and CO_2, to commercial grade methanol.

Trop et al. [158] studied methanol production from a mixture of torrefied biomass and coal. In the process, gasification of biomass and coal, synthesis gas purification and methanol synthesis from syngas have been simulated.

Authors modelled methanol synthesis as a series of plug-flow reactions occurring in a stoichiometric reactor. Products are then cooled to 303.15 K and the condensed crude methanol is sent to a flash separator and a purification system, consisting into four distillation columns, where methanol is separated from water, small amounts of ethanol and dissolved reactants. The composition (mass fractions) of the final products is made of 0.9998 methanol, 0.0001 ethanol, and traces of H_2O and CO_2. For the methanol production section of the process, the Peng-Robinson thermodynamic method was chosen.

Gamero et al. [65] developed an Aspen Plus model for methanol synthesis from syngas obtained through gasified biomass and then gas cleaning through PSA. In the model, the cleaned syngas stream is compressed and heated up to the operating pressure and temperature. Then, the stream is introduced in the methanol synthesis reactor, which has been simulated as an equilibrium reactor (REQUIL). This kind of reactor requires the stoichiometry to be specified. The equations involved in the synthesis are (9) and (11), with a conversion of 36% for CO and of 17% for CO_2. The selected catalyst is Cu/ZnO. The reaction product is then depressurized and cooled down, and then sent to a column separator, to condense and separate methanol from the gas-phase, getting at the bottom pure methanol as the final product. The H_2/CO in the feed stream is about 2.4-2.5. As regards the thermodynamic method, the Peng-Robinson with Boston Mathias function was selected as appropriate for the process application, in particular for high temperature gasification. Operating conditions have been varied, evaluated, and optimized through a sensitivity study. The optimal conditions were fixed at 493.15 K and 55.7 bar, yielding 32 kg/h methanol produced from a biomass feed rate of 100 kg/h.

Chein et al. [159] modelled methanol synthesis in Aspen Plus from syngas produced from biogas. After being compressed and cooled to the operating conditions for methanol synthesis (5 MPa and 523.15 K), the syngas enters the methanol reactor, modelled as an equilibrium reactor. This kind of reactor can simulate thermodynamic equilibrium reactions with a good accuracy. Products (methanol and water) are expanded and then separated in a flash unit. Recycling unreacted syngas to improve the methanol yield is also performed by using a splitter with specified recycle ratio. In addition, this study also estimated the performance of a green process for methanol synthesis using captured CO_2 as a feedstock. Optimized conditions for obtaining 25.48% methanol yield have been found.

Ortiz et al. [70] developed an Aspen Plus simulation model for methanol synthesis from syngas obtained by supercritical water reforming of glycerol. In the model, the syngas is compressed and heated to the MeOH synthesis operating conditions (86.13 bar and 523.15 K). Then, the stream is sent to the methanol reactor, modelled as a stoichiometric (RSTOIC) gas-phase reactor, with specified CO conversion of 20% and CO_2 conversion of 3%. According to the authors, this kind of reactor can better represent an industrial reactor, as an equilibrium reactor (REQUIL) would lead to a CO conversion and CO_2 conversion of about 76.8% and 9.6% respectively. In the study it is assumed that no by-product formation occurs. The reactor effluent is then cooled down to condensate the crude methanol, and thus separated from the gas phase, which is then recompressed and recycled to increase the overall CO conversion to methanol. A fraction of the recycled gas is purged to prevent accumulation of inert gases and sent to the furnace to support energy self-sufficiency of the process. Finally, crude methanol is sent to a distillation column, in which H_2O is separated from CH_3OH, with a recovery of 99%.

De María et al. [160] simulated methanol production from syngas in Aspen Plus to investigate a kinetic model developed by the authors. For this matter, an external model of the reactor was integrated into the simulation flowsheet instead of using a reactor block already available in Aspen. The reactor model was developed in Matlab and integrated into the Aspen Plus flowsheet using CAPE OPEN standard. The simulated process is constituted by a first part dedicated to syngas compression from 1 to 110 bar in a two-stages intercooled (311.15 K) compression train. Then, syngas is mixed with recycled streams, preheated in a feed-effluent heat exchanger, and then sent to a distillation column for raw methanol separation. The property method chosen for the whole process is the RK-Aspen (Redlich–Kwong), with the only exception of the distillation column, for which the NRTL-RK was set. The composition of the feed syngas is equal to 6.9% mol CO_2, 23% mol CO, 0.2% mol H_2O, 67.5% mol H_2, 0.3% mol N_2, 2.2% mol CH_4. The product stream is characterized by: 98.1% mol CH_3OH, 0.2% mol CO_2, 1.6% mol H_2O.

Suhada et al. [161] developed an Aspen Plus simulation model to convert the CO_2 separated from biogas to methanol. The methanol reactor, which is also fed by a stream of H_2 obtained from an electrolysis unit, has been modelled as an equilibrium reactor type (REQUIL).

Another simulation approach for modelling methanol synthesis from captured CO_2 has been developed by Atsonios et al. [162]. Two different reactor types have been investigated: a tubular catalytic reactor and a zeolite membrane reactor. The tubular catalytic reactor is composed by three main units, i.e. methanol synthesis, gas separation and product purification. The inlet gas is constituted by H_2 and CO_2, with a H_2/CO_2 ratio of 3.0, heated to 423.15 K and then sent to the methanol reactor. The authors do not specify which Aspen Plus reactor block has been chosen for the simulation. However, the process stoichiometry and kinetics is considered. In particular, the reactions involved are (9), (10) and (11), and the process kinetics follows the study of Graaf et al. [163], developed for a commercial Cu/Zn/Al

catalyst. The composition of the stream exiting the reactor is equal to 14.5% mol CO_2, 63.3% mol H_2, 6.9% mol H_2O, 1.8% mol CO, 7.5% mol CH_3OH. The crude methanol is then subject to a refining step, made of two flash separators and a distillation column, leading to a final product composition of 99.3% mol CH_3OH, 0.1% mol H_2O and 0.6% mol CO_2.

About the membrane reactor, it has been modelled as a series of equilibrium reactors with the intermediate interpolation of split separators. The split fraction of the vapours (only water and methanol) that are assumed to permeate the membrane is specified by a determined separation factor. The methanol purity of the product exiting the process is about 99.4%.

Van-Dal et al. [164] also simulated in Aspen Plus the methanol synthesis from captured CO_2 via hydrogenation. In the simulation model, CO_2 (1 bar, 298.15 K) is compressed to 78 bar in a series of intercooled compressors, while H_2 (30 bar, 298.15 K) is compressed to 78 bar in a single stage. The two gases are mixed and then re-mixed with the recycle stream, heated to 483.15 K and finally injected in the RPLUG reactor for methanol synthesis, which is a fixed bed adiabatic reactor. The stream leaving the reactor is then split into two streams, one used to heat the fresh feed and the other in the reboiler and to heat the feed of the distillation column. These streams are then re-mixed, cooled to 308.15 K by water and then sent to a knock-out drum, where condensed water and methanol get separated from the non-reacted gases, which are partially purged to minimise the accumulation of inerts and by-products in the reaction loop. The crude methanol obtained (composed of CH_3OH, H_2O and residual dissolved gases) is expanded to 1.2 bar through two expansion valves, fed into a flash separator where residual gases are almost completely removed, heated to 353.15 K, and finally sent to a distillation column (RADFRAC). Here water and methanol are separated, and the resulting CH_3OH stream, in gaseous form, contains 69 ppm wt. of H_2O and some unreacted gases. The RPLUG reactor is packed with a fixed bed of $Cu/ZnO/Al_2O_3$ catalyst. The model of Bussche and Froment [165] describing the reactions of methanol production and the RWGS reaction with this catalyst has been chosen, with readjusted parameters of Mignard and Pritchard [166]. The kinetic constants follow the Arrhenius law, while the equilibrium constants are provided by the study of Graaf et al. [163]. In Aspen Plus, the LHHW (Langmuir-Hinshelwood-Hougen-Watson) kinetics has been selected. Achieved CO_2 conversion was 33%. About the used thermodynamic method, the Redlich-Kwong-Soave equation of state with modified Huron-Vidal mixing rules (RKSMHV2) was used for streams at high pressure (>10 bar), while for low pressure streams the NRTL-RK model was employed.

In the thesis work developed by Mantoan [167], MeOH production from CO_2 hydrogenation was simulated following the model developed by Fortes et al. [168], and adopts the similar approach seen in Van-Dal et al. [164]. Also in this case, the methanol synthesis process involves: a first step, in which the feed gases are compressed up to reactor feed pressure through different intercooled compression

stage; a second process step, in which the pressurized feed stream gets is heated up and sent to the reactor; and a third process step, in which MeOH is finally separated from H_2O in a distillation column. As in the study of Van-Dal et al. [164], the kinetic model used is that of Bussche and Froment [165] with readjusted parameters of Mignard and Pritchard [166], the kinetic constants follow the Arrhenius law and the equilibrium constants are given by Graaf et al. [163]. The thermodynamic models used are the RKSMHV2 for high pressure streams (>10 bar) and NRTL-RK for low pressure. The reactor type selected is an adiabatic ideal plug flow reactor (PFR), following the equations (10) and (11) and reaction rates implemented in CHEMCAD®. The CO_2 conversion into CH_3OH in the reactor is ~21%. The distillation column has been designed to yield a high MeOH purity (>99.9% wt). The stream fed into the reactor has a composition of 13% wt H_2, 75% wt CO_2 and 12% wt CO. The product stream exiting the MeOH reactor has a composition of 12% wt CH_3OH, 7% wt H_2O, 11% wt H_2, 58% wt CO_2 and 12% wt CO. The product methanol stream leaving the system has a composition of: 99.96% wt CH_3OH, 0.01% wt H_2O and 0.03% wt CO_2.

Calogero et al. [169] also simulated methanol synthesis through CO_2 hydrogenation, referring to the models developed by Atsonios et al. [162] and Van-Dal et al. [164]. The process consists into two main parts, i.e. a preparation section, in which the reactants are brought to the process conditions, and a processing section, in which the synthesis reaction takes place, and the separation of products and recirculation occurs. The process conditions and scheme follow those of the study developed by Atsonios et al. [162], with the aim to obtain a product methanol purity equal to 99.9% mol.

Kiss et al. [170] used Aspen Plus to simulate a process for methanol synthesis from CO_2 and wet hydrogen by-product from chlor-alkali production. In the simulated process, reactants are first brought to the required temperature and pressure, mixed, and then fed to the reactor, with is simulated by a plug flow reactor (PFR) using the LHHW kinetics. The reactor outlet contains products (CH_3OH and H_2O) as well as unconverted reactants (CO_x and H_2), and then this gaseous mixture is cooled and flashed to separate the condensable products from the non-condensable reactants, which are recycled. The condensed components are then separated in a distillation column, to get into lights (dissolved CO_x and minor light impurities), MeOH and water. Authors included a stripping unit in the process, in which wet hydrogen flows in counter-current mode with the condensed water mixture from the high-pressure low-temperature separator after the reaction. In this way, there is a complete recycle of CO_2 as CO/CO_2 is removed from the methanol-water mixture, and at the same time, by removing water from the wet hydrogen, there are no negative impacts of the reaction equilibrium conversion. The chosen *Property Methods* are the Soave-Redlich-Kwong EOS and NRTL with Henry components. The feed stream entering the PRF reactor is composed of 2.96% mol CO, 25.14% mol CO_2, 71.39% mol H_2, 0.51% mol CH_3OH. The product stream exiting the PRF reactor has a composition of 3.24% mol CO, 22.78% mol CO_2,

63.95% mol H_2, 4.74% mol H_2O, 5.29% mol CH_3OH. The methanol stream exiting the system is characterized by a molar concentration of 0.01% mol H_2, 0.02% mol H_2O, 99.98% mol CH_3OH. The H_2 conversion is 18.17%, while the CO_2 conversion is 17.20% and the MeOH yield of the overall process is 99.83%. In this process, all the carbon from the CO_2 feed is converted into MeOH product, whereas only two thirds of H_2 are converted into MeOH product, while the rest is converted to the water by-product.

Table 11 summarizes the reviewed studies on modelling methanol synthesis. The analysis revealed that the process (either from syngas or CO_2 as main feedstock) has been largely simulated in Aspen Plus. On the other hand, no studies simulating the process of direct methane to methanol (DMTM) conversion in Aspen Plus have been found in literature, probably because the technology is still in the developing phase.

Table 11. Studies reviewed modelling MeOH synthesis in Aspen Plus

Authors	Publication year	Feedstock	Thermodynamic method	Main simulation blocks	MeOH % in the products	Remarks
Atsonios et al. [171]	2015	CO_2	not specified	reactor type not specified (reaction kinetics considered), flash separators, distillation column	99.3% mol	convert captured CO_2 into MeOH
Calogero et al. [169]	2018	CO_2	not specified	RPLUG reactor with LHHW kinetics	99.9% mol	convert captured CO_2 into MeOH, based on Atsonios et al. and Van-Dal et al. studies
Chein et al. [159]	2021	syngas and syngas + captured CO_2	not specified	REQUIL reactor, flash separator	not specified	methanol production from biogas
De María et al. [160]	2013	syngas	NRTL-RK	user-defined reactor developed in Matlab, distillation column	98.1% mol	methanol production from syngas to investigate a kinetic model developed by the authors
Gamero et al. [65]	2018	syngas	PR-BM	REQUIL reactor, distillation column	not specified	methanol production from biomass
Kiss et al. [170]	2015	CO_2	SRK, NRTL	RPLUG reactor with LHHW kinetics, distillation columns, flash separator	99.98% mol	MeOH from CO_2 and wet hydrogen by-product from chlor-alkali production
Mantoan [167]	2019	CO_2	NRTL-RK for low pressures (<10 bar), RKSMHV2 for high pressures (>10 bar)	RPLUG with reaction rates implemented in CHEMCAD, flash separator, distillation column	99.96% wt	convert captured CO_2 into MeOH. Follows Van-Dal et al. Simulation model
Ortiz et al. [70]	2012	syngas	PSRK	RSTOIC reactor with CO conversion per pass of 20% and CO2 conversion per pass of 3%, distillation column	99% MeOH recovery	methanol production from syngas obtained by supercritical water reforming of glycerol
Suhada et al. [161]	2020	CO_2	not specified	REQUIL	not specified	used to convert the CO_2 separated from biogas to methanol
Trop et al. [158]	2014	syngas	PENG-ROB	RPLUG rectors, flash separator, distillation columns	99.98% mass	methanol production from a mixture of torrefied biomass and coal
Van-Dal et al. [164]	2013	CO_2	NRTL-RK for low pressures (<10 bar), RKSMHV2 for high pressures (>10 bar)	RPLUG reactor with LHHW kinetics, RADFRAC distillation column, flash separator	not specified	convert captured CO_2 into MeOH

3.1.3 Preliminary quantitative assessment

In most of the reviewed modelling studies, the technologies suitable for the value chain that we investigate in this thesis work were not simulated as stand-alone units, but they are embedded in wider contexts. Therefore, it was often difficult to extrapolate, whether reported, quantitative information about each specific technology. Moreover, it must be underlined that each work is characterized by its own process conditions, stream compositions, plant configurations (e.g. products separation equipment, recycling streams, etc.) which can be hardly used to perform an accurate comparison among technologies. However, a preliminary quantitative assessment and use of mass balances, and thus process yields, of the models found in the literature is needed to complete the overview of such conversion pathways. Therefore, considering the aforementioned limitations, and focusing on the modelling studies whose application is closer to the sustainable value chain here proposed, **Table 12** has been drafted to report information regarding the mass balances of conversion technologies in the reviewed modelling studies. The table also provides extracts of mass balances related to full value chains.

The study developed by Ashraf et al. [29] is of particular interest, as the pathway encompassed is extremely coherent to that proposed in the present work. In this research, authors considered a relatively small-scale biogas to FT liquids conversion route, including biogas upgrading through PWS, biomethane reforming though DMR, syngas cleaning through chemical absorption with MEA, FT synthesis and products upgrading in distillation columns. The study showed that, for 10,000 Nm^3/h of dry biogas, the process requires 7.08 MW of power in addition to 35 of heating and 185 GJ/h for cooling, and, from 4000 kg/h of methane in the biogas feed, 1602 kg/h of FT products could be produced. The process investigated is thus characterized by a carbon conversion efficiency of 45% and energy efficiency of 30%.

Another article that could be taken as a reference to study the sustainable biofuels production chain proposed is that of Bao et al. [144], even though the feedstock considered in the process is natural gas. The simulated plant converts 900,000 kg/h natural gas to 118,000 bpd of products, through a conversion route involving reforming, FT reaction, and product upgrading.

Table 12. Mass balances reported in the reviewed modelling studies

Technology	Authors	Process feed			Process output			Remarks
		Stream	Amount	Unit	Stream	Amount	Unit	
Overall value chain	Ashraf et al. [29]	Raw biogas	10,000	Nm^3/h	Syncrude	1,602	kg/h	Biogas to FT liquids conversion (PWS, DMR, MEA, FT and upgrading)
	Bao et al. [144]	CH_4	854,961	kg/h	Diesel	139,170	gal/h	NG to FT liquids conversion (reforming, FT reaction, and upgrading)
					LPG	6,310	gal/h	
					Naphta	62,210	gal/h	
AD	Scamardella et al. [105]	Biomass	2	t/d	Biogas	157	Nm^3/d	Feed is composed of fruit waste
Upgrading - PWS	Bortoluzzi et al. [112]	Biogas	1.60E-01	kg/s	$BioCH_4$	4.81E-02	kg/s	
	Cozma et al. [172]	Biogas	604.558	kg/h	$BioCH_4$	229.11	kg/h	
	Gamba et al. [115]	Biogas	49.5	kmol/h	$BioCH_4$	29.2	kmol/h	
	Menegon et al. [111]	Biogas	500	Nm^3/h	$BioCH_4$	276.05	Nm^3/h	
		Biogas	1,000	Nm^3/h	$BioCH_4$	649.23	Nm^3/h	
Upgrading - MEA	Gamba et al. [115]	Biogas	51.9	kmol/h	$BioCH_4$	32.8	kmol/h	
Upgrading - MDEA	Gamba et al. [115]	Biogas	50.2	kmol/h	$BioCH_4$	32.8	kmol/h	
Reforming - DMR+ SMR	Er-Rbib et al. [50]	CH_4	122.326	t/h	Syngas	715.826	t/h	H_2/CO ratio about 2
		CO_2	330	t/h				
		H_2O	263.5	t/h				
FT synthesis	Er-Rbib et al. [50]	Syngas	715.826	t/h	Diesel	67.1	t/h	
					Gasoline	25	t/h	
					LPG	0.3	t/h	
					Other chemicals	0.6	t/h	
	Cinti et al. [145]	Syngas	1532	mol/h	Gasoline	0.15	bbl/day	H2/CO=2.1
					Diesel	0.43	bbl/day	

					WAXC30	0.36	bbl/day	
					Total FT products	1	bbl/day	
	Campanario et al. [123]	Syngas	15,250.2	kg/h	FT diesel	1,374	kg/h	C5-C9
					FT jet fuel	898	kg/h	C10-C13
					FT gasoline	497	kg/h	C14-C20
	Sudiro et al. [143]	Syngas	268	t/h	Gasoline	28.41	t/h	$H_2/CO=2$
					Diesel	69.9	t/h	
					GPL	1	t/h	
					Light gas + unreacted syngas	35.7	t/h	
MeOH synthesis	De María et al. [160]	Syngas	11,449.9	kmol/h	MeOH	3141.6	kmol/h	MeOH from syngas, $H_2/CO=2.94$
	Kiss et al. [170]	Syngas + unreacted prod.	122,003	kg/h	MeOH	1,2508.7	kg/h	MeOH from CO_2 hydrogenation, the reactor is fed with CO_2, H_2 and recycled unreacted products; MeOH
	Perèz-Fortes et al. [168]	CO_2	80.5	t/h	MeOH	55.1	t/h	MeOH from CO_2 hydrogenation, CO2 wt% = 100%, H_2 wt% = 100%
		H_2	11	t/h				MeOH wt% = 99.96%
	Van-Dal et al. [164]	CO_2	88	t/h	MeOH	59.3	t/h	MeOH from CO_2 hydrogenation
		H_2	12.1	t/h				

3.1.4 Discussion on the review findings

After a quality-based initial screening, a total of about 57 reviewed modelling papers were selected among the available literature; these included anaerobic digestion, biogas cleaning and upgrading to biomethane, methane reforming to syngas, syngas conversion to hydrocarbons through Fischer-Tropsch synthesis and MeOH synthesis from syngas and CO_2 hydrogenation.

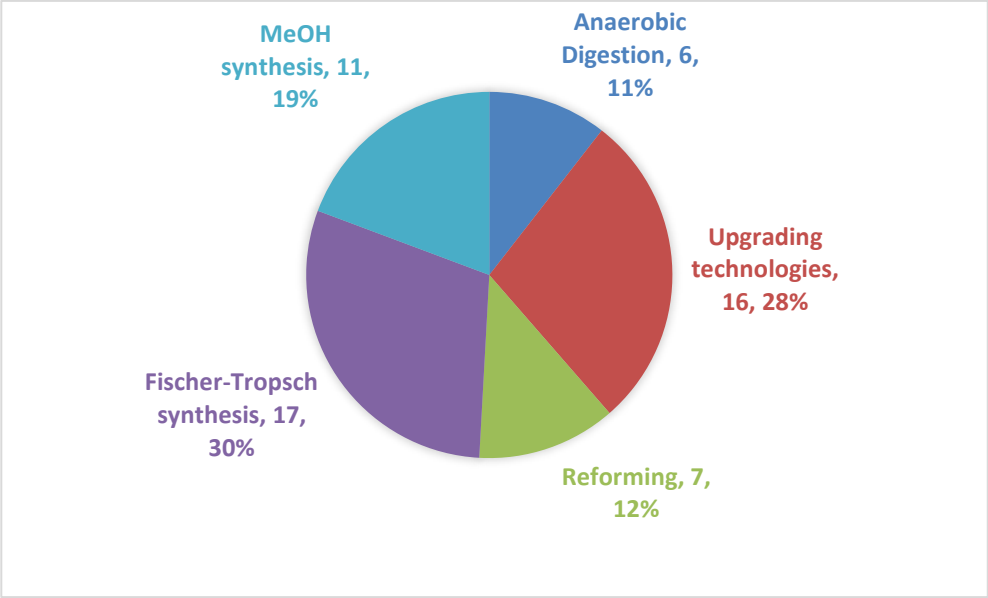

Figure 12. Number of selected studies reviewed and based on Aspen Plus modelling

In the reviewed papers, many of the technologies of interest to this work have not been modelled as stand-alone cases, but are embedded in broader contexts, with more complex flowsheets. For this reason, it was often difficult to extrapolate detailed information on yields and consumptions of the individual processes from their original framework. For example, in the study of Cinti et al. [145], aimed at simulating the production of synthetic green fuels through a system integrating Solid Oxide Electrolyser and FT synthesis, our analysis did not cover the electrolyze unit, but was focused only on modelling the Fischer-Tropsch synthesis.

As discussed, the first step of the value chain under investigation foresees the Anaerobic Digestion process following the BDR model to produce biogas in a sustainable manner. In the literature, no studies that specifically apply this model in Aspen Plus simulation environment have been found. Therefore, we searched for generalized Anaerobic Digestion models, which turned out to be not so numerous (i.e. 6); this could be due to the high complexity of the process, which turns to be particularly difficult to model, especially as regards the biological activity of microorganisms. Nguyen et al. [104] and Scamardella et al. [105] opted for a one-stage model in a single reactor, in which the whole AD phases occurs. In the RSTOIC reactor (used in Nguyen et al. [104]) the reaction kinetics is not

considered, whereas in the RCSTR (used in Scamardella et al. [105]) detailed information on the reactions and their kinetics must be input; this means that the first represents a more simplistic modelling approach. However, the two studies ([104] [105]) refer to different AD models (i.e. Buswell equation; ADM1 and comprehensive models), and the papers do not provide information showing a comparison with experimental data. Al-Rubaye et al. [100] and Rajendran et al. [173] adopted a very similar approach, i.e. a two-step model using a RSTOIC reactor for the hydrolytic phase and a RCSTR reactor for the other AD phases, in reference to the ADM1 and comprehensive models. The two studies have been validated against experimental data, resulting in both cases in a good agreement. The AD model developed by Serrano Peris [101], which involves two RSTOIC reactors in series, does not consider the hydrolytic step, and its application is thus limited to post-hydrolysed wastes. Besides, a higher modelling complexity is given in that of Llanes et al. [106], which integrates ADM1, flow pattern and biofilm characteristics implemented through FORTRAN subroutines; this model is thus not limited to completely mixed flow pattern (as in case of RCSTR reactors), and results agree with experimental data.

Biogas upgrading to biomethane is a fundamental step in the proposed sustainable value chain, as biomethane must comply with strict Country-specific technical standards to be injected in the natural gas grid. Therefore, accurately modelling this step is crucial. In the literature, there is a relevant number of papers (i.e. 16) simulating upgrading processes; these are in large part set in the context of gas sweetening, but nevertheless in some studies ([29], [65], [70]) the upgrading technologies are employed for syngas upgrading (i.e. CO_2 removal). Many of the upgrading processes modelled in Aspen Plus turned out to be the physical absorption (i.e. PWS) and chemical absorption with using amine solutions (i.e. MEA, DEA, MDEA). The modelling approach of these technologies is almost the same in every paper: a distillation column for both absorption and stripping processes. The Aspen Plus distillation unit operation chosen in most of the reviewed simulations was the RADFRAC column, which is the most generic column block type. Some models have opted for an equilibrium-stage approach for both absorption and stripping column, which assumes that each plate of the column is a theoretical plate (equilibrium plate), and thus the vapor and the liquid leave any plate at thermodynamic equilibrium [174]. In other simulations, instead, the distillation columns are rate-based, which means that the mass and energy transfer across the interface are considered using rate equation and mass transfer coefficients; therefore, this approach provides a more rigorous modelling of the columns. At the same time, there are studies ([111], [114]) that opted for a combined equilibrium-based and rate-based approach.

Not many models simulating the pressure swing adsorption process in Aspen Plus were found in the literature. As a matter of facts, the PSA process is a dynamic process and, as Aspen Plus is a steady state calculator, no dynamic options are available in the software. For this reason, many authors preferred to model the

process in Aspen Adsorption, being this a comprehensive flowsheet simulator more specific for adsorption processes. Finally, only one study (i.e. [105]) modelling the biogas upgrading through membrane separation has been found, consisting in a user-defined model developed in Excel referring to the Fick's law with diffusive model assumptions.

About the modelling of the reforming technologies, a discrete number of studies have been found (i.e. 7), most of them assessing the SMR process, which is the most consolidated one in this matter. A good number of papers addressed the process of dry reforming, which is an emerging technology whose reaction kinetics has not been fully described yet. Anyway, there are many studies in which DMR is combined with SMR, as well as POX, while a smaller number of articles assessing the ATR process was found. Most of the reviewed models are aimed at simulating processes for hydrogen production in spite of syngas production, and consequently in many studies SMR is combined to WGS. The modelling approaches of the analysed studies are various: the Aspen Plus reactor blocks employed in the simulations are RGIBBS ([29], [127], [129]), REQUIL ([125], [128]) and RPLUG with Langmuir-Hinshelwood-Hougen-Watson (LHHW) kinetics ([42], [126]). The RPLUG reactor type, that unlike the RGIBBS and the REQUIL encompasses the process reaction kinetics, allows for a complete description of the process under variable conditions and proper reactor sizing; however, a suitable reaction set and the relative kinetic model and thermodynamic data must be provided [175].

A large number of studies (i.e. 17) modelling the Fischer-Tropsch process in Aspen Plus has been found in the literature. As mentioned, the FT process is particularly complex and the full understanding of all mechanisms involved has not yet been reached, though it is not a novel technology. The reference model for most of the reviewed articles is the Anderson-Schulz-Flory (ASF) distribution, a fairly simple model which gives a reasonable description of FT products by representing the synthesis as an addition polymerization reaction with chain growth probability α [176] [137]. Nevertheless, despite the mathematical simplicity of the ASF model, studies have shown that there are deviations of the FT product composition from the ideal distribution (i.e., higher methane selectivity, lower ethylene selectivity, increasing chain growth probability, and lower olefin-to-paraffin ratio with increasing carbon number) [148], [154], [177], [152]; therefore, correlations accounting for the ASF distribution deviations and dependence of α on process conditions have been developed and are well documented in literature [135], [136], [137], [147], [155], [130], [156], [157]. In many modelling studies reviewed, the produced hydrocarbons have been assumed to be composed only by paraffins; this assumption is acceptable, as the alkanes are the main product of the FT synthesis. However, there is also a large number of studies considering olefins in the products, while only one model (i.e. Dahl [154]) among those found includes also alcohols. Moreover, it was noticed that in many studies ([141], [144], [145], [152]) the chain growth probability α has a constant value, while others use correlations to relate its values to the process conditions; the most used expression in the reviewed papers

is the one derived by Song et al. [135]. Another significant parameter for determining the accuracy of a FT model is the carbon number (*n*) for the product chain termination; in the modelling studies reviewed, this number was found to be always higher than 20 for the main products (i.e. paraffins). Setting a high *n* for the hydrocarbon chain termination definitively represents a higher accuracy in describing the Fischer-Tropsch synthesis; in facts, the product slate synthesized ranges from methane up to C-120+ [134]. However, as the product selectivity significantly decreases after peaking at around C-7 to C-13 (depending on the process conditions and the catalyst), cutting the chain from n=20 could be considered as satisfactory.

Most of the reviewed Aspen Plus models employ reactor types such as RSTOIC and RYIED, in which the reaction kinetics is not explicitly considered, and the product distribution is imposed. Nevertheless, a small number of modelling studies assessing the FT synthesis reaction kinetics (through external subroutine) were also found (i.e. [129], [148], [150], [154]); these models provide a higher flexibility when changing the process conditions.

As concerns the MeOH synthesis from syngas, 5 studies have been found, whose modelling procedures are diverse. Some authors did not consider the reaction kinetics, opting for a RSTOIC reactor ([70]) or for a REQUIL reactor ([65], [159]), which performs chemical and phase equilibrium reactions. At the same time, De Maria et al. [160] and Trop et al. [158] described the reaction kinetics of the catalytic reaction, using, in the former case, an user-defined reactor type developed in Matlab, and a RPLUG reactor in the latter case.

Additionally, opportunities for further pathways have been investigated, including methanol synthesis from captured CO_2, which represents an excellent opportunity from an environmental sustainability point of view. Indeed, CCS and CCU technologies, if associated with bioenergy, offer a promising pathway towards not just carbon neutrality, but potentially carbon negativity.. In this perspective, in the proposed bioliquids production chain, the CO_2 separated from biogas through upgrading processes acts as an additional resource for MeOH production. Lots of studies simulating this in Aspen Plus have been found (i.e. 7), meaning that this topic is of great interest to the scientific community. The modelling approaches of the MeOH synthesis from CO_2 adopted in the reviewed papers are very similar to those of the case of syngas as a feedstock: REQUIL reactor ([159], [161]) and RPLUG reactor with LHHW kinetics ([162], [164], [169], [170], [167]).

As an alternative to MeOH synthesis from syngas, the straight conversion of methane into methanol (DMTM) could be an interesting route, as it gives the possibility to by-pass the very energy intensive step of methane reforming, representing an economical-advantage and environment-friendly option. However, as mentioned, this method still needs to be improved to be suitable for industrial applications. As a matter of facts, no Aspen Plus models simulating this process have been found in literature.

3.2 Model development

The model focuses on the part of the value chain related to the GTL plant, starting with methane extracted from the grid, followed by its reforming into syngas and subsequent conversion into liquid biofuels (FT liquids, MeOH, jet fuel).

For the GTL-FT and GTL-MeOH routes, this entire process is executed within Aspen Plus. In the case of the GTL-F_ATJ route, specifically the fermentation and ATJ conversion stages, we relied on references from the literature for yield and energy consumption data.

The Aspen Plus simulation model builds upon the findings presented in Chapter 2 and published in [178]. It is the outcome of selecting and combining the analysed models, integrating them into a cohesive framework.

Both the SMR and POX methods have been modelled. The modelling strategy and process conditions draw from reference simulation models: Ayad et al. [48] for POX, and Er-Rbib et al. [179] for SMR.

While the POX process generates syngas with a hydrogen to carbon monoxide ratio (H_2/CO) of 2, which is the optimal ratio for FT and MeOH synthesis, it is important to note that the syngas produced by the SMR process has an H_2/CO ratio higher than 2, resulting in an excess of hydrogen. The model thus incorporates a separator after the SMR reforming stage in the models. This separator enables one to obtain one stream with the desired H_2/CO ratio, directing it to the synthesis reactor. Simultaneously, another stream contains the excess hydrogen, treated as a separate final and additional refinery product that can be marketed alongside the primary products.

3.2.1 GTL-FT model

As previously stated, the initial phase of the model focuses on methane reforming, either through Steam Methane Reforming (SMR) or Partial Oxidation (POX). The objective is to generate syngas with an optimal hydrogen to carbon monoxide ratio (H_2/CO) set at 2.

As concerns the section dedicated to Fischer-Tropsch synthesis, the reference model and specific process conditions are taken from the Dahl's work [180] described in Chapter 2.

Recalling and summarizing the key features of the reference model, it encompasses two RSTOIC reactors: FT-R1 and R-C2H4.

FT-R1 primarily describes FT reactions based on the Anderson–Schulz–Flory (ASF) distribution model. This reactor employs the Hillestad model, lumping higher hydrocarbons, and considers the formation of n-paraffins, 1-olefins, and 1-oxygenates (alcohols). Paraffin products up to C20 are individually listed, while

those exceeding C20 are grouped into a pseudocomponent (C21+ lump) with calculated average carbon number, average weight, and normal boiling point. Olefin products up to C10 are specified, and those beyond are lumped into a C11+ category. Oxygenate products up to C5 are individually detailed, and a lumped C6+ category is provided. An additional CH_4 reaction is incorporated to address the underestimation of methane formation given by the ASF deviation.

The second reactor specifically targets the overestimation of ethylene.

The combined output from the two reactors includes water, off-gas (C1-C4), and syncrude, categorized by carbon content: naphtha (C5-C9), kerosene (C10-C16), diesel (C17-C21), and waxes (C21+). The model is confined to this product distribution and does not account for any subsequent refinement of the waxes.

Operational conditions tested include a pressure of 27.6 bar, a temperature of 220°C.

3.2.2 GTL-MeOH model

As mentioned in the introduction, the section dedicated to reforming is identical to that of the model for the GTL-FT route. This is because both methanol synthesis and Fischer-Tropsch synthesis require a hydrogen to carbon monoxide ratio (H_2/CO) equal to 2.

As for the MeOH synthesis from syngas, the reference simulation model considered for the methanol synthesis unit is Gamero et al. [181].

3.2.3 GTL-F_ATJ model

The simulation of the methane reforming stage follows the approach used for other examined routes and is carried out in Aspen Plus. For this route, the simulation model employs the Steam Methane Reforming (SMR) technology with the goal of achieving a syngas H_2/CO ratio of 2.

To model the syngas fermentation process, just appearing on the market[2], insights from literature reviews and industrial data were utilized, particularly drawing on information from [182] for its technological details, as well as [183] and [184]. It is worth noting that the gas fermentation process demonstrates versatility, accommodating a broad range of H_2/CO gas compositions [185].

Data pertaining to the alcohol-to-jet (ATJ) process was then gathered from [90].

It is crucial to emphasize that SMR was chosen as the reforming technology for this pathway due to the ATJ process's demand for hydrogen during the CO_2 hydrogenation phase. The integration of hydrogen production within the refinery,

[2] Indeed, the ATJ pathway has been certified under ASTM specifications ASTM D7566 Annex 5 for the production of drop-in aviation fuel in April 2016 for isobutanol as feedstock, and June 2018 for ethanol [199]

in conjunction with syngas generation, presents potential advantages. Additionally, any excess hydrogen produced can be commercially utilized alongside the primary product, jet fuel.

Chapter 4 Results and discussion

4.1 Model results

This chapter reports the outcomes derived from the simulation model. The paragraph is structured into three primary segments: the initial segment discloses findings related to the GTL-FT route, followed by the subsequent segment which showcases results from the GTL-MeOH pathway. In both instances, the results are presented whether the refinery utilizes POX or SMR. Lastly, the third part encompasses assessments pertaining to the GTL-F_ATJ route.

4.1.1 GTL-FT route

POX scenario

In the assumed scenario of a 10,000 barrels per day (bpd) GTL FT-based plant using POX, results from the simulation model indicate a demand for approximately 2.8 million cubic meters per day (1.02 billion cubic meters per year) of biomethane. Assuming the refinery is supplied by biogas facilities of 1 MWe equivalent capacity, this would theoretically result in approximately 516 plants needed to adequately support this specific refinery configuration. The 1 MWe size has been considered since it was the reference dimension in the previous Italian decrees, supporting biogas for renewable heat and power generation: thus, there is a large network of plants potentially available for retrofitting to biomethane. It is however worth to remark, however, that typical biomethane plants have in average a larger size, of some 2-3 to 5 MWe capacity: therefore, the calculation of the number of plants needed is for reference only and could be considerably reduced if different biomethane sizes are considered, and the market grows as expected.

In terms of power requirements, the GTL plant calls for approximately 28.85 MW of electricity and 197.77 MW for cooling duties.

The distribution of products from this GTL plant is given in **Table 13**.

Product	[bpd]	[tonne/day]
Naphtha (C5-C9)	2,981	218.74
Kerosene (C10-C16)	2,240.6	221.91
Diesel (C17-C21)	956.8	94.92
Waxes (C21+)	3,821.6	474.56

Table 13. 10,000 bpd GTL FT-based plant: products distribution

Figure 13**Figure 13** provides the mass and energy balance of the value chain, including: the oxygen generated by the Air Separation Unit (ASU) for supply to the

Partial Oxidation (POX) segment, the resultant off gas from the overall process, and the water produced via the Fischer-Tropsch synthesis.

It is however also possible to implement smaller scale FT units - of the order of 1,000 bpd of products - given the status of technology development in this field and by decoupling biomass sourcing for biomethane from its conversion in existing refineries: this strongly reduce the need for biomass mobilization compared to a centralized approach. At the same time, the possibility to feed a full industrial scale fossil refinery with large volumes of biomethane through Guarantees of origin will deliver better performances.

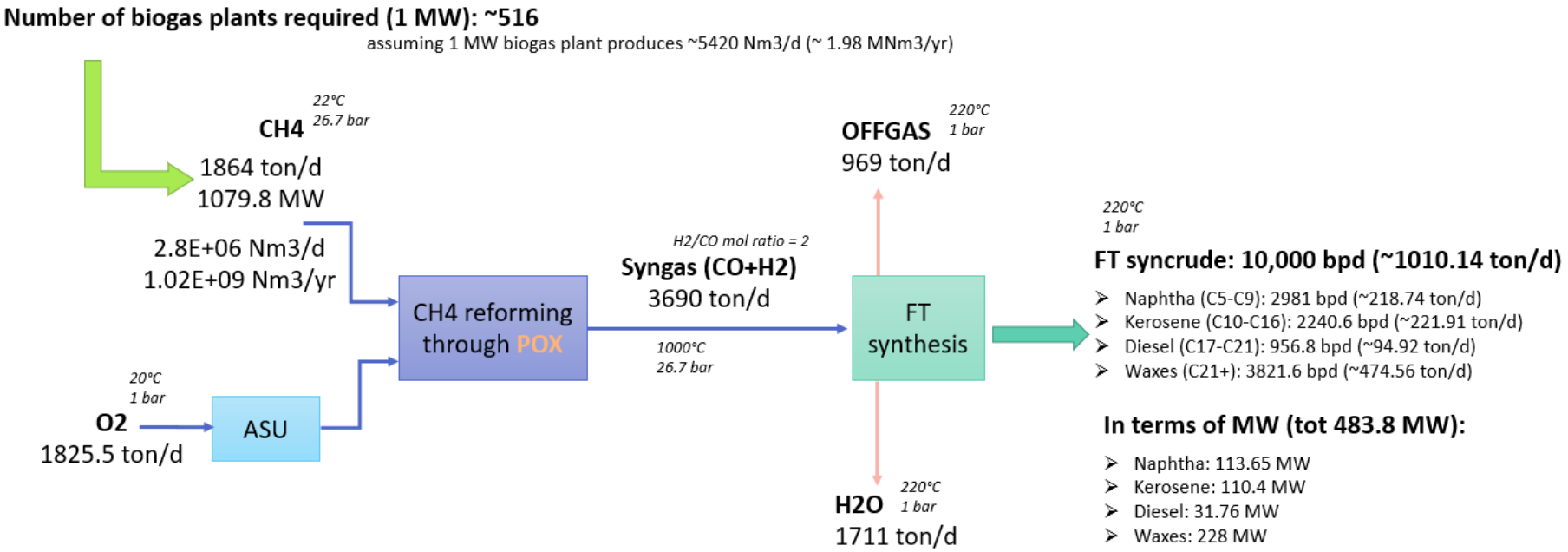

Figure 13. 10,000 bpd GTL-FT based plant (POX scenario): simulation results

SMR scenario

In the case that the 10,000 bpd GTL FT-based refinery employs SMR, the model indicates a demand for approximately 6.1 million cubic meters per day (equivalent to 2.23 billion cubic meters per year) of biomethane. Assuming again the refinery is theoretically supplied by AD facilities with a capacity of 1 MWe each, this dimension would require approximately 1.128 plants to adequately support this specific refinery configuration. As an additional product, the plant produces about 1063 tonne/d of hydrogen.

In terms of power requirements, the GTL plant requires around 985.38 MW of electricity, 664.5 MW for heating duties, and 242.94 MW for cooling duties. Results are shown in **Figure 14**.

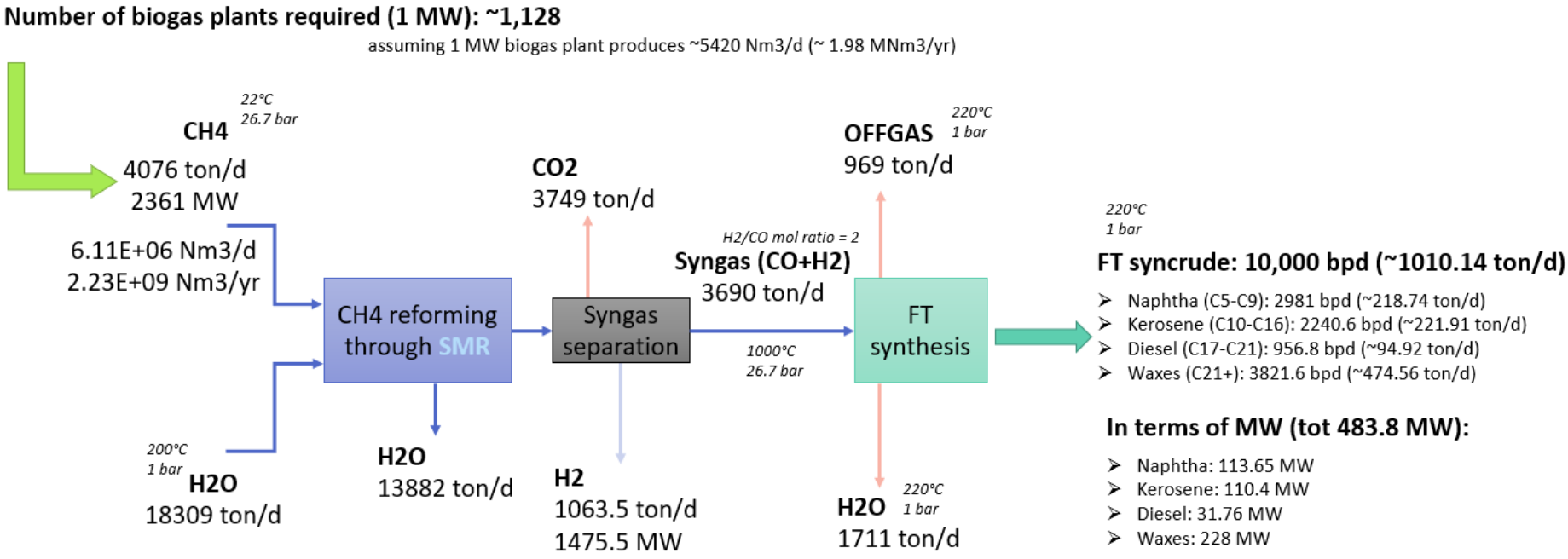

Figure 14. 10,000 bpd GTL-FT based plant (SMR scenario): simulation results

4.1.2 GTL-MeOH route

POX scenario

For a GTL MeOH industrial plant processing 2,000 tonnes per day, the model calculated a demand of around 1.82 million cubic meters per year (1.82 million cubic meters per day) of biomethane. Assuming the refinery is supplied by biogas facilities with a 1 MWe equivalent capacity, approximately 336 such plants would be required to sufficiently support this specific refinery configuration.

Regarding power requirements, the GTL plant needs about 73.48 MW of electricity (primarily for compressor operation) and 176.83 MW for cooling purposes.

Figure 15 provides a complete mass and energy balance of the modelled value chain.

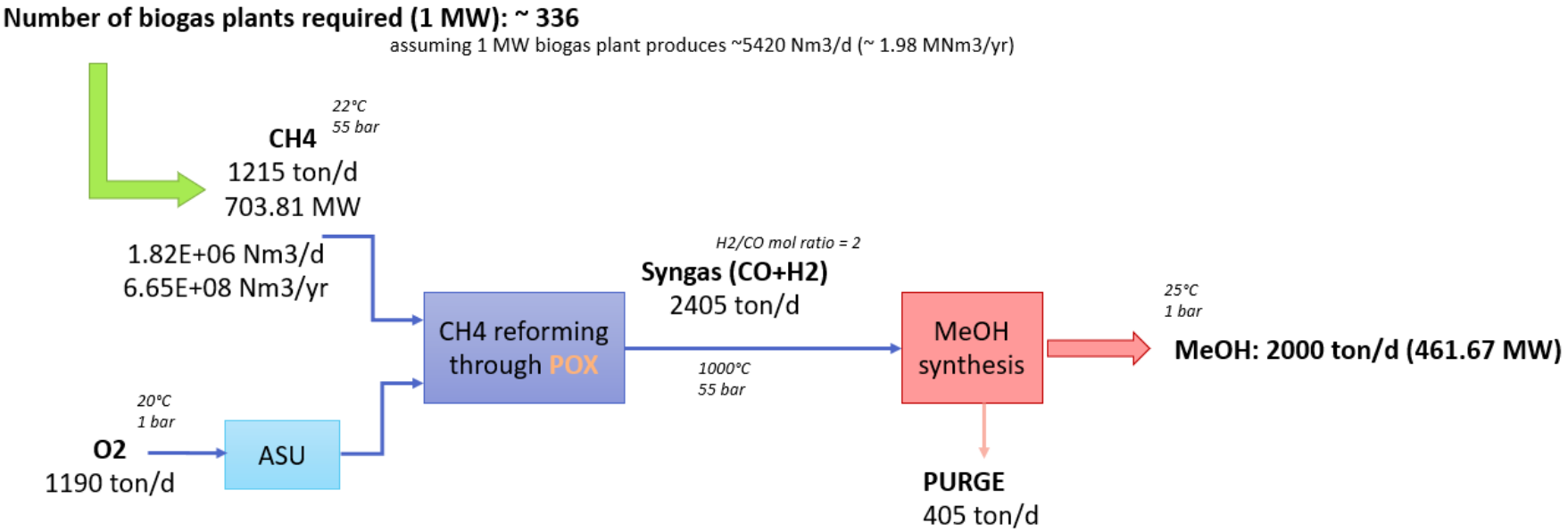

Figure 15. 2,000 tonne/day GTL-MeOH based plant (POX route): simulation results

SMR scenario

For a GTL MeOH industrial facility processing 2,000 tonnes daily with SMR, the simulation model indicates a biomethane demand of roughly 3.98 million cubic meters annually (equivalent to 1.45 million cubic meters daily). Assuming the refinery is supplied by biomethane facilities with a 1 MWe equivalent capacity, 735 such plants would be necessary to adequately feed this specific refinery configuration. Additionally, the plant generates approximately 693.2 tonnes of hydrogen per day. In terms of power requirements, the GTL plant necessitates around 690.2 MW of electricity, primarily for compressor operation, 433.2 MW for heating duties, and 256.8 MW for cooling purposes. **Figure 16** shows the mass and energy balance of this specific case.

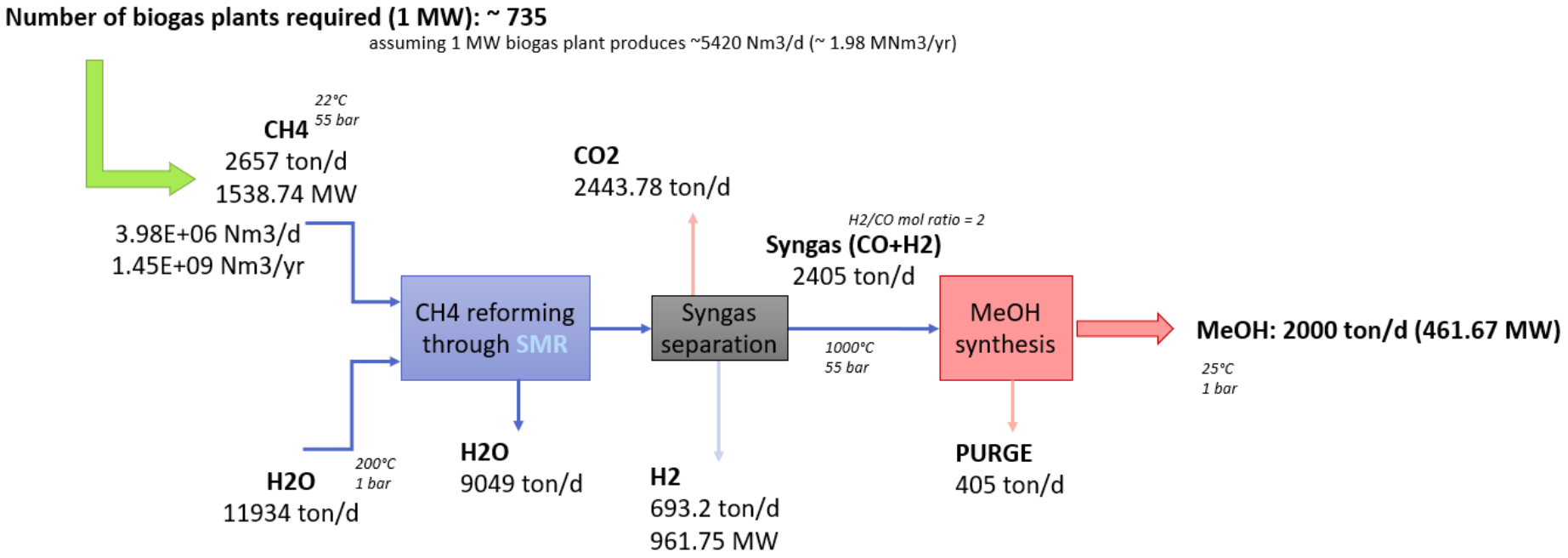

Figure 16. 2,000 tonne/day GTL-MeOH based plant (SMR route): simulation results

4.1.3 GTL-F_ATJ route

This type of GTL plant produces 1,000 tonnes per day of valuable products, such as about 100 tonnes per day of gasoline, 700 tonnes per day of jet fuel and 200 tonnes per day of diesel.

The model indicates a requirement of approximately 6.64 Mm^3 per day (2.42 billion cubic meters per year) of biomethane. This would translate into 1,226 biomethane plants at the 1 MWe reference capacity.

Additionally, as the process requires 11.1 t/d of hydrogen, it will also generate the extra yield of 1,144 t/d of hydrogen from SMR, alongside the production of jet fuel, gasoline, and diesel.

The total electric power required by the system for electricity is about 278.12 MW, the total thermal power for heating duties is about 722 MW, while for cooling duties it is about 902.23 MW. Please note that the power requirement calculation did not account for the syngas fermentation section due to the absence of comprehensive and non-aggregated information on the consumption of this innovative process in the literature. **Figure 17** reports the mass balance of the process.

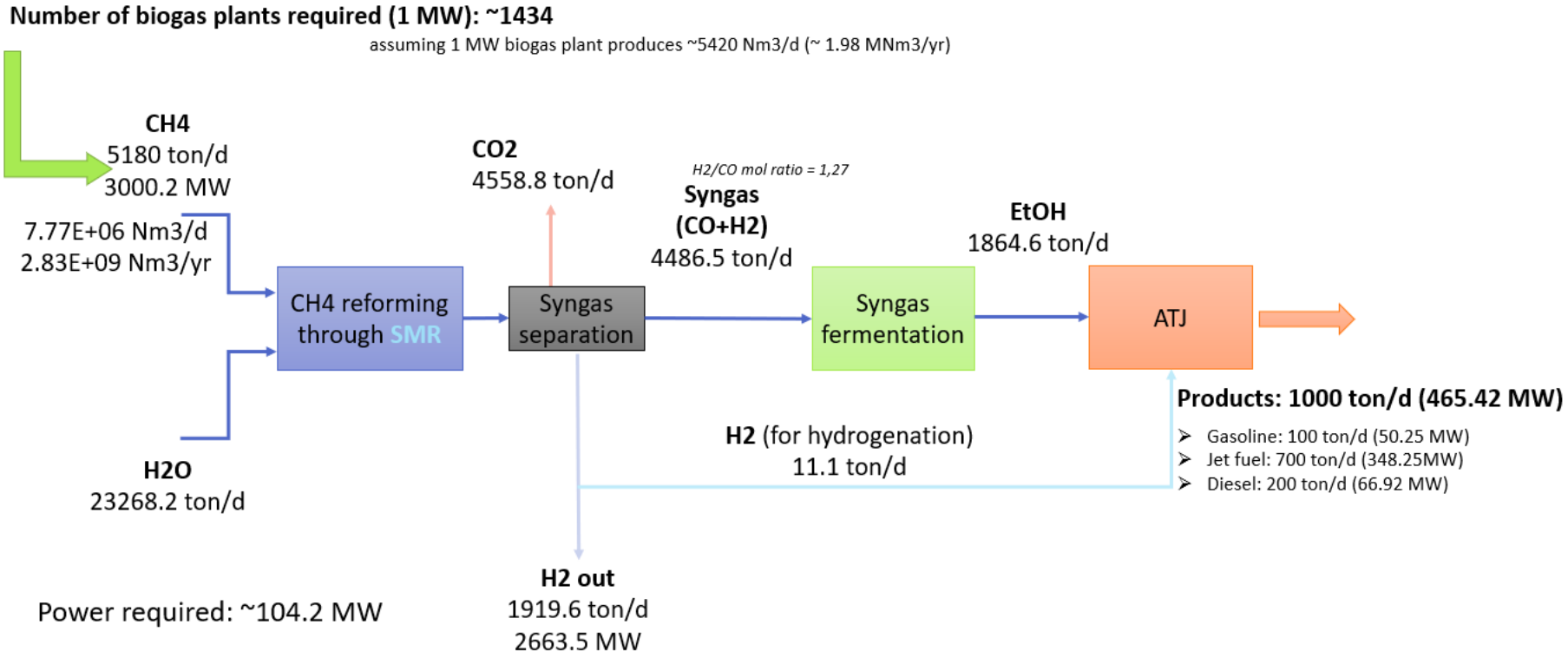

Figure 17. 1,000 tonne/day GTL-F_ATJ based plant: model results

4.2 Discussion

In this study, three distinct pathways for the production of advanced liquid biofuels are examined, all sharing a common decentralized feedstock and sustainable biomethane production model, known as the Biogasdoneright model, with biogas upgrading to biomethane and injection into the natural gas grid. Additionally, for the GTL-FT and GTL-MeOH routes, we explored two different options, namely the use of Steam Methane Reforming (SMR) and Partial Oxidation of Methane (POX) as reforming technologies, considering energy consumption, efficiencies, and resulting by-products in each case.

It is important to clarify that the results of the model represent preliminary estimates, and that further investigation and energy optimization are still necessary. For instance, in the GTL plants, heating could potentially be achieved through methane combustion rather than relying solely on electric energy, or by recovering thermal waste. Similarly, refrigeration methods could also benefit from exploration and potential optimization.

Table 14 Table 14 reports the conversion efficiencies (MJ of product per MJ of CH4 as feedstock) of the three GTL routes and their various configurations, calculated based on the higher heating values (HHV) of the fuels. The demand of electric energy is not considered in this evaluation, as it primarily focuses on the direct conversion efficiency of methane to final products. However, it is important to note that in the results chapter, we have also provided data on electricity requirements and heat. This additional information offers a more comprehensive understanding of the energy dynamics involved in the GTL processes, enabling a thorough assessment of both direct conversion efficiencies and overall energy balance.

Table 15 presents results in terms of yields (tonnes of products per tonnes of CH_4) and potentials for FT liquids, MeOH, and ATJ products production from biomethane in Italy (IT) and the European Union (EU), projected for the years 2030 and 2050. Additionally, the table highlights alternative methane reforming options to syngas and shows the potential hydrogen production for each route. Details on the potential production of biomethane in Italy and Europe are sourced from the Gas for Climate [186], and will be further discussed in the following, for comprehensive understanding of these figures.

Route	Product	POX [MJ/MJ_{CH4}]	SMR [MJ/MJ_{CH4}]
GTL-FT	*Naphtha*	0.102	0.047
	Kerosene	0.099	0.045
	Diesel	0.042	0.019

	Waxes	0.211	0.096
	Hydrogen	-	0.666
	Total	**0.454**	**0.874**
GTL-MeOH	*Methanol*	0.682	0.312
	Hydrogen	-	0.666
	Total	**0.682**	**0.978**
GTL-F_ATJ	*Gasoline*	-	0.019
	Jet fuel	-	0.132
	Diesel	-	0.037
	Hydrogen	-	0.660
	Total	**-**	**0.847**

Table 14. MJ of products per MJ of CH_4 as feedstock for the three GTL routes

Table 15. FT liquids, MeOH, ATJ products, and H_2 production potential from biomethane in IT and EU, in 2030 and 2050

	Year	CH_4 potential [Mtonne/year]	Reforming process	Conversion route	Fuel yield [tonne fuel/tonne CH_4]	H_2 yield [tonne fuel/tonne CH_4]	Liquid fuel [Mtonne/year]	H_2 [Mtonne/year]
IT	**2030**	3.68	SMR	GTL-FT	0.2478	0.2609	0.91	0.96
			POX	GTL-FT	0.5418	-	1.99	-
			SMR	GTL-MeOH	0.7500	0.2609	2.76	0.96
			POX	GTL-MeOH	1.6500	-	6.07	-
			SMR	GTL-F_ATJ	0.2258	0.2600	0.83	0.95
	2050	5.39	SMR	GTL-FT	0.2478	0.2609	1.34	1.41
			POX	GTL-FT	0.5418	-	2.92	-
			SMR	GTL-MeOH	0.7500	0.2609	4.04	1.41
			POX	GTL-MeOH	1.6500	-	8.89	-
			SMR	GTL-F_ATJ	0.2258	0.2600	1.22	1.39
EU	**2030**	24.97	SMR	GTL-FT	0.2478	0.2609	6.19	6.51
			POX	GTL-FT	0.5418	-	13.53	-
			SMR	GTL-MeOH	0.7500	0.2609	18.72	6.51
			POX	GTL-MeOH	1.6500	-	41.19	-
			SMR	GTL-F_ATJ	0.2258	0.2600	5.64	6.45
	2050	59.79	SMR	GTL-FT	0.2478	0.2609	14.82	15.60
			POX	GTL-FT	0.5418	-	32.39	-
			SMR	GTL-MeOH	0.7500	0.2609	44.84	15.60
			POX	GTL-MeOH	1.6500	-	98.65	-
			SMR	GTL-F_ATJ	0.2258	0.2600	13.50	15.45

Based on modelling results, when considering the POX option, both GTL-FT and MeOH exhibit higher yields in terms of methane conversion into the main products of interest, namely SAF (kerosene) and MeOH. **Figure 18** and **Figure 19** provide a comparative analysis of conversion efficiencies (MJ of product per MJ of CH_4 as feedstock) between the two options, POX and SMR, for both the GTL-FT and GTL-MeOH cases.

Nevertheless, in the case of SMR utilization, there is a noteworthy production of hydrogen, a highly valuable commodity in any refinery operations.

When considering the implementation of SMR and POX within an industrial complex, several crucial factors must be carefully considered. These factors encompass existing infrastructure, operational requirements, feedstock availability, and environmental impact.

SMR stands out for its ability to provide a stable and reliable hydrogen supply, a critical necessity for processes demanding consistent access to hydrogen. SMR relies on a steady supply of natural gas and steam, typically readily available in industrial settings. In contrast, POX, in addition to methane, necessitates a source of oxygen or air, which adds complexity to feedstock supply considerations within the complex. Furthermore, addressing environmental concerns is of paramount importance. Carbon capture and utilization (CCU) or storage (CCS) technologies must be implemented to mitigating these emissions if using fossil natural gas, while in case of biomethane these technologies would represent a BECCS/U path, i.e. a BioEnergy with Carbon Capture and Storage or Utilization.

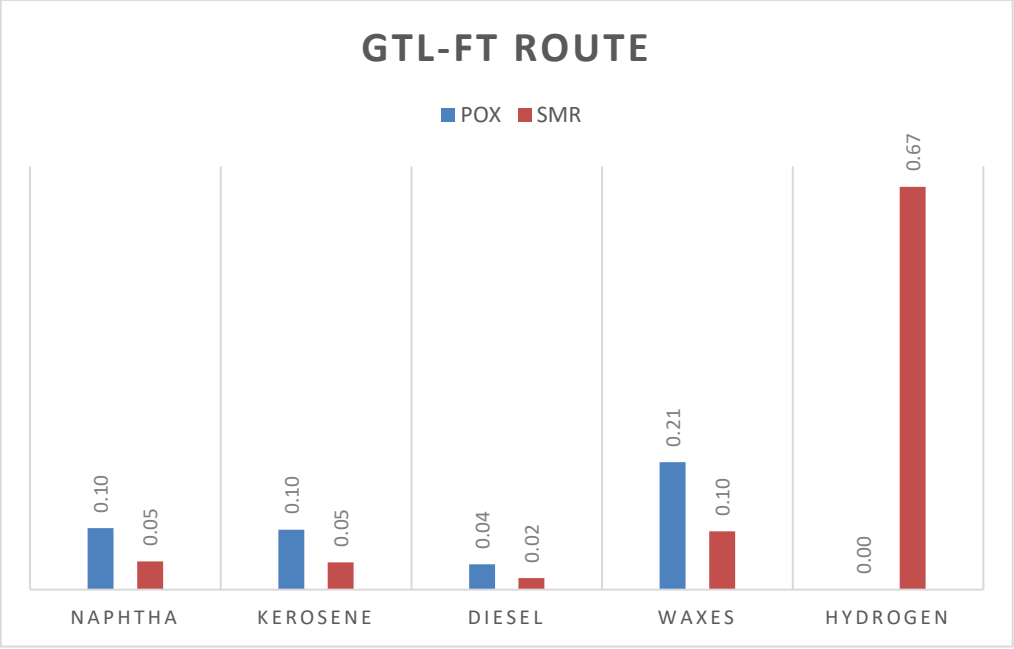

Figure 18. Comparison between POX and SMR reforming configurations in terms of feedstock conversion (MJ of product per MJ of CH_4 as feedstock) for the GTL-FT route

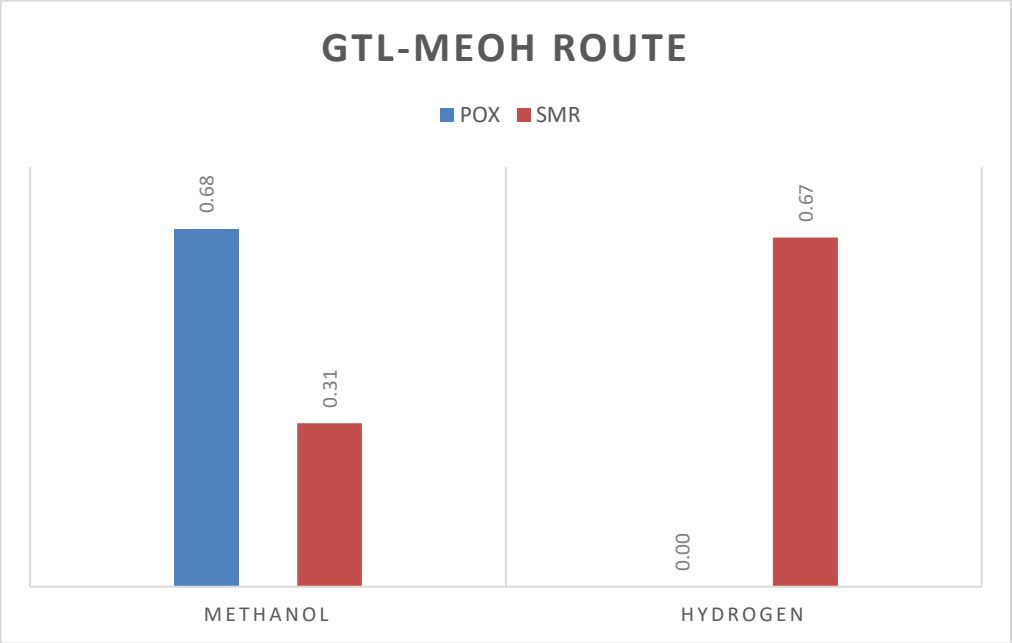

Figure 19. Comparison between POX and SMR reforming configurations in terms of feedstock conversion (MJ of product per MJ of CH4 as feedstock) for the GTL-MeOH route

The possibility of utilizing existing refineries in Europe to implement the three routes described in the article presents both opportunities and challenges. Europe currently has 89 operational refineries and 35 closed ones [187], as indicated in **Table 16**. **Figure 20** displays the corresponding geographic distribution. On one hand, leveraging existing infrastructure can offer significant economic advantages, as it avoids the substantial capital investment required for building entirely new facilities. Additionally, retrofitting existing refineries can accelerate the adoption of these pathways, potentially addressing the pressing need for cleaner and more sustainable energy sources. However, it is essential to consider that the scale of existing refineries may not always align with the optimal size for the proposed routes in terms of economics and environmental performance, and that the FT is not deployed at scale in the EU.

Refinery name	Country	Owner(s)	Capacity [Kbbl/d]	Capacity [Mt/yr]	Status
Agii Theodori (Corinth)	Greece	MotorOil Hellas	171	8.7	Open
Antwerp	Belgium	ExxonMobil	307	15.6	Open
Antwerp	Belgium	TotalEnergies	332.9	16.9	Open
Antwerp	Belgium	Gunvor	0	0	Closed
Antwerp	Belgium	APC (Vitol)	0	0	Closed
ASESA	Spain	CEPSA/REPSOL	19	1	Open
Aspropyrgos	Greece	Hellenic	140.6	7.1	Open
Augusta	Italy	Sonatrach	198	10	Open
Bayern oil	Germany	ENI/VARO/ROSNEFT	215	10.9	Open
Berre	France	LyondellBasell	0	0	Closed

Bilbao	Spain	Repsol	220	11.2	Open
Brunsbuttel	Germany	TotalEnergies	15.2	0.8	Open
Burgas	Bulgaria	Lukoil	115.2	5.8	Open
Burghausen	Germany	OMV	75.1	3.8	Open
Busalla	Italy	IPLOM	34.2	1.7	Open
Cartagena	Spain	Repsol	220	11.2	Open
Castellon	Spain	BP	104.5	5.3	Open
Collombey	Switzerland	Tamoil	0	0	Closed
Corytonne	United Kingdom	Petroplius	0	0	Closed
Cremona	Italy	TAMOIL	0	0	Closed
Cressier	Switzerland	Varo Holdings (JV of AtlasInvest & Vitol Group)	64.6	3.3	Open
Donges	France	TotalEnergies	215.9	10.9	Open
Dundee	United Kingdom	Nynas	0	0	Closed
Dunkerque	France	Colas	0	0	Closed
Dunkerque	France	TotalEnergies	0	0	Closed
Eastham	United Kingdom	Nynas/Shell	22.8	1.2	Open
Elefsis	Greece	Hellenic	100.7	5.1	Open
Falconara	Italy	API	82.9	4.2	Open
Fawley	United Kingdom	ExxonMobil	260	13.2	Open
Feyzin	France	TotalEnergies	107.7	5.5	Open
Fos	France	ExxonMobil	133	6.7	Open
Fredericia	Denmark	Shell	67	3.4	Open
Gdansk	Poland	Lotos	199.5	10.1	Open
Gela	Italy	ENI	0	0	Closed
Gelsenkirchen	Germany	BP	264.7	13.4	Open
Gonfreville	France	TotalEnergies	248.9	12.6	Open
Gothenburg	Sweden	Nynas	11.4	0.6	Open
Gothenburg	Sweden	Preem	106	5.4	Open
Gothenburg	Sweden	St1 Refinery	80	4.1	Open
Grandpuits	France	TotalEnergies	0	0	Closed
Grangemouth	United Kingdom	Petroineos	150	7.6	Open
Hamburg/Neuhoff	Germany	H&R	15.3	0.8	Open
Harburg	Germany	Nynas	31.8	1.6	Open
Harburg	Germany	Shell	0	0	Closed
Harburg (Holborn)	Germany	Tamoil	99.8	5.1	Open
Heide	Germany	RHG (Klesch)	85.9	4.4	Open
Huelva (La Rabida)	Spain	CEPSA	180.5	9.2	Open
Humber	United Kingdom	Phillips66	221	11.2	Open
Humberside (Lindsey OilRefinery)	United Kingdom	Prax Group	107.6	5.5	Open
Ingolstadt	Germany	Gunvor	104.5	5.3	Open
ISAB Priolo & Melilli	Italy	ISAB Refinery (Lukoil)	304	15.4	Open

Jaslo	Poland	Lotos	0	0	Closed
Jedlicze	Poland	PKN Orlen	2.9	0.1	Open
Kalrsruhe	Germany	MiRO (Phillips66/Exxon Mobil/Shell/Bundesnetzagentur)	287	14.5	Open
Kalundborg	Denmark	Equinor	106.4	5.4	Open
Kolin	Czech Republic	Koramo (PKN Orlen)	0	0	Closed
Kralupy	Czech Republic	CRC (PKN Orlen/ENI/Shell)	59.9	3	Open
La Coruna	Spain	Repsol	120	6.1	Open
La Mede	France	TotalEnergies	0	0	Closed
Lavera	France	Petroineos	207.1	10.5	Open
Leca	Portugal	Galp Energia	0	0	Closed
Leuna	Germany	TotalEnergies	224	11.4	Open
Lingen	Germany	BP	88.5	4.5	Open
Litvinov	Czech Republic	CRC (PKN Orlen/ENI/Shell)	97.9	5	Open
Livorno	Italy	ENI	84	4.3	Open
Lubrisur	Spain	CEPSA	0	0	Closed
Lysekil	Sweden	Preem	210	10.6	Open
Mantova (Frassino)	Italy	MOL	0	0	Closed
Mazeikiu (Lietuva)	Lithuania	PKN Orlen	190	9.6	Open
Milford Haven	United Kingdom	Murco	0	0	Closed
Mongstad	Norway	Statoil	208	10.5	Open
Naantali	Finland	Neste	0	0	Closed
Navodari (Constanza)	Romania	Petromidia (KMG International)	104.5	5.3	Open
NRC (Rotterdam)	Netherlands	BP	393.8	20	Open
Nynasham	Sweden	Nynas	30.5	1.5	Open
Pardubice	Czech Republic	Paramo (PKN Orlen)	0	0	Closed
Pembroke	United Kingdom	Valero	210	10.6	Open
Pernis	Netherlands	Shell	404	20.5	Open
Petit Couronne	France	Petroplus	0	0	Closed
Pitesti	Romania	Arpechim (Petrom)	0	0	Closed
Plock	Poland	PKN Orlen	337	17.1	Open
Ploiesti	Romania	Petrobrazi (OMV Petrom)	81.9	4.2	Open
Ploiesti	Romania	Petrotel (Lukoil)	51.6	2.6	Open
Ploiesti (Vega)	Romania	Rompetrol	0	0	Closed
Port-Jerome	France	ExxonMobil	235.5	11.9	Open
Porto Marghera	Italy	ENI	0	0	Closed
Porvoo	Finland	Neste	205	10.4	Open
Puertollano	Spain	Repsol	150	7.6	Open
RAM (Milazzo)	Italy	ENI/KPI	241.3	12.2	Open
Ravenna	Italy	ALMA	9.5	0.5	Open
Reichstett	France	Petroplus	0	0	Closed

Rheinland	Germany	Shell	325	16.5	Open
Rijeka	Croatia	INA	90.2	4.6	Open
Roma	Italy	TotalERG	0	0	Closed
Rotterdam	Netherlands	ExxonMobil	191	9.7	Open
Rotterdam	Netherlands	Gunvor	0	0	Closed
Rotterdam	Netherlands	Vitol (VPR Energy)	80	4.1	Open
Salzbergen	Germany	H&R	7	0.4	Open
San Roque	Spain	CEPSA	237.5	12	Open
Sannazzaro	Italy	ENI	200	10.1	Open
SARA	France	SARA	17.3	0.9	Open
Sarroch	Italy	SARAS	300	15.2	Open
Schwechat	Austria	OMV	193.7	9.8	Open
Schwedt	Germany	PCK (Shell/Bundesnetzgentur/ENI)	220	11.2	Open
Sines	Portugal	Galp Energia	226	11.5	Open
Sisak	Croatia	INA	0	0	Open
Sisak	Croatia	INA	0	0	Closed
Slagen	Norway	ExxonMobil	0	0	Closed
Slovnaft (Bratislava)	Slovakia	MOL	106.4	5.4	Open
Stanlow	United Kingdom	Essar	195	9.9	Open
Szazhalombata (Duna)	Hungary	MOL	153.9	7.8	Open
Taranto	Italy	ENI	84	4.3	Open
Tarragona	Spain	Repsol	180	9.1	Open
Teesside	United Kingdom	Petroplus	0	0	Closed
Teneriffe	Spain	CEPSA	0	0	Closed
Thessaloniki	Greece	Hellenic	85.5	4.3	Open
Tisza	Hungary	MOL	0	0	Closed
Trecate	Italy	ExxonMobil/API	126.5	6.4	Open
Trzebinia	Poland	PKN Orlen	7.3	0.4	Open
Vlissingen (Zeeland)	Netherlands	TotalEnergies/Lukoil	145.5	7.4	Open
Whitegate	Ireland	IRVIN OIL	71	3.6	Open
Wilhelmshaven	Germany	Hestya Energy BV	60	3	Open
Wilhelmshaven	Germany	Hestya Energy BV	0	0	Closed
Zala	Hungary	MOL	0	0	Closed

Table 16. Operating and closed refineries in Europe [187]

Figure 20. Map of existing refineries in EU [187]

Striking the right balance between utilizing existing infrastructure and potentially building new ones, appropriately sized facilities will be a crucial decision in realizing the full potential of these routes while maintaining economic and environmental viability. Although larger refineries tend to have better economies of scale and potentially superior environmental performances, smaller facilities, like a 1,000-barrel-per-day (bpd) Fischer-Tropsch (FT) plant, are today technically feasible and less impacting on the socioeconomic context, and realised in existing underexploited refinery fields (brown fields). Indeed, over the past few years, the development of smaller GTL plants has been a relevant subject-matter for innovation and nowadays technology for small-scale FT plants has been developed [188] [189]. Small-scale GTL technology has capacities ranging from 50 bpd to 5000 bpd [190]. For instance, Velocys is developing a 1,000 bpd modular system to produce diesel and naphtha at an estimated investment cost 100,000 USD/bpd [82] [191]. Other examples [189] of companies providing small-scale GTL facilities are: CompactGTL [192] [188], INFRA technology [193], Gas Technologies LLC, INERATEC, GasTechno Energy & Fuel from the USA [194], and Primus [188].

As for methanol, small-scale plant technologies are also under development: for instance, Haldor Topsoe, jointly with Modular Plant Solutions (MPS), has designed and engineered a small-scale methanol plant (215 tonne/d), namely "Methanol-To-Go™".

Compared to large-scale applications, small-scale GTL FT plants have logistical advantages, reduced capital cost, as well as a good flexibility to utilize a greater variety of carbon-containing materials as feed [195], including stranded natural gas (flared gas), landfill gas, biogas, or biomass and residual wastes [26]. These advantages have been confirmed by professionals on the Global Gas Flaring Partnership (GGFR) committee at the World Bank, who investigated small-scale GTL technology thoroughly [196].

In line with the ReFuelEU Aviation initiative [15], to attain a target of 5% SAF use for all flights leaving from EU airports by 2030, an estimated 2.3 million tonnes of SAF would be required: afterwards, flights departing from EU airports will need to use SAF for 32% and 63% of their jet fuel consumption by 2040 and 2050, respectively. It is estimated that the overall demand for aviation fuel in the EU would reach approximately 46 million tonnes in 2040 and 45 million tonnes in 2050. If the proposed SAF blending mandate is implemented, the projection indicates a need for roughly 14.8 million tonnes of SAF annually by 2040 and approximately 28.7 million tonnes by 2050.

As regards Maritime, methanol is gaining attention as a cleaner marine fuel option due to its potential to reduce emissions of pollutants and its carbon-neutral nature when produced from sustainable biomass. In terms of projections, according to Chemical Market Analytics by OPIS [197], the demand for methanol as marine bunker fuel is expected to increase significantly by 2050, from approximately 0.3 million metric tonnes today to about 7.8 million metric tonnes in 2050.

In terms of sector-specific demands, according to the EU Reference Scenario 2020 [198], the projected energy demand for international aviation is expected to reach 41,846 ktoe by 2030 and 44,375 ktoe by 2050. Simultaneously, the energy demand for international maritime transport is estimated to be 45,966 ktoe by 2030 and 55,939 ktoe by 2050.

As regards the Italian context, the EU Reference Scenario 2020 [198] still indicates that the energy demand for international aviation is expected to be approximately 4000 ktoe by 2030 and 4600 ktoe by 2050. Additionally, the energy demand for international maritime transport is projected to reach approximately 2400 ktoe by 2023 and 2700 ktoe by 2050.

Examining the biomethane potential production, today 3 billion cubic meters (bcm) are produced in the EU-27, while biogas production reaches 15 bcm. In response to the EU renewed commitment to accelerating biomethane production, the Gas for Climate [186] study, through a comprehensive analysis, has estimated a biomethane potential from anaerobic digestion in the EU-27 by 2030 to reach 38 bcm. The top 5 countries driving this growth include France, Germany, Italy, Poland, and Spain. The primary feedstocks contributing to this potential are manure (33%), agricultural residues (25%), sequential cropping (21%), and industrial

wastewater (over 10%). Looking further ahead, the estimated biomethane potential for 2050 is an impressive 91 bcm in the EU-27. Once again, the top 5 countries leading this expansion are France, Germany, Italy, Poland, and Spain. The key feedstocks expected to drive this growth see a largely leading role of sequential cropping (47%), then manure (19%), agricultural residues (17%), and industrial wastewater (over 10%). Moreover, there is the potential to unlock even more biomethane by considering additional feedstocks, such as biomass sourced from marginal or contaminated land and seaweed, as outlined in the REPowerEU plan. Additionally, renewable methane, produced from renewable electricity and biogenic CO_2 captured during biogas upgrading, along with landfill gas, can further contribute to this promising potential.

In the specific case of Italy, as per the Gas for Climate report [186], the potential production of biomethane from anaerobic digestion was estimated to be approximately 5.6 bcm by 2030, increasing to an estimated 8.2 bcm by 2050.

The potential of biomethane as a raw material for the three pathways explored in this study is, therefore, remarkable. Indeed, based on the results from our modelling, and considering the European scenario, via the GTL-FT route, at 2030 it is potentially possible to cover 9% of the demand for kerosene-based jet fuel with SAF produced from this pathway, provided the reforming technology is POX. On the other hand, if the reforming technology were SMR, it could cover 4% of the 2030 demand. Alternatively, opting for the GTL-F_ATJ route would cover about 11% of the jet fuel 2030 demand. When considering methanol as maritime fuel, the GTL-MeOH route could meet approximately 56% of the 2030 demand for maritime fuels using POX as the reforming technology and 25% using SMR as the reforming technology.

In the context of projected fuels demand for the year 2050, the GTL-FT route emerges as a promising solution. This approach has the potential to address 19% of the demand for kerosene-based jet fuel with SAF, contingent on utilizing POX as the reforming technology. Conversely, if SMR were the chosen reforming technology, it could cover 9% of the demand. Turning to alternative routes, opting for the GTL-F_ATJ route would contribute to approximately 25% of the jet fuel demand.

Shifting focus to maritime fuel options, the GTL-MeOH route, employing POX as the reforming technology, has the capacity to fulfil an impressive 105% of the demand for maritime fuels. Meanwhile, using SMR as the reforming technology would cover 48%.

Figure 21, **Figure 22**, **Figure 23**, and **Figure 24** show the European energy fuel demand (MJ) within the aviation and maritime sectors, along with the potential production of SAF and MeOH as per the suggested value chain, highlighting the investigated pathways.

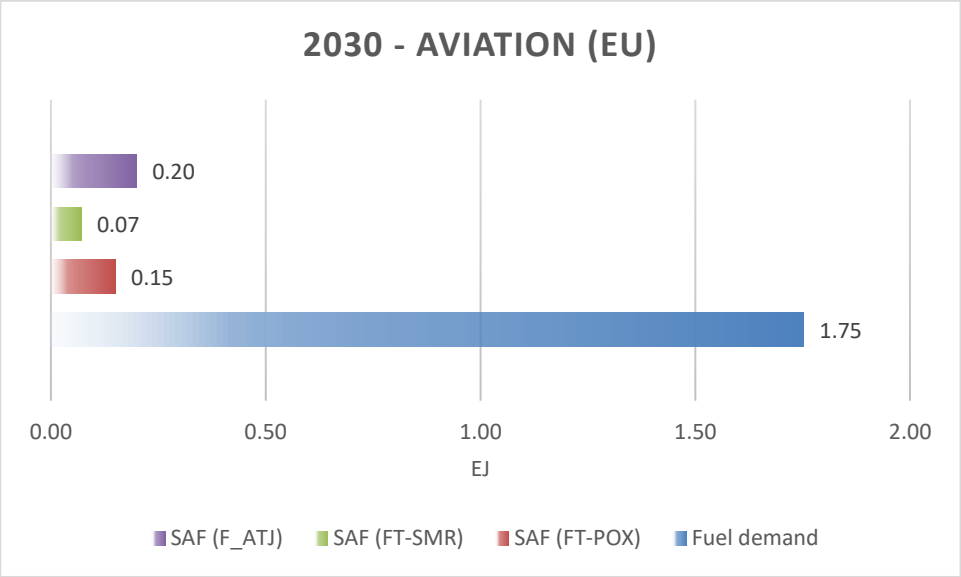

Figure 21. 2030 European fuel demand in the aviation sector (EJ) and potential production of SAF according to the different value chains

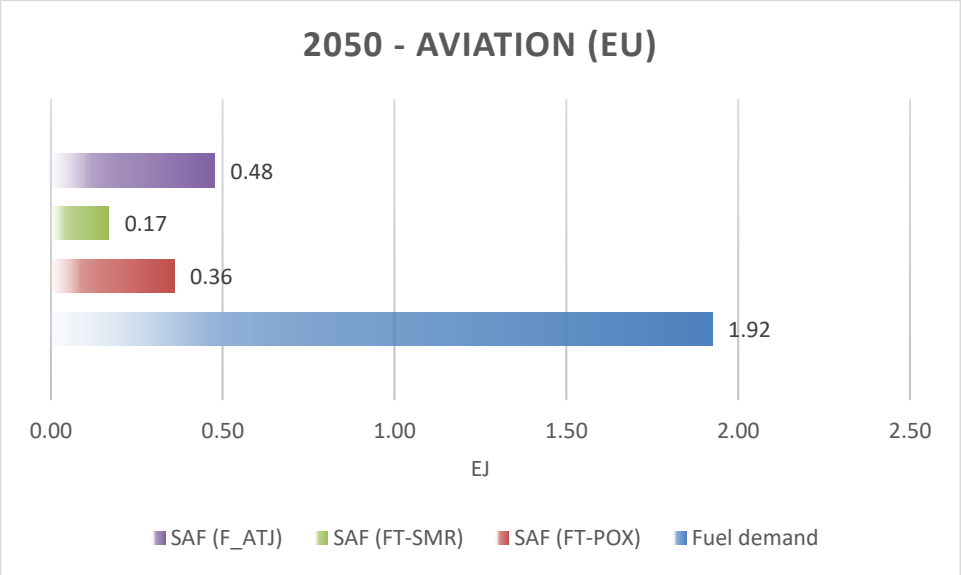

Figure 22. 2050 European fuel demand in the aviation sector (EJ) and potential production of SAF according to the different value chains

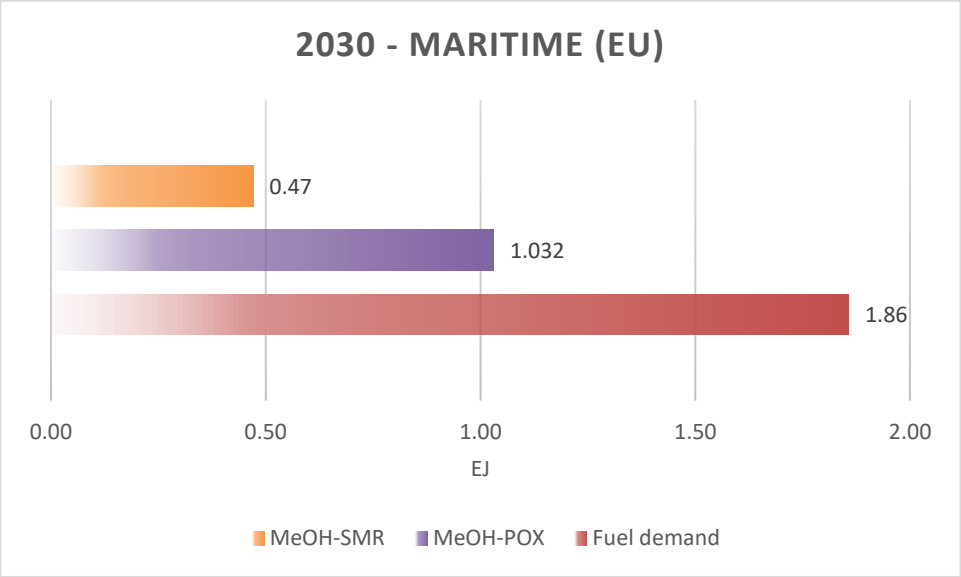

Figure 23. 2030 European fuel demand in the maritime sector (EJ) and potential production of MeOH according to the different value chains

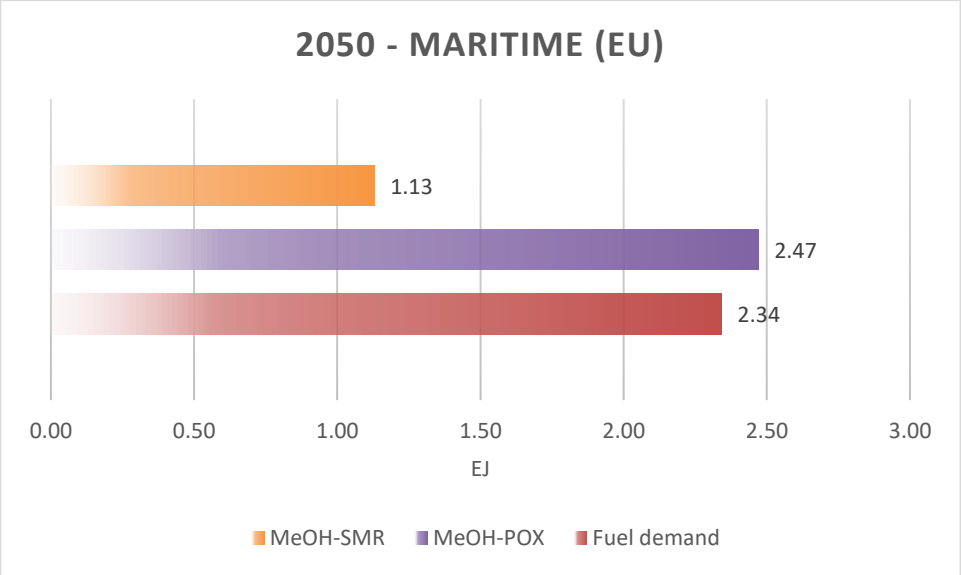

Figure 24. 2050 European fuel demand in the maritime sector (EJ) and potential production of MeOH according to the different value chains

In the 2030 Italian scenario, the GTL-FT pathway has the potential to roughly cover 13% of the demand for kerosene-based jet fuel with SAF if employing POX as the reforming technology. However, with SMR as reforming technology, it could only meet 6% of the demand, even though it simultaneously generates another valuable product, i.e. hydrogen. Alternatively, choosing the GTL-F_ATJ route would cover approximately 18% of the jet fuel demand.

Regarding the use of methanol as maritime fuel, the GTL-MeOH pathway could exceed the demand for maritime fuels (about 152% coverage) when using POX for reforming. This provides ample room for other methanol applications. If employing SMR as the reforming technology, the production of MeOH as maritime fuel through this pathway would cover approximately 69% of the demand for maritime fuels.

In the foreseen Italian scenario for 2050, the GTL-FT pathway with POX could potentially fulfil about 17% of the demand for kerosene-based jet fuel with Sustainable Aviation Fuel (SAF). At the same time, with SMR as the reforming technology, it could meet 8% of the demand, while simultaneously generating a valuable amount of hydrogen. An alternative route, the GTL-F_ATJ pathway, is estimated to cover around 22% of the jet fuel demand. Focusing on maritime fuel applications, the GTL-MeOH pathway, with POX as the reforming technology, could exceed the demand for maritime fuels, providing extensive coverage at approximately 198%. This surplus creates opportunities for various methanol applications. In contrast, using SMR as the reforming technology, the production of MeOH as maritime fuel through this pathway is anticipated to cover around 91% of the demand for maritime fuels.

Figure 25, **Figure 26**, **Figure 27**, and **Figure 28** show the Italian energy requirements in the aviation and maritime sectors, quantified in MJ. They also provide the potential production of SAF and MeOH based on the proposed value chain, outlining the diverse pathways under examination.

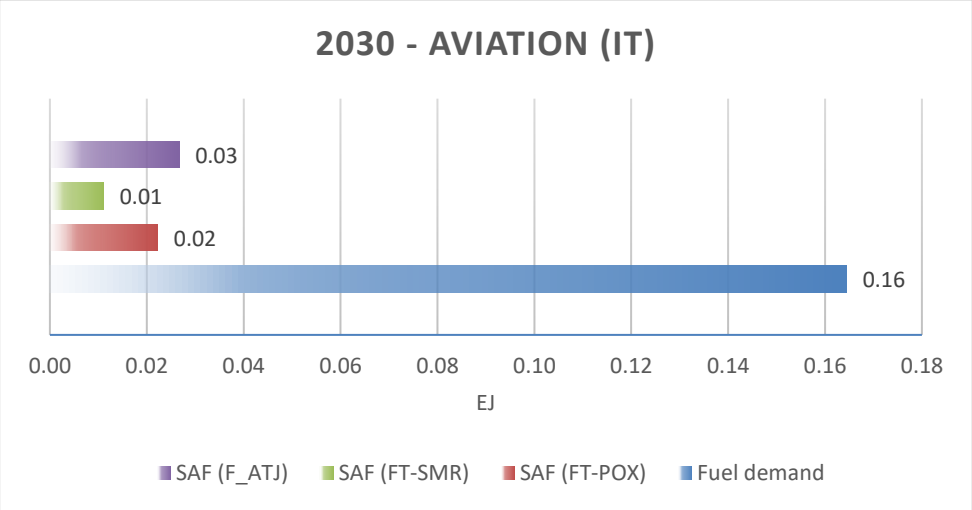

Figure 25. 2030 Italian fuel demand in the aviation sector (EJ) and potential production of SAF according to the different value chains

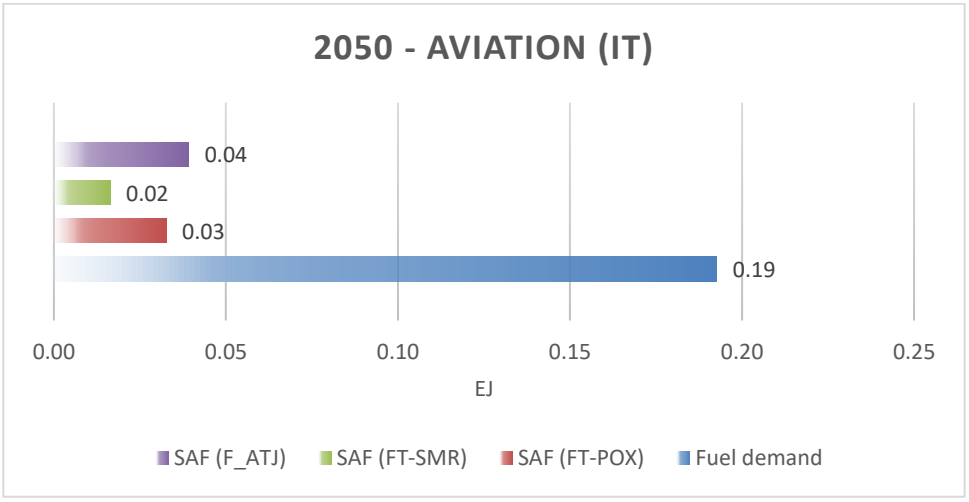

Figure 26. 2050 Italian fuel demand in the aviation sector (EJ) and potential production of SAF according to the different value chains

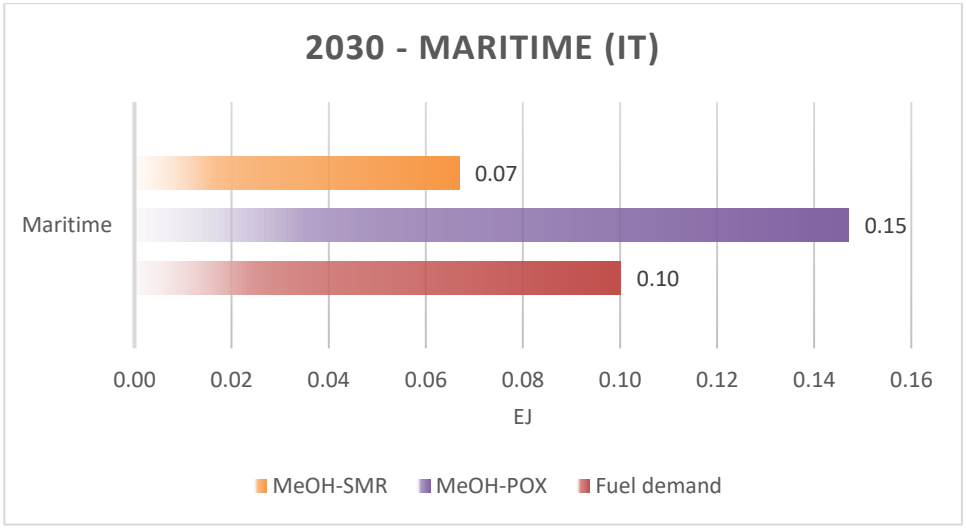

Figure 27. 2030 Italian fuel demand in the maritime sector (EJ) and potential production of MeOH according to the different value chains

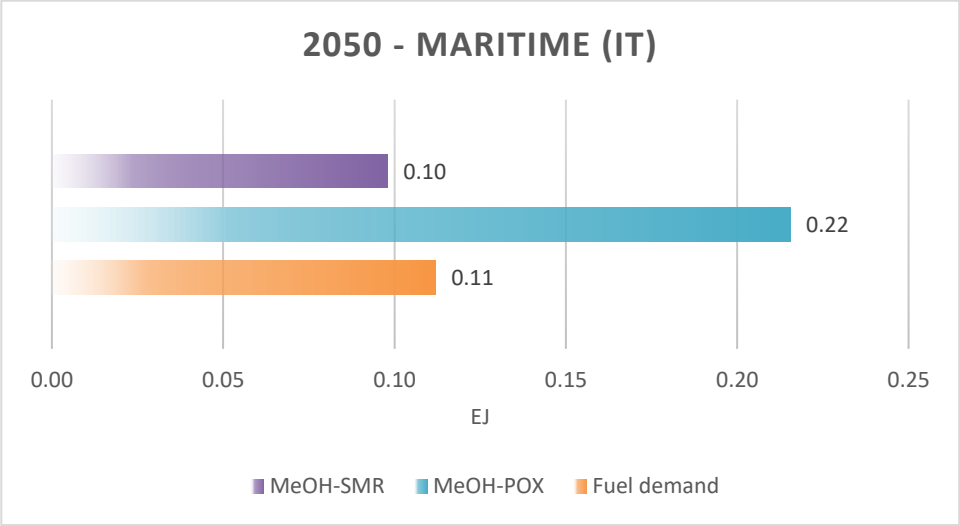

Figure 28. 2050 Italian fuel demand in the maritime sector (EJ) and potential production of MeOH according to the different value chains

Summarizing, **Table 17** recaps the products generated by each of the studied pathway per MJ_{CH4} at inlet, offering a comprehensive view, beyond the contribution to Aviation and Maritime only.

In fact, while the GTL-FT route (10,000 bpd unit) predominantly delivers Naphtha (219 t/d), Kerosene (222 t/d, here assumed for Aviation use), Diesel (95 t/d) and Waxes (474 t/d) and the GTL-MeOH (2,000 tonnes/d) only Methanol (for Maritime), the GTL-F_ATJ (1,000 t/d of products) offers Jet Fuel (700 t/d), Gasoline (100 t/d) and Diesel (200 t/d). With additional H_2 production, in the case of the SMR route.

It is important to note that Naphtha can be used in petrochemicals, while waxes can undergo hydrocracking, where they are broken down into smaller hydrocarbons to produce lighter products such as diesel or gasoline. Such an aspect has not been accounted for in the model developed; however, it would be compelling to incorporate the hydrocracking phase of waxes in a future study to delve deeper into this perspective.

Processes should therefore be selected on the base of the political priorities: the allocation of the current and future available biomethane will be decided on sector priorities, and policies/regulations will follow accordingly. For instance, if green hydrogen generation is to be prioritized against the contribution to Aviation and Maritime, the SMR route could be preferred. Otherwise, POX will offer more volumes to Aviation or Maritime, for the same given amount of biomethane.

Finally, it is worth to observe that, from a strict energy viewpoint, while POX is an exothermal reaction which generates thermal energy (even if presenting risks of explosions) – thus recoverable in the process itself, SMR is an endothermal step with requires feeding thermal energy.

Route	Reforming technology	Fuels	H_2
GTL-FT	POX	0.454	0
GTL-FT	SMR	0.207	0.666
GTL-MeOH	POX	0.682	0
GTL-MeOH	SMR	0.312	0.666
GTL-F_ATJ	POX	0	0
GTL-F_ATJ	SMR	0.188	0.660

Table 17. Liquid Fuels and Hydrogen produced from each pathway (MJ/MJ_{CH4})

Finally, focusing to the 2030 target, based on the stated EU and IT potential, the number of 1 MWe equivalent AD units necessary to serve each pathway is summarized in the following **Table 18**, together with the potential max contribution to the expected EU and IT demand at that year.

Route	Reforming technology	Nr of 1 MWe AD units	Potential contribution to EU Aviation 2030	Potential contribution to EU Maritime 2030	Potential contribution to IT Aviation 2030	Potential contribution to IT Maritime 2030
GTL-FT	POX	516	9%	-	13%	-
GTL-FT	SMR	1128	4%	-	6%	-
GTL-MeOH	POX	336	-	56%	-	152%
GTL-MeOH	SMR	735	-	25%	-	69%
GTL-F_ATJ	POX	-	-	-	-	-
GTL-F_ATJ	SMR	1126	11%	-	18%	-

Table 18. Potential max contribution of each pathway to 2030 EU and IT objectives, and nr of 1 MWe AD units necessary per process route

Chapter 5 Conclusion

This research addressed three different advanced biofuel production pathways for the aviation and maritime sectors based on sustainable (advanced) bio-based natural gas from anaerobic digestion. The biomethane has been assumed as advanced biofuel since it is derived from feedstocks obtained by applying sustainable agricultural management practices, as the Biogas Done Right model.

The research is framed within the European context, and Italy as case study, given the relevance of Anaerobic Digestion in the Country and the existing scheme supporting sustainable biomethane production. This approach offers the valuable potential of securing a raw material, certified with a guarantee of origin, to produce advanced liquid biofuels, thereby ensuring their renewable sourcing.

The proposed systems consider a combination of centralized and decentralized approach, which integrates farm-level biomethane production, its injection into the natural gas grid, and the centralized production of liquid biofuels within a Gas-to-Liquids (GTL) plant at an existing refinery site. This scheme, beyond Anaerobic Digestion, deploy other high TRL advanced technologies such as Fischer-Tropsch synthesis (GTL-FT), methanol synthesis (GTL-MeOH), and syngas fermentation to ethanol, coupled with the alcohol-to-jet process (GTL-F_ATJ). Thus, it is ready for scale up to full industrial production, with a significant potential.

At the core of this study lies the utilization of a value chain model, developed through a comprehensive literature review and modelling, which considers industrial data from existing facilities. Additionally, within the study, we compared two types of technologies for converting methane into syngas (i.e. SMR and POX), at the basis of the conversion processes considered.

The outcomes of the study emphasize the crucial interplay between technological innovation, infrastructure development, regulatory frameworks, and incentive schemes.

For a GTL-FT plant with a capacity of 10,000 bpd, the required number of biogas facilities, following the metric of AD plants of 1 MWe equivalent, is 516 for POX and 1,128 for SMR. This configuration produces approximately 222 tonnes/d of kerosene (assuming it is all Jet Fuel A) and an additional 95 tonnes/d of diesel. Notably, a significant portion of the diesel could potentially serve as Marine fuel, although using it entirely for this purpose might be less optimal in the market, considering its potential application in conventional road vehicles, cars, or heavy-duty vehicles.

In the case of the GTL-MeOH route, the required AD plants are 336 for POX and 735 for SMR. This configuration yields a substantial production of 2,000 tonnes/d of MeOH.

For the GTL-F_ATJ route, the configuration involves 1,226 AD plants and results in the production of 700 tonnes/d of jet fuel, 100 tonnes/d of gasoline, and 200 tonnes/d of diesel.

The advantages of POX are evident, notably in the reduction of the required number of plants to meet each demand in various configurations. Conversely, the GTL-F_ATJ route presents a considerable drawback, demanding nearly three times the number of plants compared to POX/GTL-FT. In terms of product output, while FT produces 957 tonnes/d of diesel, GTL-F_ATJ generates 100 tonnes/d of gasoline and 200 tonnes/d of diesel. Consequently, on a wider perspective, the GTL-FT route proves significantly more efficient than GTL-F_ATJ.

In the case of SMR, the consideration extends to the hydrogen produced, adding another layer to the comparative analysis.

Given the significantly high biomethane production potential within Europe, our work suggests that, within the 2030 European context, the GTL-FT route could potentially fulfil about 9% of the demand for kerosene-based jet fuel using SAF produced from this pathway with POX technology. If SMR technology is used, it could cover 4% of the demand. Alternatively, the GTL-F_ATJ route might cover roughly 11% of the jet fuel demand. Regarding methanol as maritime fuel, the GTL-MeOH route, with POX reforming technology, could potentially meet approximately 56% of the demand for maritime fuels. Utilizing SMR technology, it could cover around 25% of the demand.

On the other hand, in the European context for 2050, the GTL-FT route, utilizing POX technology, has the potential to cover 19% of kerosene-based jet fuel demand with SAF, while SMR technology could cover 9%. The GTL-F_ATJ route may contribute roughly 25% to the jet fuel demand. As for methanol as maritime fuel, the GTL-MeOH route, employing POX technology, could meet even 105% of the demand, and with SMR technology, it could cover about 48%.

For the specific case of Italy in 2030, the GTL-FT route using SAF from POX technology could fulfil around 13% of the kerosene-based jet fuel demand, while the SMR technology could cover about 6%. The GTL-F_ATJ route may meet around 18% of jet fuel demand. For methanol as maritime fuel, GTL-MeOH with POX technology could exceed demand by about 52%, and with SMR technology, it could cover approximately 69% of the demand.

Conversely, in Italy by 2050, the GTL-FT route, leveraging SAF from POX technology, could satisfy about 17% of the demand for kerosene-based jet fuel, while SMR technology might cover about 8%. The GTL-F_ATJ route, on the other hand, is anticipated to fulfil approximately 22% of the jet fuel demand. Regarding

methanol as maritime fuel, GTL-MeOH with POX technology could exceed demand by about 98%, and with SMR technology, it could cover approximately 91% of the demand.

It is worth emphasizing that the utility of these processes extends beyond the aviation and maritime sectors. The production pathways discussed not only fulfil specific demands within these two sectors, but also contribute valuable by-products such as naphtha, diesel, waxes, hydrogen, gasoline, and more, underscoring their versatility and potential applications across diverse industries. Naphtha may find application in petrochemicals, while waxes can be subjected to further refining, such as hydrocracking, for producing lighter products like diesel or gasoline. While this aspect was not included in this study, integrating the hydrocracking of waxes in future studies could offer valuable insights.

The study also provides preliminary and averaged insights into the investment costs for these routes, derived from a literature review of existing facilities. The estimated capital investment cost per unit of product for the considered routes is as follows: 791,970 USD per tonne per day for the GTL-FT route (considering all the FT products), 130,275 USD per metric tonne per day for the GTL-MeOH route. In the case of the GTL-F_ATJ route, the costs are projected at approximately 669,740 USD per tonne per day of product generated along the chain.

The possibility to use the existing refineries in Europe for the three routes (i.e. GTL-FT, GTL-MeOH, GTL-F_ATJ) presents both opportunities and challenges. While leveraging established infrastructure in brown fields promises economic advantages and accelerated adoption of these cleaner routes, there is the need for alignment between existing refinery scales and the biomethane ideal capacity for optimal economic and environmental performance. Small-scale GTL plants have also emerged as a viable alternative, offering logistical advantages, reduced capital costs, and enhanced flexibility.

While this analysis aimed at offering an insightful view into the EU and IT potential of these pathways, it also underlines the imperative need for continuous advancements, scaling, and investments. The journey towards a sustainable energy future demand concerted efforts, reliable yet innovative technologies, and aligned policies, stable in the long-term, to ensure investment risks due to change in regulations can be properly addressed and secured.

Publications

The work of this thesis has led to the publication of the articles listed below.

Journal papers

- Testa, L., Chiaramonti, D., Prussi, M. et al. Challenges and opportunities of process modelling renewable advanced fuels. Biomass Conv. Bioref. (2022). https://doi.org/10.1007/s13399-022-03057-0

- David Chiaramonti, Lorenzo Testa, Deploying EU biomethane potential for transports: Centralized/decentralized biogasrefinery schemes to SAF and maritime fuels, Applied Energy, Volume 366, 2024, 123306, ISSN 0306-2619, https://doi.org/10.1016/j.apenergy.2024.123306 .

References

[1] L. Testa, D. Chiaramonti, M. Prussi, and S. Bensaid, *Challenges and opportunities of process modelling renewable advanced fuels*, no. 0123456789. Springer Berlin Heidelberg, 2022. doi: 10.1007/s13399-022-03057-0.

[2] J. G. J. Olivier and P. J.A.H.W, "TRENDS IN GLOBAL CO2 AND TOTAL GREENHOUSE GAS 2019 Report," vol. 2020, no. May, 2020.

[3] U. Nations, *Paris Agreement*, no. 8. 2015.

[4] L. R. Lynd *et al.*, "The role of biomass in America's energy future: Framing the analysis," *Biofuels, Bioproducts and Biorefining*, vol. 3, no. 2, doi: https://doi.org/10.1002/bbb.134.

[5] K. P. Overmars, E. Stehfest, J. P. M. Ros, and A. G. Prins, "Indirect land use change emissions related to EU biofuel consumption: An analysis based on historical data," *Environ Sci Policy*, vol. 14, no. 3, pp. 248–257, 2011, doi: 10.1016/j.envsci.2010.12.012.

[6] "Indirect Land Use Change (ILUC)," European Commission. [Online]. Available: https://ec.europa.eu/commission/presscorner/detail/en/MEMO_12_787

[7] "Sustainability criteria for biofuels specified," European Commission. [Online]. Available: https://ec.europa.eu/commission/presscorner/detail/en/MEMO_19_1656

[8] European Union, "Directive (EU) 2018/2001 of the European Parliament and of the Council of 11 December 2018 on the promotion of the use of energy from renewable sources (recast)." Accessed: Sep. 12, 2023. [Online]. Available: https://eur-lex.europa.eu/legal-content/EN/TXT/?uri=uriserv:OJ.L_.2018.328.01.0082.01.ENG

[9] European Commission, "European Green Deal: Commission proposes transformation of EU economy and society to meet climate ambitions." Accessed: Sep. 12, 2023. [Online]. Available: https://ec.europa.eu/commission/presscorner/detail/en/IP_21_3541

[10] J. Larsson, A. Elofsson, T. Sterner, and J. Åkerman, "International and national climate policies for aviation: a review," *Climate Policy*, vol. 19:6, pp. 787–799, 2019, doi: https://doi.org/10.1080/14693062.2018.1562871.

[11] European Commission, "REPowerEU: Affordable, secure and sustainable energy for Europe." Accessed: Sep. 12, 2023. [Online]. Available:

https://commission.europa.eu/strategy-and-policy/priorities-2019-2024/european-green-deal/repowereu-affordable-secure-and-sustainable-energy-europe_en

[12] European Commission, "DIRECTIVE (EU) 2023/2413 OF THE EUROPEAN PARLIAMENT AND OF THE COUNCIL," Official Journal of the European Union. Accessed: Dec. 18, 2023. [Online]. Available: https://eur-lex.europa.eu/legal-content/EN/TXT/?uri=CELEX%3A32023L2413&qid=1699364355105

[13] D. for T. GOV UK, "Sustainable Aviation Fuels Mandate: Summary of consultation responses," no. March 2022, 2023.

[14] M. Shehab, K. Moshammer, M. Franke, and E. Zondervan, "Analysis of the Potential of Meeting the EU's Sustainable Aviation Fuel Targets in 2030 and 2050," *Sustainability*, vol. 15, no. 12, p. 9266, 2023, doi: 10.3390/su15129266.

[15] European Parliament, "ReFuelEU Aviation initiative: Sustainable aviation fuels and the fit for 55 package," no. August, 2023.

[16] IEA, "International shipping." Accessed: Sep. 12, 2023. [Online]. Available: https://www.iea.org/energy-system/transport/international-shipping

[17] Global Energy Monitor, "Global Gas Infrastructure Tracker." Accessed: Dec. 18, 2023. [Online]. Available: https://globalenergymonitor.org/projects/global-gas-infrastructure-tracker/tracker/

[18] GSE, "ATLAIMPIANTI." Accessed: Apr. 28, 2023. [Online]. Available: https://www.gse.it/dati-e-scenari/atlaimpianti

[19] Ministro dello Sviluppo Economico, "Decreto Ministeriale 2 Marzo 2018," pp. 1–43, 2018.

[20] European Biogas Association (EBA), "Biomethane Map 2021." Accessed: May 05, 2023. [Online]. Available: https://www.europeanbiogas.eu/biomethane-map-2021/

[21] Y. Yoshizawa, "Germany' s biogas industry and the prospective business opportunities — use of biomethane and bio-LNG to grow in the transportation sector," 2022.

[22] Ministro dell'Ambiente e della Sicurezza Energetica, "Decreto Ministeriale 6 Luglio 2012, n. 120," 2012.

[23] Official Journal of the European Union, "DIRECTIVE 2009/28/EC OF THE EUROPEAN PARLIAMENT AND OF THE COUNCIL of 23 April 2009 on the promotion of the use of energy from renewable sources and amending and subsequently repealing Directives 2001/77/EC and 2003/30/EC," vol. 1, pp. 32–38, 2008.

[24] B. E. Dale *et al.*, "Biogasdoneright^{TM}: An innovative new system is commercialized in Italy," *Biofuels, Bioproducts and Biorefining*, vol. 10, no. 4, pp. 341–345, 2016, doi: https://doi.org/10.1002/bbb.1671.

[25] X. Wang and M. Economides, *Advanced Natural Gas Engineering*. Gulf Publishing Company, 2010. doi: https://doi.org/10.1016/C2013-0-15532-8.

[26] M. Konarova, W. Aslam, and G. Perkins, "Chapter 3 - Fischer-Tropsch synthesis to hydrocarbon biofuels: Present status and challenges involved," in *Hydrocarbon Biorefinery*, 2022, pp. 77–96. doi: https://doi.org/10.1016/B978-0-12-823306-1.00006-6.

[27] L. Kelley, "US methanol boom in billion dollar investment phase." Accessed: Sep. 10, 2023. [Online]. Available: https://www.icis.com/explore/resources/news/2018/05/17/10222821/us-methanol-boom-in-billion-dollar-investment-phase/

[28] Ministero della Transizione Ecologica, "Decreto Ministeriale 15 Settembre 2022," *Gazzetta Ufficiale della Repubblica Italiana*, 2022.

[29] M. T. Ashraf, J. E. Schmidt, and J.-R. B. Oyanedel, "Conversion Efficiency of Biogas to Liquids Fuels through Fischer-Tropsch Process," Jun. 2015, doi: 10.5071/23RDEUBCE2015-3CO.15.5.

[30] H. Gruber *et al.*, "Fischer-Tropsch products from biomass-derived syngas and renewable hydrogen," *Biomass Convers Biorefin*, pp. 1–12, Jun. 2019, doi: 10.1007/s13399-019-00459-5.

[31] C. Perego, R. Bortolo, and R. Zennaro, "Gas to liquids technologies for natural gas reserves valorization: The Eni experience," *Catal Today*, vol. 142, no. 1–2, pp. 9–16, 2009, doi: 10.1016/j.cattod.2009.01.006.

[32] M. A. Ershov *et al.*, "An evolving research agenda of merit function calculations for new gasoline compositions," *Fuel*, vol. 322, no. April, p. 124209, 2022, doi: 10.1016/j.fuel.2022.124209.

[33] M. A. Ershov *et al.*, "Perspective towards a gasoline-property-first approach exhibiting octane hyperboosting based on isoolefinic hydrocarbons," *Fuel*, vol. 321, no. November 2021, p. 124016, 2022, doi: 10.1016/j.fuel.2022.124016.

[34] M. A. Ershov, T. M. M. Abdellatief, D. A. Potanin, N. A. Klimov, E. A. Chernysheva, and V. M. Kapustin, "Characteristics of Isohexene as a Novel Promising High-Octane Gasoline Booster," *Energy and Fuels*, vol. 34, no. 7, pp. 8139–8149, 2020, doi: 10.1021/acs.energyfuels.0c00945.

[35] S. Jung, J. Lee, D. H. Moon, K. H. Kim, and E. E. Kwon, "Upgrading biogas into syngas through dry reforming," *Renewable and Sustainable Energy Reviews*, vol. 143, no. February, p. 110949, 2021, doi: 10.1016/j.rser.2021.110949.

[36] J. Baltrusaitis and W. L. Luyben, "Methane Conversion to Syngas for Gas-to-Liquids (GTL): Is Sustainable CO2 Reuse via Dry Methane Reforming (DMR) Cost Competitive with SMR and ATR Processes?," *ACS Sustain Chem Eng*, vol. 3, no. 9, pp. 2100–2111, 2015, doi: 10.1021/acssuschemeng.5b00368.

[37] "10.3. SYNGAS CONVERSION TO METHANOL," National Energy Technology Laboratory (NETL). [Online]. Available: Methanol is a liquid at

ambient conditions and is widely considered as a transportation fuel. Methanol, especially M85, can be burned in engines designed to burn gasoline, but methanol may be corrosive to materials designed to contact gasoline. Methanol i

[38] R. G. dos Santos and A. C. Alencar, "Biomass-derived syngas production via gasification process and its catalytic conversion into fuels by Fischer Tropsch synthesis: A review," *Int J Hydrogen Energy*, vol. 45, no. 36, pp. 18114–18132, 2020, doi: 10.1016/j.ijhydene.2019.07.133.

[39] GSE, "Biometano." [Online]. Available: https://www.gse.it/servizi-per-te_site/rinnovabili-per-i-trasporti_site/biometano_site/Pagine/Biometano.aspx

[40] A. M. Ranjekar and G. D. Yadav, "Dry reforming of methane for syngas production: A review and assessment of catalyst development and efficacy," *Journal of the Indian Chemical Society*, vol. 98, no. 1, p. 100002, 2021, doi: 10.1016/j.jics.2021.100002.

[41] L. Yang and X. Ge, *Advances in Bioenergy, Chapter Three - Biogas and Syngas Upgrading*. 2016. doi: https://doi.org/10.1016/bs.aibe.2016.09.003.

[42] P. Gangadharan, K. C. Kanchi, and H. H. Lou, "Evaluation of the economic and environmental impact of combining dry reforming with steam reforming of methane," *Chemical Engineering Research and Design*, vol. 90, no. 11, pp. 1956–1968, 2012, doi: 10.1016/j.cherd.2012.04.008.

[43] R. Carapellucci and L. Giordano, "Steam, dry and autothermal methane reforming for hydrogen production: A thermodynamic equilibrium analysis," *J Power Sources*, vol. 469, no. October 2019, p. 228391, 2020, doi: 10.1016/j.jpowsour.2020.228391.

[44] Q. Zhu, X. Zhao, and Y. Deng, "Advances in the partial oxidation of methane to synthesis gas," *Journal of Natural Gas Chemistry*, vol. 13, no. 4, pp. 191–203, 2004, doi: 10.1016/S1003-9953-2004-13-4-191-203.

[45] Shell Global, "Gas-to-liquids." Accessed: Sep. 12, 2023. [Online]. Available: https://www.shell.com/energy-and-innovation/natural-gas/gas-to-liquids.html

[46] M. Senden;, F. Martens;, W. Steenge;, and R. K. Nagelvoort, "Shell's GTL: Its Technology and Design, Its Operation and Products," in *International Petroleum Technology Conference, Doha, Qatar, November 2005*, 2005. doi: https://doi.org/10.2523/IPTC-10683-MS.

[47] Sasol, "Sasol Slurry Phase Distillate." Accessed: Sep. 12, 2023. [Online]. Available: https://www.sasol.com/innovation/gas-liquids/technology

[48] M. A. Ayad and N. A. E.-E. T. M. Aboul-Fotouh, "A study on the different reforming techniques in gas to liquid technology," *Petroleum and Coal*, no. 60(5). pp. 822–831, ISSN 1337-7027, 2018.

[49] R. A. Fiato; and P. W. Sibal, "ExxonMobil's Advanced Gas-to-Liquids Technology–AGC-21," in *SPE Middle East Oil and Gas Show and*

Conference, Kingdom of Bahrain, March 2005, 2005. doi: https://doi.org/10.2118/93653-MS.

[50] H. Er-rbib, C. Bouallou, and F. Werkoff, "Dry reforming of methane - Review of feasibility studies," *Chem Eng Trans*, vol. 29, no. April 2016, pp. 163–168, 2012, doi: 10.3303/CET1229028.

[51] M. A. Ershov, D. A. Potanin, S. V. Tarazanov, T. M. M. Abdellatief, and V. M. Kapustin, "Blending Characteristics of Isooctene, MTBE, and TAME as Gasoline Components," *Energy and Fuels*, vol. 34, no. 3, pp. 2816–2823, 2020, doi: 10.1021/acs.energyfuels.9b03914.

[52] S. Mehariya *et al.*, *Fischer-Tropsch synthesis of syngas to liquid hydrocarbons*. 2019. doi: 10.1016/B978-0-12-815936-1.00007-1.

[53] R. Rauch, A. Kiennemann, and A. Sauciuc, *Chapter 12 - Fischer-Tropsch Synthesis to Biofuels (BtL Process)*. 2013. doi: https://doi.org/10.1016/B978-0-444-56330-9.00012-7.

[54] H. Mahmoudi *et al.*, "A review of Fischer Tropsch synthesis process, mechanism, surface chemistry and catalyst formulation," *Biofuels Engineering*, vol. 2, no. 1, pp. 11–31, Jan. 2018, doi: 10.1515/bfuel-2017-0002.

[55] H. Gruber *et al.*, "Fischer-Tropsch products from biomass-derived syngas and renewable hydrogen," *Biomass Convers Biorefin*, pp. 1–12, Jun. 2019, doi: 10.1007/s13399-019-00459-5.

[56] C. Perego, R. Bortolo, and R. Zennaro, "Gas to liquids technologies for natural gas reserves valorization: The Eni experience," *Catal Today*, vol. 142, no. 1–2, pp. 9–16, 2009, doi: 10.1016/j.cattod.2009.01.006.

[57] M. A. Ershov *et al.*, "An evolving research agenda of merit function calculations for new gasoline compositions," *Fuel*, vol. 322, no. April, p. 124209, 2022, doi: 10.1016/j.fuel.2022.124209.

[58] M. A. Ershov *et al.*, "Perspective towards a gasoline-property-first approach exhibiting octane hyperboosting based on isoolefinic hydrocarbons," *Fuel*, vol. 321, no. November 2021, p. 124016, 2022, doi: 10.1016/j.fuel.2022.124016.

[59] T. M. M. Abdellatief, M. A. Ershov, and V. M. Kapustin, "New recipes for producing a high-octane gasoline based on naphtha from natural gas condensate," *Fuel*, vol. 276, no. January, p. 118075, 2020, doi: 10.1016/j.fuel.2020.118075.

[60] M. A. Ershov, T. M. M. Abdellatief, D. A. Potanin, N. A. Klimov, E. A. Chernysheva, and V. M. Kapustin, "Characteristics of Isohexene as a Novel Promising High-Octane Gasoline Booster," *Energy and Fuels*, vol. 34, no. 7, pp. 8139–8149, 2020, doi: 10.1021/acs.energyfuels.0c00945.

[61] S. Adelung, S. Maier, and R. U. Dietrich, "Impact of the reverse water-gas shift operating conditions on the Power-to-Liquid process efficiency," *Sustainable Energy Technologies and Assessments*, vol. 43, no. July 2020, p. 100897, 2021, doi: 10.1016/j.seta.2020.100897.

[62] C. I. Méndez and J. Ancheyta, “Kinetic models for Fischer-Tropsch synthesis for the production of clean fuels,” *Catal Today*, vol. 353, no. November 2019, pp. 3–16, 2020, doi: 10.1016/j.cattod.2020.02.012.

[63] L. A. I. B. Nassr, “SIMULATION OF FISCHER-TROPSCH FIXED-BED REACTOR IN DIFFERENT REACTION MEDIA,” Texas A&M University, 2013.

[64] F. M. Yanti *et al.*, “Methanol production from biomass syngas using Cu / ZnO / Al 2 O 3 catalyst Methanol Production from Biomass Syngas using Cu / ZnO / Al2O3 Catalyst,” vol. 020006, no. April, 2020.

[65] M. Puig-Gamero, J. Argudo-Santamaria, J. L. Valverde, P. Sánchez, and L. Sanchez-Silva, “Three integrated process simulation using aspen plus®: Pine gasification, syngas cleaning and methanol synthesis,” *Energy Convers Manag*, vol. 177, no. September, pp. 416–427, 2018, doi: 10.1016/j.enconman.2018.09.088.

[66] R. Chein, W. Chen, H. C. Ong, P. L. Show, and Y. Singh, “Analysis of methanol synthesis using CO2 hydrogenation and syngas produced from biogas-based reforming processes,” *Chemical Engineering Journal*, p. 130835, 2021, doi: 10.1016/j.cej.2021.130835.

[67] O. Y. Abdelaziz, M. A. Gadalla, and F. H. Ashour, “Simulation of Biomethanol Production from Green Syngas Through Sustainable Process Design”, doi: 10.5220/0005002906770684.

[68] A. Akça, “Conversion of methane to methanol on C-doped boron nitride: A DFT study,” *Comput Theor Chem*, vol. 1202, no. February, p. 113291, 2021, doi: 10.1016/j.comptc.2021.113291.

[69] M. J. Da Silva, “Synthesis of methanol from methane: Challenges and advances on the multi-step (syngas) and one-step routes (DMTM),” *Fuel Processing Technology*, vol. 145, pp. 42–61, 2016, doi: 10.1016/j.fuproc.2016.01.023.

[70] F. J. Gutiérrez Ortiz, A. Serrera, S. Galera, and P. Ollero, “Methanol synthesis from syngas obtained by supercritical water reforming of glycerol,” *Fuel*, vol. 105, pp. 739–751, 2013, doi: 10.1016/j.fuel.2012.09.073.

[71] T. Kiyokawa and N. Ikenaga, “Oxidative dehydrogenation of n-butene to buta-1,3-diene with novel iron oxide-based catalyst: Effect of iron oxide crystalline structure,” *Molecular Catalysis*, vol. 507, no. April, p. 111560, 2021, doi: 10.1016/j.mcat.2021.111560.

[72] I. Landälv, L. Waldheim, and K. Maniatis, “Continuing the work of the Sub Group on Advanced Biofuels - Technology status and reliability of the value chains : 2018 Update,” no. December, 2018.

[73] D. A. Bell, B. F. Towler, and M. Fan, “Chapter 12 - Methanol and Derivatives,” in *Coal Gasification and Its Applications*, 2011, pp. 353–371. doi: 10.1016/B978-0-8155-2049-8.10012-9.

[74] S. A. Al-Sobhi, A. Elkamel, F. S. Erenay, and M. A. Shaik, "Simulation-optimization framework for synthesis and design of natural gas downstream utilization networks," *Energies (Basel)*, vol. 11, no. 2, pp. 1–19, 2018, doi: 10.3390/en11020362.

[75] L. E. Lücking, "Methanol Production from Syngas," Delft University of Technology, 2017.

[76] S. Majhi and K. K. Pant, "Direct conversion of methane with methanol toward higher hydrocarbon over Ga modified Mo/H-ZSM-5 catalyst," *Journal of Industrial and Engineering Chemistry*, vol. 20, no. 4, pp. 2364–2369, 2014, doi: 10.1016/j.jiec.2013.10.014.

[77] Z. Zakaria and S. K. Kamarudin, "Direct conversion technologies of methane to methanol: An overview," *Renewable and Sustainable Energy Reviews*, vol. 65, pp. 250–261, 2016, doi: 10.1016/j.rser.2016.05.082.

[78] C. Ma, X. Tan, H. Zhang, Q. Shen, N. Sun, and W. Wei, "Direct conversion of methane to methanol over Cu exchanged mordenite: Effect of counter ions," *Chinese Chemical Letters*, vol. 31, no. 1, pp. 235–238, 2020, doi: 10.1016/j.cclet.2019.03.039.

[79] P. Khirsariya and R. K. Mewada, "Single step oxidation of methane to methanol - Towards better understanding," in *Procedia Engineering*, Elsevier Ltd, Jan. 2013, pp. 409–415. doi: 10.1016/j.proeng.2013.01.057.

[80] J. Pechstein, U. Neuling, J. Gebauer, and M. Kaltschmitt, *Biokerosene*. Berlin, Heidelberg: Springer, 2018.

[81] I. K. Stoll, N. Boukis, and J. Sauer, "Syngas Fermentation to Alcohols: Reactor Technology and Application Perspective," *Chemie-Ingenieur-Technik*, vol. 92, no. 1–2. Wiley-VCH Verlag, pp. 125–136, Jan. 01, 2020. doi: 10.1002/cite.201900118.

[82] Pascoela Marciana Da Silva Sequeira, "Economy analysis comparison for liquefied natural gas and gas-toliquid project in monetizing excessive natural gas production," UNIVERSITY OF OKLAHOMA, 2019.

[83] A. de Klerk, *Fischer-Tropsch Refining*. Wiley-VCH Verlag GmbH & Co. KGaA, 2011. doi: 10.1002/9783527635603.

[84] National Energy Technology Laboratory (NETL), "SYNGAS CONVERSION TO METHANOL." Accessed: Aug. 15, 2023. [Online]. Available: https://www.netl.doe.gov/research/carbon-management/energy-systems/gasification/gasifipedia/methanol

[85] Methanex, "Geismar 3: An industry-leading methanol plant with lower emissions intensity." Accessed: Oct. 27, 2023. [Online]. Available: https://www.methanex.com/geismar-3/

[86] K. Newsroom, "Koch Methanol, Yuhuang Chemical enter into methanol offtake agreement." Accessed: Oct. 27, 2023. [Online]. Available: https://news.kochind.com/news/2018/koch-methanol,-yuhuang-chemical-enter-into-methano

[87] OCI Global, “Fueling a Cleaner Future.” Accessed: Oct. 27, 2023. [Online]. Available: https://oci-global.com/products-solutions/methanol/hyfuels/

[88] OCI Global, “Interview: After shattering records in green-methanol bunkering, OCI Global stresses the power of collaboration for a smooth transition.” Accessed: Oct. 27, 2023. [Online]. Available: https://oci-global.com/news-stories/opinion/interview-after-shattering-records-in-green-methanol-bunkering-oci-global-stresses-the-power-of-collaboration-for-a-smooth-transition/

[89] Methanex, “Media Resources.” Accessed: Oct. 27, 2023. [Online]. Available: https://www.methanex.com/news/media-resources/

[90] Dr. S. Geleynse, K. Brandt, Dr. M. Garcia-Perez, Dr. M. Wolcott, and Dr. X. Zhang, “The Alcohol-to-Jet Conversion Pathway for Drop-In Biofuels: Techno-Economic Evaluation,” *ChemSusChem*, vol. 11, no. 21, pp. 3728–3741, 2018, doi: https://doi.org/10.1002/cssc.201801690.

[91] B. Han *et al.*, “Recent advancements in catalytic conversion pathways for synthetic jet fuel produced from bioresources,” vol. 251, no. September 2021, 2022, doi: 10.1016/j.enconman.2021.114974.

[92] M. Tsagkari, A. France, A. Kokossis, J. Dubois, and A. France, “A method for quick capital cost estimation of biorefineries beyond the state of the art,” pp. 1061–1088, 2020, doi: 10.1002/bbb.2114.

[93] E. Ficara, S. Hassam, A. Allegrini, A. Leva, F. Malpei, and G. Ferretti, *Anaerobic Digestion Models: a Comparative Study*, vol. 45, no. 2. IFAC, 2012. doi: 10.3182/20120215-3-at-3016.00186.

[94] Graef, S. P., and J. F. Andrews., “Stability and Control of Anaerobic Digestion,” *Journal (Water Pollution Control Federation), JSTOR,* vol. 46, n, 1974.

[95] O. Bernard *et al.*, “Dynamical model development and parameter identification for an anaerobic wastewater treatment process. Biotechnology and bioengineering 75.4 (2001) 424-438..pdf,” *Biotechnol Bioeng*, vol. 75, 2001.

[96] D. J. Batstonnee, J. Keller, I. Angelidaki, S. V Kalyuzhnyi, S. G. Pavlostathis, and A. Rozzi, “The IWA Anaerobic Digestion Model No 1 (ADM1),” *Enzyme.Chem.Msu.Ru*, vol. 1, no. 1, pp. 65–74.

[97] S. W. Sötemann, N. E. Ristow, M. C. Wentzel, and G. A. Ekama, “A steady state model for anaerobic digestion of sewage sludges SW,” 2005.

[98] Vavilin, V.A., Vasiliev, V.B., Ponomarev, A.V., Rytow, S.V., “Simulation model ‘methane’ as a tool for effective biogas production during anaerobic conversion of complex organic matter,” *Bioresour. Technol. 48 (1), 1–8.*, doi: https://doi.org/10.1016/0960-8524(94)90126-0.

[99] I. Angelidaki, L. Ellegaard, and B. K. Ahring, “A comprehensive model of anaerobic bioconversion of complex substrates to biogas,” *Biotechnol Bioeng*, vol. 63, no. 3, pp. 363–372, 1999, doi: 10.1002/(SICI)1097-0290(19990505)63:3<363::AID-BIT13>3.0.CO;2-Z.

[100] H. Al-Rubaye, S. Karambelkar, M. M. Shivashankaraiah, and J. D. Smith, "Process Simulation of Two-Stage Anaerobic Digestion for Methane Production," *Biofuels*, vol. 10, no. 2, pp. 181–191, 2019, doi: 10.1080/17597269.2017.1309854.

[101] R. S. Peris, "Biogas Process Simulation using Aspen Plus," *Department of Chemical engineering, Biotechnology and Environmental Technology. Syddansk University.*, pp. 1–88, 2011.

[102] "Aspen Plus User Guide, Version 10.2," *Aspen Technology, Inc.* 2000.

[103] K. Rajendran, H. R. Kankanala, M. Lundin, and M. J. Taherzadeh, "A novel process simulation model (PSM) for anaerobic digestion using Aspen Plus," *Bioresour Technol*, vol. 168, pp. 7–13, 2014, doi: 10.1016/j.biortech.2014.01.051.

[104] H. H. Nguyen, S. Heaven, and C. Banks, "Energy potential from the anaerobic digestion of food waste in municipal solid waste stream of urban areas in Vietnam," *International Journal of Energy and Environmental Engineering*, vol. 5, no. 4, pp. 365–374, 2014, doi: 10.1007/s40095-014-0133-1.

[105] D. Scamardella *et al.*, "Simulation and optimization of pressurized anaerobic digestion and biogas upgrading using aspen plus," *Chem Eng Trans*, vol. 74, no. July 2018, pp. 55–60, 2019, doi: 10.3303/CET1974010.

[106] J. Lorenzo-Llanes, J. Pagés-Díaz, E. Kalogirou, and F. Contino, "Development and application in Aspen plus of a process simulation model for the anaerobic digestion of vinasses in UASB reactors: Hydrodynamics and biochemical reactions," *J Environ Chem Eng*, vol. 8, no. 2, p. 103540, 2020, doi: 10.1016/j.jece.2019.103540.

[107] P. Cozma, C. Ghinea, I. Mămăligă, W. Wukovits, A. Friedl, and M. Gavrilescu, "Environmental impact assessment of high pressure water scrubbing biogas upgrading technology," *Clean (Weinh)*, vol. 41, no. 9, pp. 917–927, 2013, doi: 10.1002/clen.201200303.

[108] P. Cozma, W. Wukovits, I. Mămăligă, A. Friedl, and M. Gavrilescu, "Modeling and simulation of high pressure water scrubbing technology applied for biogas upgrading," *Clean Technol Environ Policy*, vol. 17, no. 2, 2014, doi: 10.1007/s10098-014-0787-7.

[109] M. Götz, W. Köppel, R. Reimert, and F. Graf, "Optimierungspotenzial von Wäschen zur Biogasaufbereitung: Teil 1 - Physikalische Wäschen," *Chem Ing Tech*, vol. 83, no. 6, pp. 858–866, 2011, doi: 10.1002/cite.201000211.

[110] M. Götz, W. Köppel, R. Reimert, and F. Graf, "Optimierungspotenzial von Wäschen zur Biogasaufbereitung: Teil 1 - Physikalische Wäschen," *Chem Ing Tech*, vol. 83, no. 6, pp. 858–866, 2011, doi: 10.1002/cite.201000211.

[111] S. Menegon, "Tesi di Laurea Magistrale in DAL BIOGAS AL BIOMETANO: SIMULAZIONE DI PROCESSO ED ANALISI TECNO-ECONOMICA DELLE PRINCIPALI," p. 148, 2017.

[112] G. Bortoluzzi, M. Gatti, A. Sogni, and S. Consonni, “Biomethane production from agricultural resources in the Italian scenario: Techno-Economic analysis of water wash,” *Chem Eng Trans*, vol. 37, pp. 259–264, 2014, doi: 10.3303/CET1437044.

[113] N. Abu Seman and N. Harun, “Simulation of pressurized water scrubbing process for biogas purification using Aspen Plus,” *IOP Conf Ser Mater Sci Eng*, vol. 702, no. 1, 2019, doi: 10.1088/1757-899X/702/1/012040.

[114] H.-U. Lingelem, “Process Optimization of Biogas Upgrading with AMP Using Pilot Plant Data and Simulations with Aspen Plus,” p. 124, 2016.

[115] S. Gamba and L. A. Pellegrini, “Biogas Upgrading : Analysis and Comparison between Water and Chemical Scrubbings,” *Chem Eng Trans*, vol. 32, 2013, doi: 10.3303/CET1332213.

[116] L. A. Pellegrini, S. Moioli, and S. Gamba, “Energy saving in a CO2 capture plant by MEA scrubbing,” *Chemical Engineering Research and Design*, vol. 89, no. 9, pp. 1676–1683, 2011, doi: 10.1016/j.cherd.2010.09.024.

[117] S. Gamba, L. A. Pellegrini, and S. Langè, “Energy analysis of different municipal sewage sludge-derived biogas upgrading techniques,” *Chem Eng Trans*, vol. 37, 2014, doi: 10.3303/CET1437139.

[118] L. A. Pellegrini, G. De Guido, S. Consonni, G. Bortoluzzib, and M. Gatti, “From biogas to biomethane: How the biogas source influences the purification costs,” *Chem Eng Trans*, vol. 43, pp. 409–414, 2015, doi: 10.3303/CET1543069.

[119] G. Bortoluzzi, M. Gatti, A. Sogni, and S. Consonni, “Biomethane production from agricultural resources in the Italian scenario: Techno-Economic analysis of water wash,” *Chem Eng Trans*, vol. 37, pp. 259–264, 2014, doi: 10.3303/CET1437044.

[120] C. WORAWIMUT, S. VIVANPATARAKIJ, A. WATANAPA, W. WIYARATN, and S. ASSABUMRUNGRAT, “Purification and Upgrading from Biogas to Biomethane,” *Journal of the Japan Institute of Energy*, vol. 97, no. 7, pp. 176–179, 2018, doi: 10.3775/jie.97.176.

[121] M. W. Niu and G. P. Rangaiah, “Retrofitting amine absorption process for natural gas sweetening via hybridization with membrane separation,” *International Journal of Greenhouse Gas Control*, vol. 29, pp. 221–230, 2014, doi: 10.1016/j.ijggc.2014.08.019.

[122] A. Abdeljaoued, F. Relvas, A. Mendes, and M. H. Chahbani, “Simulation and experimental results of a PSA process for production of hydrogen used in fuel cells,” *J Environ Chem Eng*, vol. 6, no. 1, pp. 338–355, 2018, doi: 10.1016/j.jece.2017.12.010.

[123] F. J. Campanario and F. J. Gutiérrez Ortiz, “Fischer-Tropsch biofuels production from syngas obtained by supercritical water reforming of the bio-oil aqueous phase,” *Energy Convers Manag*, vol. 150, no. June, pp. 599–613, 2017, doi: 10.1016/j.enconman.2017.08.053.

[124] G. F. F. Jianguo Xu, "Methane steam reforming, methanation and water-gas shift: I. Intrinsic kinetics," *AIChE Journal*, 1989, doi: https://doi.org/10.1002/aic.690350109.

[125] A. Giwa and S. O. Giwa, "Simulation, Sensitivity Analysis and Optimization of Hydrogen Production by Steam Reforming of Methane Using Aspen Plus," *International Journal of Engineering Research & Technology*, vol. 2, no. 7, pp. 1719–1729, 2013.

[126] U. I. Amran, A. Ahmad, and M. R. Othman, "Kinetic based simulation of methane steam reforming and water gas shift for hydrogen production using aspen plus," *Chem Eng Trans*, vol. 56, pp. 1681–1686, 2017, doi: 10.3303/CET1756281.

[127] S. G. Gopaul and A. Dutta, "Dry reforming of multiple biogas types for syngas production simulated using Aspen Plus: The use of partial oxidation and hydrogen combustion to achieve thermo-neutrality," *Int J Hydrogen Energy*, vol. 40, no. 19, pp. 6307–6318, 2015, doi: 10.1016/j.ijhydene.2015.03.079.

[128] H. Er-Rbib, C. Bouallou, and F. Werkoff, "Production of synthetic gasoline and diesel fuel from dry reforming of methane," *Energy Procedia*, vol. 29, pp. 156–165, 2012, doi: 10.1016/j.egypro.2012.09.020.

[129] X. Hao, M. E. Djatmiko, Y. Xu, Y. Wang, J. Chang, and Y. Li, "Simulation analysis of a gas-to-liquid process using aspen plus," *Chem Eng Technol*, vol. 31, no. 2, pp. 188–196, 2008, doi: 10.1002/ceat.200700336.

[130] U. Pandey, "Modelling Fischer-Tropsch Kinetics and Product Distribution over a Cobalt Catalyst," *Norwegian University of Science and Technology*, 2020.

[131] J. Patzlaff, Y. Liu, C. Graffmann, and J. Gaube, "Interpretation and kinetic modeling of product distributions of cobalt catalyzed Fischer-Tropsch synthesis," *Catal Today*, vol. 71, no. 3–4, pp. 381–394, 2002, doi: 10.1016/S0920-5861(01)00465-5.

[132] G. P. Van Der Laan and A. A. C. M. Beenackers, "Kinetics and selectivity of the Fischer-Tropsch synthesis: A literature review: A literature review," *Catalysis Reviews-Science and Engineering*, vol. 41, no. 3–4, p. 64, 1999, doi: https://doi.org/10.1081/CR-100101170.

[133] T. Damartzis and A. Zabaniotou, "Thermochemical conversion of biomass to second generation biofuels through integrated process design — A review," vol. 15, pp. 366–378, 2011, doi: 10.1016/j.rser.2010.08.003.

[134] L. Zhou, J. Gao, X. Hao, Y. Yang, and Y. Li, "Chain Propagation Mechanism of Fischer–Tropsch Synthesis: Experimental Evidence by Aldehyde, Alcohol and Alkene Addition," *Reactions*, vol. 2, no. 2, pp. 161–174, 2021, doi: 10.3390/reactions2020012.

[135] H. S. Song, D. Ramkrishn, S. Trinh, and H. Wright, "Operating strategies for Fischer-Tropsch reactors: A model-directed study," *Korean Journal of*

Chemical Engineering, vol. 21, no. 2, pp. 308–317, 2004, doi: 10.1007/BF02705414.

[136] D. Vervloet, F. Kapteijn, J. Nijenhuis, and J. Van Ommen, "Fischer-Tropsch reaction-diffusion in a cobalt catalyst particle: Aspects of activity and selectivity for a variable chain growth probability," *Catal Sci Technol*, 2012, doi: 10.1039/C2CY20060K.

[137] K. D. Kruit, D. Vervloet, F. Kapteijn, and J. R. Van Ommen, "Selectivity of the Fischer-Tropsch process: Deviations from single alpha product distribution explained by gradients in process conditions," *Catal Sci Technol*, vol. 3, no. 9, pp. 2210–2213, 2013, doi: 10.1039/c3cy00080j.

[138] M. S. Niasar, "Development and Optimization of an Integrated Process Configuration for," no. January 2018, 2019, doi: 10.22108/gpj.2018.112760.1038.

[139] L. Zheng and E. Furimsky, "ASPEN simulation of cogeneration plants," *Energy Convers Manag*, vol. 44, no. 11, pp. 1845–1851, 2003, doi: 10.1016/S0196-8904(02)00190-5.

[140] V. Dlugosel'skii, V. Belyaev, N. Mishustin, and V. Rybakov, "Gas-turbine units for cogeneration.," *Thermal Engineering*, no. 54(12), pp. 1000–1003, 2007.

[141] S. Michailos, D. Parker, and C. Webb, "A techno-economic comparison of Fischer–Tropsch and fast pyrolysis as ways of utilizing sugar cane bagasse in transportation fuels production.," *Chemical Engineering Research and Design*, vol. 118, pp. 206–214, 2017, doi: 10.1016/j.cherd.2017.01.001.

[142] H. Er-Rbib, C. Bouallou, and F. Werkoff, "Production of synthetic gasoline and diesel fuel from dry reforming of methane," *Energy Procedia*, vol. 29, pp. 156–165, 2012, doi: 10.1016/j.egypro.2012.09.020.

[143] M. Sudiro and A. Bertucco, "Production of synthetic gasoline and diesel fuel by alternative processes using natural gas and coal: Process simulation and optimization," *Energy*, vol. 34, no. 12, pp. 2206–2214, 2009, doi: 10.1016/j.energy.2008.12.009.

[144] B. Bao, M. M. El-Halwagi, and N. O. Elbashir, "Simulation, integration, and economic analysis of gas-to-liquid processes," *Fuel Processing Technology*, vol. 91, no. 7, pp. 703–713, 2010, doi: 10.1016/j.fuproc.2010.02.001.

[145] G. Cinti, A. Baldinelli, A. Di Michele, and U. Desideri, "Integration of Solid Oxide Electrolyzer and Fischer-Tropsch: A sustainable pathway for synthetic fuel," *Appl Energy*, vol. 162, pp. 308–320, 2016, doi: 10.1016/j.apenergy.2015.10.053.

[146] M. Pondini and M. Ebert, "Process synthesis and design of low temperature Fischer-Tropsch crude production from biomass derived syngas," Chalmers University of Technology, 2013.

[147] S. Rane, O. Borg, E. Rytter, and A. Holmen, "Relation between hydrocarbon selectivity and cobalt particle size for alumina supported cobalt Fischer-

Tropsch catalysts," *Appl Catal A Gen*, vol. 437–438, pp. 10–17, 2012, doi: 10.1016/j.apcata.2012.06.005.

[148] M. Marchese, E. Giglio, M. Santarelli, and A. Lanzini, "Energy performance of Power-to-Liquid applications integrating biogas upgrading, reverse water gas shift, solid oxide electrolysis and Fischer-Tropsch technologies," *Energy Conversion and Management: X*, vol. 6, no. January, p. 100041, 2020, doi: 10.1016/j.ecmx.2020.100041.

[149] M. Marchese, N. Heikkinen, E. Giglio, A. Lanzini, J. Lehtonneen, and M. Reinikainen, "Kinetic study based on the carbide mechanism of a Co-Pt/γ-Al2 O3 Fischer–Tropsch catalyst tested in a laboratory-scale tubular reactor," *Catalysts*, vol. 9, no. 9, 2019, doi: 10.3390/catal9090717.

[150] M. Marchese, G. Buffo, M. Santarelli, and A. Lanzini, "CO2from direct air capture as carbon feedstock for Fischer-Tropsch chemicals and fuels: Energy and economic analysis," *Journal of CO2 Utilization*, vol. 46, no. December, 2021, doi: 10.1016/j.jcou.2021.101487.

[151] M. Marchese, S. Chesta, M. Santarelli, and A. Lanzini, "Techno-economic feasibility of a biomass-to-X plant: Fischer-Tropsch wax synthesis from digestate gasification," *Energy*, vol. 228, p. 120581, 2021, doi: 10.1016/j.energy.2021.120581.

[152] K. J. Gabriel, P. Linke, A. Jiménez-Gutiérrez, D. Y. Martínez, M. Noureldin, and M. M. El-Halwagi, "Targeting of the water-energy nexus in gas-to-liquid processes: A comparison of syngas technologies," *Ind Eng Chem Res*, vol. 53, no. 17, pp. 7087–7102, 2014, doi: 10.1021/ie4042998.

[153] N. A. Hamad, M. M. El-halwagi, N. O. Elbashir, and S. M. Mannan, "Safety and Techno-Economic Analysis of Solvent Selection for Supercritical Fischer-Tropsch Synthesis Reactors," Texas A&M University, 2011.

[154] R. Dahl, "Evaluation of the new Power & Biomass to Liquid (PBtL) concept for production of biofuels from woody biomass," Norwegian University of Science and Technology, Faculty of Natural Sciences, 2020.

[155] M. Hillestad, "Modeling the Fischer-Tropsch Product Distribution and Model Implementation," *Chemical Product and Process Modeling*, vol. 10, no. 3, pp. 147–159, 2015, doi: 10.1515/cppm-2014-0031.

[156] B. Todic, W. Ma, G. Jacobs, B. H. Davis, and D. B. Bukur, "CO-insertion mechanism based kinetic model of the Fischer-Tropsch synthesis reaction over Re-promoted Co catalyst," *Catal Today*, vol. 228, pp. 32–39, 2014, doi: 10.1016/j.cattod.2013.08.008.

[157] W. D. Shafer *et al.*, "Fischer-tropsch: Product selectivity-the fingerprint of synthetic fuels," *Catalysts*, vol. 9, no. 3, 2019, doi: 10.3390/catal9030259.

[158] P. Trop, B. Anicic, and D. Goricanec, "Production of methanol from a mixture of torrefied biomass and coal," *Energy*, vol. 77, pp. 125–132, 2014, doi: 10.1016/j.energy.2014.05.045.

[159] R. Y. Chein, W. H. Chen, H. Chyuan Ong, P. Loke Show, and Y. Singh, "Analysis of methanol synthesis using CO2 hydrogenation and syngas

produced from biogas-based reforming processes," *Chemical Engineering Journal*, vol. 426, no. June, p. 130835, 2021, doi: 10.1016/j.cej.2021.130835.

[160] R. De María, I. Díaz, M. Rodríguez, and A. Sáiz, "Industrial methanol from syngas: Kinetic study and process simulation," *International Journal of Chemical Reactor Engineering*, vol. 11, no. 1, pp. 469–477, 2013, doi: 10.1515/ijcre-2013-0061.

[161] N. Suhada, N. Azma, M. Mel, and S. Sulaiman, "Optimization of Methanol Production using Aspen Plus," vol. 1, no. 1, pp. 1–10, 2020.

[162] K. Atsonios, K. D. Panopoulos, and E. Kakaras, "Thermocatalytic CO2 hydrogenation for methanol and ethanol production: Process improvements," *Int J Hydrogen Energy*, vol. 41, no. 2, pp. 792–806, 2016, doi: 10.1016/j.ijhydene.2015.12.001.

[163] G. H. Graaf, E. J. Stamhuis, and A. A. C. M. Beenackers, "Kinetics of low-pressure methanol synthesis," *Chem Eng Sci*, vol. 43, no. 12, pp. 3185–3195, 1988, doi: 10.1016/0009-2509(88)85127-3.

[164] É. S. Van-Dal and C. Bouallou, "Design and simulation of a methanol production plant from CO2 hydrogenation," *J Clean Prod*, vol. 57, pp. 38–45, 2013, doi: 10.1016/j.jclepro.2013.06.008.

[165] K. M. Vanden Bussche and G. F. Froment, "A steady-state kinetic model for methanol synthesis and the water gas shift reaction on a commercial Cu/ZnO/Al2O3 catalyst," *J Catal*, vol. 161, no. 1, pp. 1–10, 1996, doi: 10.1006/jcat.1996.0156.

[166] D. Mignard and C. Pritchard, "On the use of electrolytic hydrogen from variable renewable energies for the enhanced conversion of biomass to fuels," *Chemical Engineering Research and Design*, vol. 86, no. 5, pp. 473–487, 2008, doi: 10.1016/j.cherd.2007.12.008.

[167] F. Mantoan, F. Bezzo, and E. Barbera, "Design and Simulation of Hydrogenation Processes for Co 2 Conversion To C-1 Chemicals," UNIVERSITÀ DEGLI STUDI DI PADOVA, 2019.

[168] M. Pérez-Fortes, J. C. Schöneberger, A. Boulamanti, and E. Tzimas, "Methanol synthesis using captured CO2 as raw material: Techno-economic and environmental assessment," *Appl Energy*, vol. 161, pp. 718–732, 2016, doi: 10.1016/j.apenergy.2015.07.067.

[169] F. Calogero, M. Santarelli, E. Giglio, and D. Ferrero, "Methanol synthesis through CO2 hydrogenation: reactor and process modelling (M.Sc. thesis)," Politecnico di Torino, 2018.

[170] A. A. Kiss, J. J. Pragt, H. J. Vos, G. Bargeman, and M. T. de Groot, "Novel efficient process for methanol synthesis by CO2 hydrogenation," *Chemical Engineering Journal*, vol. 284, pp. 260–269, 2016, doi: 10.1016/j.cej.2015.08.101.

[171] K. Atsonios, K. D. Panopoulos, and E. Kakaras, "Thermocatalytic CO2 hydrogenation for methanol and ethanol production: Process

improvements," *Int J Hydrogen Energy*, vol. 41, no. 2, pp. 792–806, 2016, doi: 10.1016/j.ijhydene.2015.12.001.

[172] P. Cozma, W. Wukovits, I. Mămăligă, A. Friedl, and M. Gavrilescu, "Modeling and simulation of high pressure water scrubbing technology applied for biogas upgrading," *Clean Technol Environ Policy*, vol. 17, no. 2, pp. 373–391, 2014, doi: 10.1007/s10098-014-0787-7.

[173] K. Rajendran, H. R. Kankanala, M. Lundin, and M. J. Taherzadeh, "A novel process simulation model (PSM) for anaerobic digestion using Aspen Plus," *Bioresour Technol*, vol. 168, pp. 7–13, 2014, doi: 10.1016/j.biortech.2014.01.051.

[174] A. Almoslh, F. Alobaid, C. Heinze, and B. Epple, "Comparison of equilibrium-stage and rate-based models of a packed column for tar absorption using vegetable oil," *Applied Sciences (Switzerland)*, vol. 10, no. 7, pp. 8–10, 2020, doi: 10.3390/app10072362.

[175] A. Tripodi, M. Compagnoni, R. Martinazzo, G. Ramis, and I. Rossetti, "Process simulation for the design and scale up of heterogeneous catalytic process: Kinetic modelling issues," *Catalysts*, vol. 7, no. 5, 2017, doi: 10.3390/catal7050159.

[176] O. O. James, B. Chowdhury, M. A. Mesubi, and S. Maity, "Reflections on the chemistry of the Fischer-Tropsch synthesis," *RSC Adv*, vol. 2, no. 19, pp. 7347–7366, 2012, doi: 10.1039/c2ra20519j.

[177] M. J. Prins, K. J. Ptasinski, and F. J. J. G. Janssen, "Exergetic optimisation of a production process of Fischer-Tropsch fuels from biomass," *Fuel Processing Technology*, vol. 86, no. 4, pp. 375–389, 2005, doi: 10.1016/j.fuproc.2004.05.008.

[178] L. Testa, D. Chiaramonti, M. Prussi, and S. Bensaid, *Challenges and opportunities of process modelling renewable advanced fuels*, no. 0123456789. Springer Berlin Heidelberg, 2022. doi: 10.1007/s13399-022-03057-0.

[179] H. Er-Rbib, C. Bouallou, and F. Werkoff, "Production of synthetic gasoline and diesel fuel from dry reforming of methane," *Energy Procedia*, vol. 29, pp. 156–165, 2012, doi: 10.1016/j.egypro.2012.09.020.

[180] R. Dahl, "Evaluation of the new Power & Biomass to Liquid (PBtL) concept for production of biofuels from woody biomass," 2020.

[181] M. Puig-Gamero, J. Argudo-Santamaria, J. L. Valverde, P. Sánchez, and L. Sanchez-Silva, "Three integrated process simulation using aspen plus ® : Pine gasification , syngas cleaning and methanol synthesis," *Energy Convers Manag*, vol. 177, no. June, pp. 416–427, 2018, doi: 10.1016/j.enconman.2018.09.088.

[182] R. M. Handler, D. R. Shonnard, E. M. Griffing, A. Lai, and I. Palou-Rivera, "Life Cycle Assessments of Ethanol Production via Gas Fermentation: Anticipated Greenhouse Gas Emissions for Cellulosic and Waste Gas

Feedstocks," *Ind Eng Chem Res*, vol. 55, no. 12, pp. 3253–3261, 2016, doi: 10.1021/acs.iecr.5b03215.

[183] P. Roy, A. Dutta, and Bill Deen, "Greenhouse gas emissions and production cost of ethanol produced from biosyngas fermentation process," *Bioresour Technol*, vol. 192, pp. 185–191, 2015, doi: https://doi.org/10.1016/j.biortech.2015.05.056.

[184] Rudy Michel *et al.*, "Steam gasification of Miscanthus X Giganteus with olivine as catalyst production of syngas and analysis of tars (IR, NMR and GC/MS)," *Biomass Bioenergy*, vol. 35, no. 7, pp. 2650–2658, 2011, doi: https://doi.org/10.1016/j.biombioe.2011.02.054.

[185] D. W. Griffin and M. A. Schultz, "Fuel and chemical products from biomass syngas: A comparison of gas fermentation to thermochemical conversion routes," *Environ Prog Sustain Energy*, vol. 31, no. 2, pp. 219–224, 2012, doi: https://doi.org/10.1002/ep.11613.

[186] A Gas for Climate report, "Feasibility of REPowerEU 2030 targets, production potentials in the Member Biomethane production potentials in the EU," no. July, 2022.

[187] ConcaweEU, "Refinery Sites in Europe." Accessed: Oct. 27, 2023. [Online]. Available: https://www.concawe.eu/refineries-map/

[188] E. Brancaccio, "GTL: Small Scale and Modular Technologies for Gas to Liquid Industry." Accessed: Sep. 12, 2023. [Online]. Available: https://www.oil-gasportal.com/gtl-small-scale-and-modular-technologies-for-gas-to-liquid-industry/

[189] H. M. Howells and T. H. Fleisch, "MINI-GTL TECHNOLOGY BULLETIN," vol. 2, no. July 2016, pp. 1–4, 2016.

[190] K. Zayer, A. Teimouri, S. Changizian, and P. Ahmadi, "Techno-economic assessment of small-scale gas to liquid technology to reduce waste flare gas in a refinery plant," *Sustainable Energy Technologies and Assessments*, vol. 55, no. December 2022, p. 102955, 2023, doi: 10.1016/j.seta.2022.102955.

[191] P. Kelly-Detwiler, "Gas-to-Liquids Plants: No Longer Exclusive to Larger Players." Accessed: Sep. 12, 2023. [Online]. Available: https://www.forbes.com/sites/peterdetwiler/2013/01/17/gas-to-liquids-plants-no-longer-exclusive-to-larger-players/

[192] CompactGTL, "CompactGTL." Accessed: Sep. 12, 2023. [Online]. Available: https://www.compactgtl.com/

[193] INFRA, "Small-scale GTL." Accessed: Sep. 12, 2023. [Online]. Available: https://infra-sf.com/products/smallscalegtl/

[194] INFRA, "GasTechno and INFRA to jointly market Mini-GTL technology." Accessed: Sep. 12, 2023. [Online]. Available: https://infra-sf.com/info/news/213/

[195] J. Shen *et al.*, "Design of a Fischer-Tropsch multi-tube reactor fitted in a container: A novel design approach for small scale applications," *J Clean Prod*, vol. 362, 2022, doi: https://doi.org/10.1016/j.jclepro.2022.132477.

[196] Fleisch and T. H, “Associated Gas Monetization via miniGTL: Conversion of Flared Gas into Liquid Fuels and Chemicals,” Washingtonne, DC, 2015.
[197] Chemical Market Analytics, “Methanol as a Marine Bunker Fuel.” Accessed: Nov. 05, 2023. [Online]. Available: https://chemicalmarketanalytics.com/blog/methanol-market-outlook-2/
[198] European Commission, “EU Reference Scenario 2020.” Accessed: Nov. 05, 2023. [Online]. Available: https://energy.ec.europa.eu/data-and-analysis/energy-modelling/eu-reference-scenario-2020_en
[199] James Hileman, “ICAO - Fuel Approval Process & Status.” Accessed: Feb. 15, 2024. [Online]. Available: https://www.icao.int/Meetings/SAFStocktaking/Documents/ICAO%20SAF%20Stocktaking%202019%20-%20AI1-1%20Jim%20Hileman.pdf